

**APPLICATION OF DUAL MODELS IN
I. MESON-BARYON POLARIZATION
AND
II. NON-LINEAR BOOTSTRAP**

A Thesis Submitted
In Partial Fulfilment of the Requirements
for the Degree of
DOCTOR OF PHILOSOPHY

**BY
JNANADEVIA MAHARANA**

to the

59125

**DEPARTMENT OF PHYSICS
INDIAN INSTITUTE OF TECHNOLOGY KANPUR
JULY 1972**

To

GAGA and BA

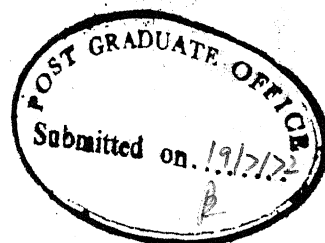
V
JUNE '76

I. I. T. KANPUR
CENTRAL LIBRARY
422125

Thesis
539.72
J 569

4 JAN 1973

PHY-1972-D-MAH-APP



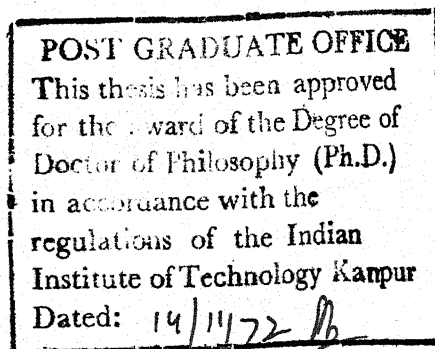
CERTIFICATE

Certified that the work presented in this thesis entitled " Application of Dual Models in (I) Meson-Baryon Polarization and (II) Nonlinear Bootstrap" by Jnanadeva Maharana has been done under my supervision and it has not been submitted elsewhere for a degree.

R. Ramachandran

(R. Ramachandran)
Assistant Professor
Department of Physics
Indian Institute of Technology
Kanpur-16

July, 1972



ACKNOWLEDGEMENTS

I am deeply indebted to Professor R. Ramachandran and express my grateful thanks for his patient guidance and invaluable advice throughout the course of this investigation. He has been a continual source of enthusiasm and encouragement during my stay at I.I.T. Kanpur.

Thanks are due to Professors Gyan Mohan, Tulsi Dass and H.S. Mani for their kind inspirations and useful discussions at various stages. My colleagues, Drs. P.K. Patnaik, A.K. Bhargava, S.K. Bose and M/S A.K. Kapoor, V.M. Raval, S. Krishna, Radhey Shyam, Pankaj Sharan and V.K. Agrawal need mention for numerous helpful comments and discussions and I have enjoyed their association during my stay at Kanpur. Thanks are also due to M/S N.V. Dandekar, M.P. Das, S.N. Gadekar, H.M. Gupta, P.K. Misra and many others for providing me their pleasant company.

I am grateful to Professor J. Mahanty for his kind interest and encouragements.

I am thankful to Mr. J.K. Misra for his patient typing of the manuscript and to H.K. Panda for cyclostyling the thesis.

Financial supports from the Department of Atomic Energy; Government of India and Council of Scientific and Industrial Research, New Delhi are gratefully acknowledged.

J. Maharana
J. Maharana

CONTENTS

	Page
CHAPTER I: : 1.1 Introduction	1
1.2 Finite Energy Sum Rules and Duality	4
1.3 Construction of Dual Amplitudes	12
CHAPTER II:	18
2.2 Pion Nucleon Scattering in the Veneziano Model	20
2.2.1 Kinematics and Notations	21
2.2.2 Igi's Model	26
2.3 Fenster and Wali Model	32
2.4 η Production in πN Scattering	44
CHAPTER III	50
3.2.1 Charge-Exchange Processes in the $\bar{K}N$ Scattering	51
3.2.2 Hypercharge - Exchange Processes	53
3.3 Pion Conspiracy in Charged Pion Photo-production	67
3.3.1 Kinematics and Invariant Amplitudes	68
CHAPTER IV	78
4.2 Single Particle Distribution and Total Cross-Sections	81
4.2.1 Total Cross-Section for Two Particle Scattering	81
4.2.2 Kinematics of Single Particles Distribution	82
4.2.3 The Total Cross-Section and Inclusive Cross-Section	90

4.2.4	The Process $\pi^-K^+ \rightarrow \pi^-K^+$ and the Inclusive Reaction $\pi^-K^+ \rightarrow \pi^0 +$ anything	94
4.2.5	$\pi\eta \rightarrow \pi\eta$ and the Inclusive Reaction $\pi\eta \rightarrow \pi + \text{anything}$	97
4.3	Discontinuity Functions	99
4.4	Results	112
CHAPTER	V	115
REFERENCES		124
APPENDIX		130

LIST OF FIGURES

<u>Figure</u>		<u>Page</u>
1.	Shows the kinematics of meson baryon scattering. $q_1(p_1)$ and $q_2(p_2)$ refer to the four-momenta of the incoming and outgoing meson (baryon) respectively.	22
2.	Shows prediction of polarization, for πN CEX, as calculated using the baryon trajectories are degenerate. Polarization data has been taken from Rs. 50.	36
3.	Fits to polarization have been obtained using Igi's set for πN CEX scattering.	37
4.	Shows the polarization calculated using FESR parametrization for πN CEX scattering	38
5.	Shows the polarization as calculated using Fenster and Wali model.	39
6.	Shows the differential cross-section obtained using degenerate trajectory set and the Igi's set of parameters.	40
7.	Shows the predictions for the differential cross-section using FESR parametrization and Fenster and Wali model.	41

FigurePage

8. Prediction for polarization in the high momentum transfer region in the case when baryon trajectories are taken to be degenerate. Data has been taken from Ref. 51. 42
9. The predictions for polarization in the high momentum transfer region with Igi's set of parameters. 43
10. Shows fits to the differential cross-section for $\pi^-p \rightarrow \eta n$ at 5.9 and 13.3 GeV. Data has been taken from Ref. 54. 47
11. Shows fits to the differential cross-section for $\pi^-p \rightarrow \eta n$ at 9.8 GeV. 48
12. Shows our predictions for the polarization in the process $\pi^-p \rightarrow \eta n$. The data has been taken from Ref. 54. 49
13. Shows fits to the differential cross-section for the process $K^-p \rightarrow \bar{K}^0 n$, data has been taken from Ref. 64. 58
14. Shows the differential cross-section for $K^+n \rightarrow K^0 p$ as obtained using s - u crossing of the amplitude for $K^-p \rightarrow \bar{K}^0 n$. Data has been taken from Ref. 65. 59

FigurePage

15. Gives the polarization for $K^-p \rightarrow \bar{K}^0 n$. 60
16. Fits to the differential cross-section for $K^-p \rightarrow \pi^- \Sigma^+$ is shown in this figure. Data has been taken from Ref. 68. 62
17. Shows fits to the differential cross-section for the process $K^-n \rightarrow \pi^- \Lambda$. The data has been taken from Ref. 69. 63
18. Shows the prediction of polarization for the process $K^-n \rightarrow \pi^- \Lambda$. The data has been taken from Ref. 69. 64
19. The prediction of polarization for $\pi^+ p \rightarrow K^+ \Sigma^+$ is shown in this Figure. The data has been taken from Ref. 70. 65
20. Fits to the differential cross-section for $\gamma + p \rightarrow \pi^+ n$ is shown in this Figure. The data has been taken from Ref. 84. 74
21. The prediction for the asymmetry parameter is shown in this Figure. The data has been taken from Ref. 85. 76
22. (a) Represents the case when $a+b$ form a resonance and decay into anything.
(b) Depicts the case when $a+b$ form two resonances R_1 and R_2 which decay into anything. 83

FigurePage

22. (a) Represents the case when $a+b$ form a resonance and decay into anything.
(b) Depicts the case when $a+b$ form two resonances R_1 and R_2 which decay into anything. 83
23. (a) Shows that square of Fig. 22(a) is related to the elastic forward scattering amplitude of $a+b \rightarrow a+b$.
(b) Shows that square of Fig. 22(b) gives rise to twisted nonplanar dual loop. 84
24. (a) Shows the diagram that contributes in the pionization region.
(b) is the diagram in the TEX region.
(c) is the diagram relevant in the tripple Regge region. 87
25. Shows the diagrams which contribute to the inclusive process $a+b \rightarrow c + \text{anything}$ a single resonance decays into anything. 89
26. (a-d) Represent the diagrams we have considered to find the discontinuity functions for the inclusive process $a+b \rightarrow c + \text{anything}$. 92

SYNOPSIS

We have studied some applications of Dual Resonance Model in this thesis. The thesis consists of two parts, the first part contains the study of charge and hypercharge exchange processes in meson-baryon scattering using the Veneziano model. The second part is devoted to the study of the consistency condition imposed on the coupling constants using the information on total cross-section and inclusive cross-section. The content of the thesis is as follows.

The first chapter is devoted to the general introduction to the S-matrix theory and its application to the low-energy and high energy scattering processes. We introduce Dolen-Horn-Schmid duality hypothesis in this chapter and mention some of its applications. Then we consider Veneziano model as one of the models which exhibits principle of duality explicitly.

In the second chapter, we study single Regge pole exchange processes in pion-nucleon scattering using the Veneziano model. The polarization phenomena in pion-nucleon charge exchange process is studied in the intermediate energy range. This process is studied in the two models (i) proposed by Igi and (ii) Fenster and Wali. The results of the two models are compared with experimental data. We also study the γ production in the Veneziano model. We obtain a fairly good fit to the

differential cross-sections in the intermediate energy range for the γ production process.

The third chapter contains the study of the charge and hypercharge exchange processes in kaon nucleon scattering. We obtain fits to the differential cross-section with a relatively small number of parameters and predict polarization for these processes. We also predict differential cross-section for some of the crossed channel processes which are in fairly good agreement with the experimental data. In this chapter we include the application of the Veneziano model to charged pion photo-production. We obtain a good fit to the differential cross-section and the asymmetry parameter for the charged pion photo-production is predicted.

In the fourth chapter we take up study of the inclusive reactions like $a + b \rightarrow c + \text{anything}$. We use the fact that, there is already enough information about unitarity in the four point Veneziano amplitude, to calculate total cross-section for $a + b \rightarrow \text{anything}$ using optical theorem. Then we use generalized optical theorem of Mueller to obtain an expression for the inclusive cross-section from the six point Veneziano amplitude for the forward scattering amplitude of the process $a+b+\bar{c} \rightarrow a+b+\bar{c}$. The inclusive cross-section is calculated explicitly in different kinematical regions of the inclusive reaction $a+b \rightarrow c + \text{anything}$. The cross-section obtained, in this manner, for the inclusive process is integrated to obtain the total cross-section. The

theorem together with the total cross-section obtained from the inclusive cross-section give a nonlinear equation for the coupling constants. We have used this method for the calculation of the coupling constants that occur in the meson-meson scattering. The masses of the mesons and the leading Regge trajectories that are exchanged in different channels have been used as inputs. Following the arguments of Tye and Veneziano we assume that the Reggeon part and the Pomeron part satisfy the nonlinear bootstrap equations separately, therefore the Pomeron is not included in all these calculations. Our results for the coupling constants $g_{K^*K\pi}^2$ and $g_{A_2\rho\pi}^2$ are of the same order of magnitude when compared with available results.

We discuss our results in the fifth and last chapter. We also suggest the possible improvement that can be made in our models. A possible modification is suggested to study the nonlinear dual models in order to obtain better results.

CHAPTER I

The S-matrix theory¹ has been of great use in the study of the properties of strongly interacting particles during the last two decades. This approach is important, both, for its direct relation to experimental data and for its role in the theoretical study of strong interactions. The general principles of the S-matrix theory, such as unitarity, crossing and analyticity, together with the dynamical content of the Regge pole theory have produced encouraging results. It is hoped that this scheme will put strong restrictions on the scattering amplitude so that the Regge trajectories and their residue functions could be uniquely determined. As a consequence, the spectrum of the particles and their couplings would be completely determined accomplishing a bootstrap scheme.

The principle of maximal analyticity of the first kind requires that the only singularities of the S-matrix should be the poles corresponding to stable or unstable particles, and further singularities are generated from those poles by unitarity. The analytic behavior of the scattering amplitude as function of energy and momentum transfer plays a central role in establishing rigorous results at high energies and in providing the basis for approximation procedure.

The principle of maximal analyticity of the second kind states that the S-matrix should be continuable in angular momentum throughout the complex angular momentum plane, with only isolated singularities. (The cuts in the angular momentum plane can be generated from poles.) The principle of maximal analyticity of second kind together with crossing and the maximal analyticity of the first kind has become very useful, during the last decade, in the study of the high energy collisions of hadrons.

In the scattering experiments one observes the following general features in the low energy region:

- (i) There are large number of resonances in the low energy region. The peaks in the scattering cross-sections can be regarded as the manifestation of these resonances.
- (ii) The angular distribution of particles in the scattering experiments is understood in terms of a few low-lying partial waves.

To a good approximation the low energy scattering phenomena can be understood in the resonance saturation scheme. In this approximation one assumes that the scattering amplitude is well approximated by resonance poles and the non resonating background is negligible.

Whereas in the high energy experiments one finds:

- (i) Each total cross-section decreases rapidly towards a constant value in each case.
- (ii) The differential cross-sections show sharp forward and backward peaks.
- (iii) Total cross-sections for particle target and the anti-particle target in majority of processes are tending towards an equality.
- (iv) In the case of certain processes the differential cross-section has dips at fixed values of momentum transfer at different energies.

All these gross features of the experimental data have been described successfully using the Regge pole theory. According to this theory the high energy behavior of the scattering amplitude is controlled by the moving poles in the complex angular momentum plane of the crossed channel.

Now what happens in the intermediate energy region? The scattering process in this region can be described either in terms of only direct channel resonances or in terms of only Regge poles in the crossed channel. A third possibility is that we can construct the scattering amplitude as sum of a Regge part and a resonance part²⁻⁴. The latter model is referred to as the interference model. It is also possible to explain the scattering process in the intermediate energy region in terms of single particle exchanges in the t -channel. But this model fails to reproduce the observed energy dependence of the

scattering cross-sections at high energies. This apparent contradiction between the Regge pole theory and the single particle exchange model was resolved by van Hove. According to van Hove⁵⁻⁷ the Regge behavior, at high energies, can be understood as the effect of the exchange of infinite number of particles in the t -channel, occurring in an indefinitely rising Regge trajectory. Another question that crops up is whether there is any relation between the Regge poles in the crossed channel and the resonances in the direct channel. The finite energy sum rules provided the connection between the two.

1.2 Finite Energy Sum Rules and Duality:

The analytic structure of the scattering amplitude enables us to write a fixed t dispersion relation in the cut \rightarrow (energy) plane. One requires the knowledge of the behavior of the scattering amplitude as $\nu \rightarrow \infty$ in order to write such a dispersion relation. According to the resonance saturation scheme the low energy region of the scattering amplitude is well approximated by resonances, whereas, at the asymptotic energies, the behavior of the scattering amplitude is determined by the Regge poles that are exchanged in the crossed channel. Using these two bits of information it has been possible to impose certain consistency conditions on the scattering amplitude to satisfy the demands of analyticity.^{8,9}

Consider a typical unsubtracted fixed t dispersion relation:

$$A(\nu, t) = \frac{1}{\pi} \int_{\nu_0}^{\infty} \frac{\text{Im } A(\nu', t) d\nu'}{\nu' - \nu} \quad (1.2.1)$$

which tells us that $A(\nu, t)$ is a real analytic function defined in the complex ν plane cut from ν_0 to ∞ along the real axis. $A(\nu, t)$ is purely real for ν below ν_0 and its discontinuity across the cut is $2i \text{Im } A(\nu, t)$ and $A(\nu) \rightarrow 0$ as $\nu \rightarrow \infty$. If $A(\nu, t)$ does not tend to zero as $\nu \rightarrow \infty$ we need to introduce subtractions.

To derive the finite energy sum rules (FESR) we consider a function $A(\nu, t)$ which is antisymmetric in ν for fixed t and which can be represented by a series of Regge poles for $\nu \geq N$. The Regge poles can be divided into following three classes: (i) the class of poles for which $\alpha > -1$ denoted by α_i , (ii) the poles for which $\alpha < -1$ denoted by α_j and (iii) α_k denotes the set of poles for which $\alpha = -1$. The presence of α_i 's demand subtractions in the dispersion integral and α_j 's do not require any subtraction.

If we subtract the part which gets contribution from α_i then the amplitude $A(\nu, t)$ will satisfy the following equation.

$$\int_0^{\infty} \left[\text{Im } A(\nu, t) - \sum_{\alpha_i > -1} \frac{\beta_i \nu^{\alpha_i(t)}}{(\alpha_i + 1)} \right] d\nu = \beta_k \quad (1.2.2)$$

where β_k is the residue of the pole $\alpha_k = -1$.

We have assumed that the Regge behavior of the amplitude is given by

$$A(\nu, t) \sim \sum_{l=1}^{\infty} \beta_l(t) \frac{(\pm 1 - e^{-i\pi\alpha_l(t)}) \nu^{\alpha_l(t)}}{\sin \pi \alpha_l(t) \Gamma(1 + \alpha_l(t))}, \quad (1.2.3)$$

where l includes the i , j and k type Regge poles.

The point to note here is that the individual terms in the left hand side of the eqn. (1.2.2) diverge whereas the integral as a whole converges. Let us cut off the integral into two parts. Integral from $\nu = \nu_{\min}$ to $\nu = N$ and $\nu = N$ to $\nu = \infty$. N is such that at $\nu = N$ the amplitude shows Regge behavior. So we can then write eqn. (1.2.2) as,

$$\begin{aligned} \int_0^N [\text{Im } A(\nu, t) - \sum_{\alpha_i > -1} \frac{\beta_i(t) \nu^{\alpha_i(t)}}{(\alpha_i(t) + 1)}] d\nu \\ + \int_N^{\infty} \sum_{\alpha_j < -1} \frac{\beta_j(t) \nu^{\alpha_j(t)}}{\Gamma(\alpha_j(t) + 1)} d\nu = \beta_k(t) \end{aligned} \quad (1.2.4)$$

Performing each integral we get,

$$\begin{aligned} S(N) &\equiv \frac{1}{N} \int_0^N \text{Im } A(\nu, t) d\nu \\ &= \sum_{\alpha_i > -1} \frac{\beta_i(t) N^{\alpha_i(t)}}{\Gamma(\alpha_i(t) + 2)} + \sum_{\alpha_j < -1} \frac{\beta_j(t) N^{\alpha_j(t)}}{\Gamma(\alpha_j(t) + 2)} \\ &\quad + \frac{\beta_k(t)}{N} \end{aligned} \quad (1.2.5)$$

It is straight-forward to derive higher moment sum rules, given by

$$S_n = \frac{1}{N^{n+1}} \int_0^N \nu^n \operatorname{Im} A(\nu, t) d\nu$$

$$= \sum_l \frac{\beta_l(t) N^{\alpha_l(t)}}{\Gamma(1+\alpha_l(t)) (\alpha_l(t)+n+1)} \quad (1.2.6)$$

The advantage of FESR is that all the calculations are done at finite energies and the information is available both in the low energy region and high energy region to verify the sum rules. It is worth mentioning here that the left hand side of the eqn. (1.2.5) gets contribution from the low energy resonances whereas the right hand side of the equation contains the Regge parameters of the crossed channel. The averaged effect of the direct channel resonances reproduces the t-channel Regge parameters. In fact this was verified by Dolen, Horn and Schmid¹⁰ for πN charge exchange scattering. They showed that the Regge formula can be extrapolated to much lower energy and the average effect of the πN resonances smooths out to the Regge behavior.

One can use finite energy sum rules in several ways.

(i) The Regge parameters, as obtained from the high energy data, can be used to determine the parameters of s-channel resonances^{11,12}. (ii) The FESR can be used as a bootstrap scheme¹³⁻¹⁵. In this scheme we can use low energy resonance parameters as well as the Regge parameters of the crossed channel to check the consistency of the FESR equations, (iii) To use the direct

channel resonances to determine the Regge trajectories¹⁰⁻¹⁶. In particular when there is a single Regge pole exchanged in the t-channel we can determine the trajectory function and the residue by taking different moments of FESR. The algebraic equation for different moments is used to determine the trajectory and residue functions in the following manner:

$$S_n: S_m = (\alpha(t) + m + 1) : (\alpha(t) + n + 1) \quad (1.2.7)$$

In more complicated cases, when more than one Regge trajectories are exchanged in the crossed channel, a suitable combination of different invariant amplitudes can be used to determine trajectory functions and the residues using the FESR.

Among the many uses of FESR, what we wish to emphasize is the neat connection between the low energy resonances and the high energy behaviour. This forms the basis of the principle of duality^{17,18}. If one assumes that the scattering amplitude can be represented by series of poles to a good approximation at low energies and this series has an asymptotic expansion given by,

$$A(s, t) \sim \beta(t) (s)^{\alpha(t)} \quad (1.2.8)$$

then the scattering amplitude is completely determined by its meromorphic part in one invariant variable for fixed values of the other invariant variable.

If we assume $A(s, t)$ has poles on the real axis and the amplitude is determined by the meromorphic part only then $A(s, t)$ can be written as,

$$A(s, t) = \sum_{n=1}^{\infty} \frac{R_n(t)}{n-\alpha(s)} \quad (1.2.9)$$

The residues are known polynomials,

$$R_n(t) = \sum_{k=0}^n C_k(n) t^k, \quad (1.2.10)$$

which define the resonance content of the amplitude at the energy s_n such that $\alpha(s_n) = n$. The eqn. (1.2.9) is defined for values of t for which the series converges. Then the dual amplitude is completely determined as a function of two complex variables by its meromorphic part in one complex variable.

The $s \leftrightarrow t$ symmetry of the function allows us to write

$$A(s, t) = \sum_{n=1}^{\infty} \frac{R_n(s)}{n-\alpha(t)} \quad (1.2.11)$$

It should be possible to generate the poles in the t -channel from the asymptotic expansion of $R_n(t)$ given the meromorphic part in the s -channel. The t -channel poles can be generated from the controlled divergence of the infinite sum. In order that $A(s, t)$ has a leading asymptotic term (Regge term) we must require that the leading term in $R_n(t)$ is also of the form,

$$R_n(t) \sim \sum_{k=0}^{\infty} b_k(\alpha(t)) n^{\alpha(t)-k} \quad (1.2.12)$$

for $n \rightarrow \infty$. The equation (1.2.8) can be split into two parts a sum from $n = 1$ to $n = n_a$ and $n = n_a$ to $n = \infty$ with $n_a \gg 1$.

Now $A(s, t)$ can be written as

$$A(s, t) = \sum_{n=n_a}^{\infty} \sum_{k=0}^{\infty} \frac{b_k(\alpha(t)) n^{\alpha(t)-k}}{n-\alpha(s)} + \text{an entire function in } s \text{ and } t \quad (1.2.13)$$

For $|\operatorname{Re} \alpha(s)| < n_a$ eqn. (1.2.13) can be written as,

$$A(s, t) = \sum_{n=n_a}^{\infty} \sum_{k=0}^{\infty} \sum_{r=0}^{\infty} b_r(\alpha(t)) (\alpha(s))^r n^{\alpha(t)-k-r-1} + F(s, t) \quad (1.2.14)$$

where $F(s, t)$ is an entire function in s and t . Using the fact that

$$\sum n^{-z} = \frac{1}{z-1} + \text{Entire function in } z$$

and interchanging summations in eqn. (1.2.14) we get,

$$\begin{aligned} \sum_{r=0}^{\infty} \sum_{k=0}^{\infty} b_k(r+k) (\alpha(s))^r \frac{1}{r+k-\alpha(t)} \\ = \sum_{n=0}^{\infty} \frac{1}{n-\alpha(t)} \left(\sum_{k=0}^n b_k(n) (\alpha(s))^{n-k} \right) \end{aligned} \quad (1.2.15)$$

Now it is easy to see that the asymptotic expansion of $R_n(t)$ has generated the t -channel poles in a domain where s is such that the sum converges.

This fact can be seen from the dispersion theoretic point of view also. Consider the fixed t dispersion integral for $A(s, t)$ as written in eqn. (1.2.1). The t -channel poles which

are contained in $A(\nu, t)$ are generated by the divergence of the integral over the s -channel singularities. When we consider such an approach or the case mentioned above we are talking about s - t duality. But FESR tells us that the information about $\text{Im } A(\nu, t)$ for $\nu < N$ is enough to give us the knowledge about t -channel singularities through the crossed channel Regge parameters. Therefore instead of considering duality between s and t channel we talk of duality between Regge and resonance.

Under this assumption, the prescription of writing the amplitude as sum of the Regge part and the direct channel resonance part in the intermediate energy region involves double counting. This is because when one uses FESR the average of the resonances already gives Regge behavior. Therefore it is not at all necessary to include resonances separately.

Though the connection between the Regge poles and the direct channel resonances and their dynamical contents is understood fairly well in the frame work of FESR duality, the nature of the Pomeranchukon trajectory is not understood in a similar manner. The Pomeranchukon trajectory contributes in all elastic scattering processes and is primarily responsible for the diffraction phenomena in high energy processes. At the same time no known resonance seems to lie on the Pomeranchukon trajectory and the slope of the trajectory is rather small. In order to treat the Pomeranchukon on the same footing as the other Regge trajectories Freund and Harari^{19,20} conjectured that

Pomeranchukon is dual to the mysterious background in the direct channel. In other words the background in the direct channel builds up the Pomeranchuk trajectory in the crossed channel.

1.3 Construction of Dual Amplitudes:

We have mentioned earlier that in addition to analyticity, crossing and unitarity, if the scattering amplitude satisfies the principle of duality it might be possible to accomplish a scheme so that the spectrum of elementary particles and their coupling constants are determined uniquely. It is a well known experimental fact that the resonances lie on linearly rising trajectories and, widths of these resonances are rather narrow. Therefore it is desirable to construct an amplitude which

- (a) has resonance poles in all required channels in the low energy region
- (b) is Regge behaved at asymptotic energies and
- (c) incorporates the principle of duality, in order to describe the strong interaction processes.

Veneziano²¹ constructed an amplitude for linearly rising Regge trajectories, in the narrow resonance approximation, which satisfies above mentioned properties. Veneziano's original model was applied to the process $\pi\pi \rightarrow \pi\omega$. This process is easy to study because there is only one trajectory, namely the ρ -trajectory, exchanged in all channels and there is only one invariant amplitude for the process.

The crossing symmetric Regge behaved amplitude for this process may be written as,

$$A(s, t, u) = \frac{\beta}{\pi} \left[\frac{\Gamma(1-\alpha(s)) \Gamma(1-\alpha(t))}{\Gamma(2-\alpha(s) - \alpha(t))} + \frac{\Gamma(1-\alpha(u)) \Gamma(1-\alpha(t))}{\Gamma(2-\alpha(u) - \alpha(t))} + \frac{\Gamma(1-\alpha(u)) \Gamma(1-\alpha(s))}{\Gamma(2-\alpha(u) - \alpha(s))} \right], \quad (1.3.1)$$

where $\alpha(s) = \alpha(0) + \alpha's$.

It is easy to see that the amplitude has a pole in a given channel whenever the trajectory has a positive integer value other than zero. It is also interesting to note that the residue of the pole, say at $\alpha(s) = n$, is a polynomial in the other invariant variable t , as required by the principle of duality.

In addition to the leading trajectory the amplitude has a large number of daughter trajectories. But some of these secondary poles can be eliminated by adding nonleading terms to the leading amplitude.

In the high energy limit we use Stirling's approximation to obtain the asymptotic Regge behavior of the scattering amplitude. Consider the limit $s \rightarrow (-\infty)$ and t fixed and small, then using Stirling's approximation for the gamma functions we get,

$$A(s, t) = \frac{\beta}{\Gamma(\alpha(t))} \left(\frac{1 - e^{-i\pi\alpha(t)}}{\sin \pi \alpha(t)} \right) (\alpha(s))^{\alpha(t)-1} \quad (1.3.2)$$

This expression has been obtained by retaining only the leading term of the asymptotic expansion of the gamma functions.

In spite of some of the nice features of the Veneziano amplitude it also has some draw-backs.

(i) The amplitude contains infinite number of daughter trajectories in addition to leading trajectories. Though in principle one can remove some of the secondary poles by adding satellite terms, however, in practice it is not possible to follow this procedure. Introduction of infinite number of secondary terms, to remove the daughters, calls for introduction of infinite number of parameters in the amplitude. This will make the whole program meaningless.

(ii) The amplitude as given by eqn. (1.3.1) is real and contains poles only along the real axis. Therefore the amplitude does not satisfy the requirements of unitarity. Strictly speaking the amplitude is not defined on the real axis due to the presence of poles. Therefore the Stirling's formula is valid in a region off the real axis. But on the contrary the addition of an $s(t)$ dependent imaginary part to $\alpha(s)$ ($\alpha(t)$), above the threshold introduces ancestors in addition to daughters.

The Veneziano model has been an useful tool for the study of strong interaction processes in spite of the short comings that we have mentioned above. Lovelace²² has demonstrated the use of Veneziano model in $\pi\pi$ scattering without using any secondary terms. This investigation reproduced a

large number of results of soft pion current algebra, like relation between the masses of ρ and ϵ meson and their widths. This model also has been successfully applied to the decay processes like $\bar{p}n \rightarrow \pi^+\pi^-\pi^-$ and $K^{\pm} \rightarrow 3\pi$ and $K^0 \rightarrow 3\pi$. In particular the invariant mass distribution of pions and the Dalitz plot for the process $\bar{p}n \rightarrow \pi^+\pi^-\pi^-$ were in very good agreement with the experimental results. The Veneziano model²³ was also applied to $\pi\pi$, πK , KK and $K\bar{K}$ scattering by Kawarabayashi, Kitakado and Yabuki. Some of their results are in fairly good agreement with the predictions of current algebra. Lovelace has abstracted from these studies that the Veneziano formula without any secondary terms is equivalent to chiral symmetry for soft mesons without exotic resonances.

Apart from the various applications mentioned earlier the Veneziano model has been generalized to production processes. Bardakçi and Ruegg²⁴ and Virasoro²⁵ have constructed amplitudes for the five point functions. The advantage of this formulation is that it contains low energy resonances in the appropriate channels and exhibits multi-Regge behavior in the required asymptotic values of kinematic variables. The generalization of the Veneziano amplitude to N-point functions was immediately done by Chan Hong Mo²⁶ and Goebel and Sakita²⁷ after Bardakçi and Ruegg gave their formula for the five point functions. A different approach to study the multi-Veneziano amplitude was given by Koba and Nielsen²⁸. In generalising the Veneziano amplitude these authors use the technique of projective

transformation. The elegant method of representing N-point function in a harmonic oscillator basis was introduced by Susskind.²⁹ Fubini and Veneziano³⁰ used the operator formalism to study the factorization properties of the N-point amplitude. This method has led to extensive study of the various properties of dual amplitudes.

In addition to the phenomenological applications to production processes the multi-Veneziano amplitude has been used to carry out the unitarization program of the Veneziano model. We have mentioned earlier that the four point amplitude does not satisfy unitarity condition. Therefore it has been proposed that the four point function can be considered as the Born term of the scattering amplitude and various higher order terms may be considered as the corrections which will ultimately build up the unitarity in the amplitude.³² Feynman rules have been developed to compute the loop contributions. However this unitarization procedure has faced several difficulties. There are divergence difficulties associated with the calculations of dual loops. In addition to the type of divergences present in quantum electrodynamics there are divergences due to exponentially increasing density of states. Therefore there have been efforts to carry out a renormalization procedure for dual models in order to remove these divergences. The divergences of the first kind like those of quantum electrodynamics are removable whereas the divergences of the second kind due to

infinite density of particles are not removable. This program is not yet complete.³³

It is well known from the experimental results that the widths of the observed resonances are rather narrow and the resonances lie on linearly rising Regge trajectories. The Veneziano model incorporates these features in a natural fashion. Therefore, it is reasonable to assume that the Veneziano model describes the strong interaction process to a good approximation. The narrowness of the resonances suggests that the corrections to Regge trajectories are rather small. In all our calculations we have introduced a small imaginary part to the trajectory function in obtaining the behavior of the scattering amplitude at large energies. This enables us to study the meson-baryon scattering processes in the medium high energy region. In the fourth chapter we study the possibility of imposing further constraints on the Veneziano residue functions. It is assumed, in deriving these constraint equations, that the Veneziano amplitude satisfies the requirements of unitarity in the narrow resonance approximation and the corrections due to the dual loops are, presumably, small. The connection of the Pomeron trajectory with the non-planar dual loops will be discussed in the fourth chapter.

CHAPTER II

In this chapter we study pion-nucleon charge-exchange process and η -production in pion nucleon scattering. These processes are relatively simple to study since a single Regge trajectory is exchanged (ρ -trajectory in case of $\pi^-p \rightarrow \pi^0n$ and A_2 in case of $\pi^-p \rightarrow \eta n$) in the t-channel. Moreover, the Pomeranchukon trajectory cannot be exchanged in these processes. Therefore, the difficulty associated with the inclusion of Pomeranchukon trajectory in the four point Veneziano model can be avoided. The Veneziano amplitude contains resonance poles and it can reproduce the asymptotic Regge behavior at high energies. Therefore, we feel that this model can be useful to describe the scattering phenomena in the intermediate and moderately high energies.

It is a well known experimental fact that there exists nonzero polarization in the processes like $\pi^-p \rightarrow \pi^0n$ and $\pi^-p \rightarrow \eta n$, at energies like 5.9 GeV and 11.2 GeV. A single Regge pole exchange model gives a good description to the differential cross-section at these energies. However, the single Regge pole exchange model will introduce identical phase in the spin-flip and spin-nonflip amplitude predicting a vanishing polarization at these energies, which is quite contrary to the experimental evidence. The polarization phenomena calls for a modification of a single

Regge pole exchange model where the scattering amplitude contains a background term in addition to the Regge term.

Several models have been proposed to explain both the polarization, and the differential cross-section for the charge-exchange process. All of them involve, as mentioned above, adding a background term to the ρ trajectory (in the case of πN charge-exchange process) contribution and justifying such an addition. The addition of a secondary trajectory³⁴ ρ' with the same quantum number as that of ρ trajectory, but with a different intercept, can introduce the required phase difference between the spin flip and spin-nonflip amplitude without changing the cross-section significantly. An alternative model³⁵ requires a Regge cut - which presumably is connected with the Gribov-Pomeranchuk phenomena - to provide the necessary background. A fairly successful model was to treat the polarization as arising from the interference³⁶ between the Regge-trajectory contribution and the direct channel resonances, occurring on indefinitely rising baryon trajectories. It may be recalled that in this model the significant contributions were derived in the neighbourhood of resonance energy value, and that the Breit-Wigner tails of the resonances were not important. However, it has been pointed out earlier that the interference model involves double counting and hence it contradicts the hypothesis of duality.

The Veneziano representation of the scattering amplitude explicitly contains both the resonance poles corresponding to a

rising trajectory and the Regge asymptotic behavior at high energies. Naturally we should expect that it automatically contains the necessary interference terms to give the appropriate polarization³⁷. In this chapter first we study πN charge-exchange process and then η -production in πN scattering.

2.2 Pion Nucleon Scattering in the Veneziano Model:

There has been several attempts³⁸⁻⁴⁶ to construct Veneziano like amplitude for pion nucleon scattering processes. The residue functions of the Veneziano amplitude are required to be constants, independent of s , t and u , in order to preserve crossing symmetry and reproduce high energy behavior in all channels. One of the perennial problems of the Veneziano model baryon scattering is that the baryons occur in parity doublets due to the McDowell⁴⁷ symmetry. Moreover, as we shall see later, the Veneziano amplitude cannot be determined uniquely. Some of the wrong parity baryon poles can be eliminated by adding satellite terms to the leading Veneziano amplitudes thereby imposing certain constraints among the residue functions. The remaining residue functions can be determined either (i) by using information about low energy scattering data³⁹⁻⁴¹ or (ii) by fitting the high energy data. However, in the ideal world a single residue function should be able to describe the scattering process at all energies.

2.2.1 Kinematics and Notations:

The kinematics of the meson baryon scattering is as follows:

$$\begin{aligned} s &= -(p_1 + q_1)^2 = -(p_2 + q_2)^2 \\ t &= -(q_1 - q_2)^2 = -(p_2 - p_1)^2 \\ u &= -(q_1 - p_2)^2 = -(p_1 - q_2)^2 \end{aligned} \quad (2.2.1)$$

and

$$s + t + u = \sum_{i=1}^4 m_i^2 \quad (2.2.2)$$

where $q_1(p_1)$ and $q_2(p_2)$ refer to four-momenta of the incoming and outgoing meson (baryon) respectively. As shown in Fig. 1, s and u are meson-baryon channels and t is a meson-meson channel.

The T-matrix is defined by

$$S = 1 + i(2\pi)^4 \delta(P_f - P_i) T \quad (2.2.3)$$

$$\text{where } P_f = q_2 + p_2 \quad \text{and} \quad P_i = p_1 + q_1 \quad (2.2.4)$$

We write the T-matrix for the reaction $0^- + \frac{1}{2}^+ \rightarrow 0^- + \frac{1}{2}^+$ in terms of the invariant amplitudes A and B:

$$T = A + \frac{i \gamma \cdot (q_1 + q_2)}{2} B \quad (2.2.5)$$

The helicity nonflip and helicity flip amplitudes in the t-channel can be written as,

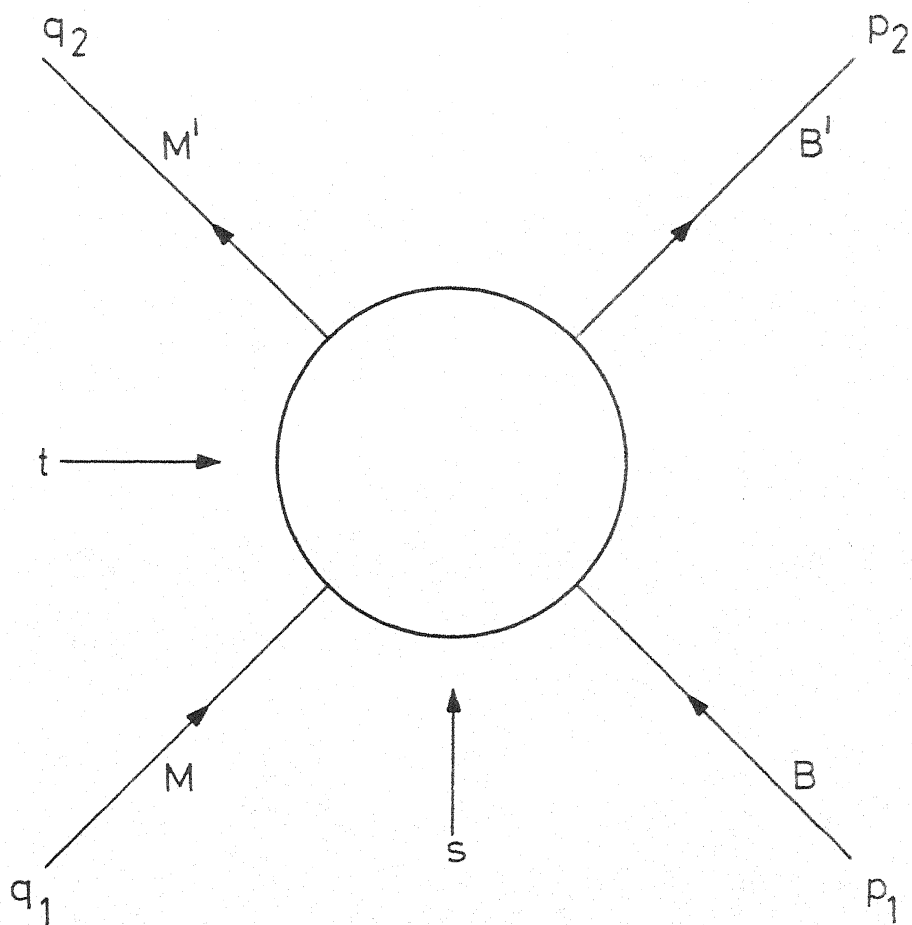


Fig. 1

$$F_{++}^t = - \left\{ - A(t - 4\bar{M}^2)^{1/2} + \frac{B\bar{M}}{(t-4\bar{M}^2)^{1/2}} \right. \\ \left. \left[2s+t - \sum m_i^2 + \frac{(m_1-m_2)(m_3^2-m_4^2)}{2\bar{M}} \right] \right\} \quad (2.2.6)$$

and

$$F_{+-}^t = - \left[\frac{\Phi^{1/2} B}{(t-4\bar{M}^2)^{1/2}} \right] \quad (2.2.7)$$

where $m_1(m_3)$ and $m_2(m_4)$ are masses of incoming and outgoing baryons (mesons) respectively.

$$\bar{M} = \frac{1}{2} (m_1 + m_2) \quad (2.2.8)$$

$$\Phi = st (\sum m_i^2 - s - t) - t(m_3^2 - m_1^2)(m_4^2 - m_2^2) \\ - s(m_1^2 - m_2^2)(m_3^2 - m_4^2) - (m_1^2 m_2^2 - m_3^2 m_4^2) \\ \times (m_3^2 + m_2^2 - m_4^2 - m_1^2) \quad (2.2.9)$$

We define,

$$G_{++} = - (t - 4\bar{M}^2)^{1/2} F_{++}^t \quad (2.2.10)$$

$$G_{+-} = + B$$

Then,

$$\frac{d\sigma}{dt} = \frac{1}{64\pi s p_1^2 (4\bar{M}^2 - t)} \left[|G_{++}|^2 + |\Phi^{1/2} G_{+-}|^2 \right] \quad (2.2.)$$

and

$$P \frac{d\sigma}{dt} = \frac{(1-z^2)^{1/2}}{16\pi\sqrt{s}} \frac{p_2}{p_1} \frac{1}{(4\bar{M}^2 - t)^{1/2}} \text{Im} (G_{++}^* G_{+-}) \quad (2.2)$$

p_1 and p_2 being the centre of mass momenta of the initial and final particles. P is the polarization.

The Veneziano representation for the invariant amplitude can be written in the following manner:

$$\begin{aligned}
 A^I(s,t,u) = & \sum_{m=1, n=1, p=1, B, M}^{\infty} \left[C^I(m, n, p, B, M) \right. \\
 & \frac{\Gamma(m - \alpha_M(t)) \Gamma(n - \frac{1}{2} - \alpha_B(s))}{\Gamma(p - \frac{1}{2} - \alpha_M(t) - \alpha_B(s))} \\
 & \left. + D^I(m, n, p, B, M)(s \rightarrow u) \right] + \sum_{m'=1, n'=1, p'=1, B, B'}^{\infty} \\
 & E^I(m', n', p', B, B') \frac{\Gamma(m' - \frac{1}{2} - \alpha_B(s)) \Gamma(n' - \frac{1}{2} - \alpha_B(u))}{\Gamma(p' - \alpha_B(s) - \alpha_B(u))} \\
 & (2.2.13)
 \end{aligned}$$

Similarly,

$$\begin{aligned}
 B^I(s,t,u) = & \sum_{m=1, n=1, p=1, B, M}^{\infty} \left[\frac{\Gamma(m - \alpha_M(t)) \Gamma(n - \frac{1}{2} - \alpha_B(s))}{\Gamma(p - \frac{1}{2} - \alpha_M(t) - \alpha_B(s))} \right. \\
 & \left. F^I(m, n, p, B, M) + G^I(m, n, p, B, M)(s \rightarrow u) \right] \\
 & + \sum_{m'=1, n'=1, p'=1, B', B}^{\infty} H^I(m', n', p', B, B') \\
 & \frac{\Gamma(m' - \frac{1}{2} - \alpha_B(s)) \Gamma(n' - \frac{1}{2} - \alpha_B(u))}{\Gamma(p' - \alpha_B(s) - \alpha_B(u))} \\
 & (2.2.14)
 \end{aligned}$$

Here I denotes the appropriate isospin index of the invariant amplitudes, α_M and α_B represent the meson and baryon trajectories respectively, and B, B', M and M' are various baryon and meson states which are summed over. The coefficients C, D etc. are constants independent of s, t and u as required in the Veneziano model. Further constraints on the coefficients C, D, E etc. are imposed by requiring the amplitude to satisfy the following conditions.

- (i) Crossing properties
- (ii) Absence of exotic states in a given amplitude, e.g. mesons with quantum numbers $B = 0, I = 2$ and baryons with quantum numbers $B = 1, S = 1$.
- (iii) Absence of wrong isospin poles from a given amplitude which corresponds to a definite isospin in a particular channel. For instance, absence of $\Delta_\delta (N_\alpha, N_\gamma)$ pole in $I = \frac{1}{2}$ ($I = \frac{3}{2}$) s or u -channel amplitude.
- (iv) Appropriate signature factor for a given amplitude.
- (v) Appropriate Regge behavior in different channels,

$$\begin{aligned}
 A(s, t) & \underset{s \rightarrow \text{large}}{\sim} s^{\alpha_M(t)} && \text{for fixed } t \\
 & \underset{s \rightarrow \text{large}}{\sim} s^{\alpha_B(u) - \frac{1}{2}} && \text{for fixed } u
 \end{aligned} \tag{2.2.15}$$

$$\begin{aligned}
 B(s, t) & \underset{s \rightarrow \text{large}}{\sim} s^{\alpha_M(t) - 1} && \text{for fixed } t \\
 & \underset{s \rightarrow \text{large}}{\sim} s^{\alpha_B(u) - \frac{1}{2}} && \text{for fixed } u
 \end{aligned} \tag{2.2.16}$$

Eqns. (2.2.13) and (2.2.14) contain infinite number of parameters. Therefore use of such an amplitude to describe the scattering processes is useless. So, we have to truncate the series. We keep only leading terms of the series following Igi's prescription. Fenster and Wali, in their model, have added some non-leading terms to the Veneziano amplitude in order to remove some of the low lying wrong parity baryon poles. First we study the charge exchange scattering process in Igi's model and then in the model proposed by Fenster and Wali.

2.2.2 Igi's Model:

The invariant amplitudes³⁸ are constructed by imposing the constraints mentioned in Sec. 2.2.1. In the t-channel ρ and f trajectories are exchanged whereas N_α , Δ_δ and N_γ trajectories are exchanged in the s and u - channels. We identify amplitudes with t-channel isospin $I_t = 0(1)$ by means of subscript of $f(\rho)$.

$$\begin{aligned}
 A_f(s,t,u) = & \frac{\beta_{f,N_\alpha}}{\pi} \left[C(1-\alpha_f(t), \frac{3}{2} - \alpha_{N_\alpha}(s)) \right. \\
 & \left. + C(1-\alpha_f(t), \frac{3}{2} - \alpha_{N_\alpha}(u)) + C(\frac{3}{2} - \alpha_{N_\alpha}(s), \frac{3}{2} - \alpha_{N_\alpha}(u)) \right] \\
 & + \frac{\beta_{f,\Delta_\delta}}{\pi} \left[C(1-\alpha_f(t), \frac{3}{2} - \alpha_{\Delta_\delta}(s)) \right. \\
 & \left. + C(1-\alpha_f(t), \frac{3}{2} - \alpha_{\Delta_\delta}(u)) + C(\frac{3}{2} - \alpha_{\Delta_\delta}(s), \frac{3}{2} - \alpha_{\Delta_\delta}(u)) \right] \\
 & + \frac{\beta_{f,N_\gamma}}{\pi} \left[C(1-\alpha_f(t), \frac{3}{2} - \alpha_{N_\gamma}(s)) + C(1-\alpha_f(t), \right. \\
 & \left. \frac{3}{2} - \alpha_{N_\gamma}(u)) + C(\frac{3}{2} - \alpha_{N_\gamma}(s), \frac{3}{2} - \alpha_{N_\gamma}(u)) \right] \quad (2.2.17)
 \end{aligned}$$

$$\begin{aligned}
B_f(s, t, u) = \frac{\beta_f}{\pi} \Big\{ & B(1-\alpha_f(t), \frac{1}{2} - \alpha_{N_\alpha}(s)) - B(1-\alpha_f(t), \frac{1}{2} - \alpha_{N_\alpha}(u)) \\
& + p \left[B(1-\alpha_f(t), \frac{1}{2} - \alpha_{\Delta_\delta}(s)) - B(1-\alpha_f(t), \frac{1}{2} - \alpha_{\Delta_\delta}(u)) \right] \\
& + q \left[B(1-\alpha_f(t), \frac{1}{2} - \alpha_{N_\gamma}(s)) - B(1-\alpha_f(t), \frac{1}{2} - \alpha_{N_\gamma}(u)) \right] \\
& + p \left[B(\frac{1}{2} - \alpha_{N_\alpha}(s), \frac{1}{2} - \alpha_{\Delta_\delta}(u)) - B(\frac{1}{2} - \alpha_{\Delta_\delta}(s), \frac{1}{2} - \alpha_{N_\alpha}(u)) \right] \\
& + q \left[B(\frac{1}{2} - \alpha_{N_\alpha}(s), \frac{1}{2} - \alpha_{N_\gamma}(u)) - B(\frac{1}{2} - \alpha_{N_\alpha}(u), \frac{1}{2} - \alpha_{N_\gamma}(s)) \right] \Big\} \\
& (2.2.18)
\end{aligned}$$

with $p+q = 1$

$$\begin{aligned}
A_p(s, t, u) = \frac{\beta}{\pi} \Big\{ & C(1-\alpha_p(t), \frac{3}{2} - \alpha_{N_\alpha}(s)) - C(1-\alpha_p(t), \frac{3}{2} - \alpha_{N_\alpha}(u)) \\
& + p' \left[C(1-\alpha_p(t), \frac{3}{2} - \alpha_{\Delta_\delta}(s)) - C(1-\alpha_p(t), \frac{3}{2} - \alpha_{\Delta_\delta}(u)) \right] \\
& + q' \left[C(1-\alpha_p(t), \frac{3}{2} - \alpha_{N_\gamma}(s)) - C(1-\alpha_p(t), \frac{3}{2} - \alpha_{N_\gamma}(u)) \right] \\
& + p' \left[C(\frac{3}{2} - \alpha_{N_\alpha}(s), \frac{3}{2} - \alpha_{\Delta_\delta}(u)) - C(\frac{3}{2} - \alpha_{\Delta_\delta}(s), \frac{3}{2} - \alpha_{N_\alpha}(u)) \right] \\
& + q' \left[C(\frac{3}{2} - \alpha_{N_\alpha}(s), \frac{3}{2} - \alpha_{N_\gamma}(u)) - C(\frac{3}{2} - \alpha_{N_\alpha}(u), \frac{3}{2} - \alpha_{N_\gamma}(s)) \right] \Big\} \\
& (2.2.19)
\end{aligned}$$

with $p' + q' = 1$.

$$\begin{aligned}
B_{\rho}(s,t,u) = & \frac{\beta_{\rho,N_{\alpha}}}{\pi} \left[B(1-\alpha_{\rho}(t), \frac{1}{2} - \alpha_{N_{\alpha}}(s)) \right. \\
& + B(1-\alpha_{\rho}(t), \frac{1}{2} - \alpha_{N_{\alpha}}(u)) + B(\frac{1}{2} - \alpha_{N_{\alpha}}(s), \frac{1}{2} - \alpha_{N_{\alpha}}(u)) \Big] \\
& + \frac{\beta_{\rho,\Delta_{\delta}}}{\pi} \left[B(1-\alpha_{\rho}(t), \frac{1}{2} - \alpha_{\Delta_{\delta}}(s)) + B(1-\alpha_{\rho}(t), \right. \\
& \left. \frac{1}{2} - \alpha_{\Delta_{\delta}}(u)) + B(\frac{1}{2} - \alpha_{\Delta_{\delta}}(s), \frac{1}{2} - \alpha_{\Delta_{\delta}}(u)) \Big] \\
& + \frac{\beta_{\rho,N_{\gamma}}}{\pi} \left[B(1-\alpha_{\rho}(t), \frac{1}{2} - \alpha_{N_{\gamma}}(s)) + B(1-\alpha_{\rho}(t), \right. \\
& \left. \frac{1}{2} - \alpha_{N_{\gamma}}(u)) + B(\frac{1}{2} - \alpha_{N_{\gamma}}(s), \frac{1}{2} - \alpha_{N_{\gamma}}(u)) \right] \quad (2.2.20)
\end{aligned}$$

$$\text{and} \quad B(X,Y) = \frac{\Gamma(X) \Gamma(Y)}{\Gamma(X+Y)}, \quad C(X,Y) = \frac{\Gamma(X) \Gamma(Y)}{\Gamma(X+Y-1)} \quad (2.2.21)$$

The invariant amplitudes at this stage satisfy crossing symmetry explicitly. It may be noticed that each of these amplitudes has the right (t, s) and (t, u) terms to give the appropriate Regge behavior together with the right signature factors. Thus as $s \rightarrow \infty$:

$$A_{\rho,f} \sim s^{\alpha_{\rho,f}(t)} (1 + e^{-i\pi\alpha_{\rho,f}(t)}) \quad (2.2.22)$$

$$B_{\rho,f} \sim s^{\alpha_{\rho,f}(t)-1} (1 + e^{-i\pi\alpha_{\rho,f}(t)}) \quad (2.2.23)$$

We have implicitly assumed that as $s \rightarrow \infty$, $\tan \pi\alpha(s) \rightarrow i$, which is easily incorporated in evaluating our gamma functions through Stirling's approximation. By this trick we have introduced a phase to the apparently real scattering amplitude. It is worthwhile to remark here that the nonleading terms in the above amplitude will carry the requisite phase difference between the spin flip and the non-spin flip amplitudes; together with this

we have real background terms coming from (s, u) terms of the amplitudes. All these will produce a nonzero polarization.

We may impose now the constraints due to isospin crossing. From the t-channel amplitudes A_f and A_ρ we can obtain amplitudes with s or u channel isospin $I_{s,u} = \frac{1}{2}$ or $\frac{3}{2}$ through crossing. They are for example

$$A_{1/2}^S(s, t, u) = -(A_f + 2A_\rho) \quad , \quad (2.2.24)$$

$$A_{3/2}^S(s, t, u) = A_f - A_\rho \quad (2.2.25)$$

We must ensure that, say, in the $I_s = 1/2$ amplitude there will be no pole term corresponding to the $I = 3/2, \Delta_\delta$ trajectory and that there will be poles corresponding to N_α and N_γ trajectories only.

The absence of pole terms corresponding to the Δ_δ trajectory in eqn. (2.2.24) requires,

$$\alpha_f(t) = \alpha_\rho(t), \quad \beta_{f, \Delta_\delta} = -2p' \beta_\rho, \quad \alpha_{N_\alpha}(s) = \alpha_{\Delta_\delta}(s).$$

Similar conditions can be obtained from the other invariant amplitude B and the $I_s = 3/2$ amplitudes. We may collect all the conditions implied by isospin constraints as follows.

$$\alpha_f(t) = \alpha_\rho(t) \quad , \quad (2.2.26)$$

$$\alpha_{N_\alpha}(s) = \alpha_{\Delta_\delta}(s) = \alpha_{N_\gamma}(s) \quad , \quad (2.2.27)$$

$$B_{f, \Delta_\delta} = -2p' \beta_\rho, \quad B_{\rho, \Delta_\delta} = -\frac{1}{2} p \beta_f \quad ,$$

$$\beta_{f, N_\alpha} = \beta_\rho, \quad \beta_{\rho, N_\alpha} = \beta_f \quad ,$$

$$\beta_{f, N_\gamma} = (1-p') \beta_\rho, \quad \beta_{\rho, N_\gamma} = (1-p) \beta_f \quad . \quad (2.2.28)$$

Eqn. (2.2.26) is the familiar exchange degeneracy conditions for mesons and the Chew-Frautschi plot for mesons seems to support it. The eqn. (2.2.28) is the set of conditions used by Igi. The degeneracy implied by eqn. (2.2.27) is a consequence of isospin crossing relation. It is, however, true that the baryon trajectories do not appear exchange degenerate and this condition is only approximately satisfied. However, even when the trajectories are not degenerate, the fact that their slopes are equal together with eqns. (2.2.26) and (2.2.28) would imply the absence of unwanted poles, from the leading trajectory. It is the daughters that will cause trouble and will have their poles appearing simultaneously in $I = 1/2$ as well as the $I = 3/2$ amplitudes. We have chosen two alternatives. First, we have kept the eqns. (2.2.26) - (2.2.28) intact and have assumed an average trajectory for baryons. We then hope, at least, to derive some qualitative features implied by Igi's model. Next we have considered a more realistic set of baryon trajectories (however, with the same slope), ignoring the presence of unwanted poles in the baryon channels at the daughter level. In both these alternatives we have assumed, after Igi, a universal slope for the trajectories. Thus,

$$\text{slope} = \alpha' = .86 \text{ GeV}^{-2} \quad (2.2.29)$$

$$\alpha_p(0) = \alpha_f(0) = .5 \quad (2.2.30)$$

This leaves us with four parameters β_p , β_f , p and p' , in terms of which the amplitudes will be completely specified.

A more convenient set of amplitudes that were defined by Singh⁴⁸ is given by

$$A'(s, t) = A(s, t) + \left(\frac{\omega + t/4M_N^2}{1 - t/4M_N^2} \right) B(s, t) \quad , \quad (2.2.31)$$

where pion laboratory energy ω is given by

$$\omega = (s - M_N^2 - M_\pi^2)/2M_N \quad . \quad (2.2.32)$$

The charge-exchange (CEX) amplitude can be written in terms of the corresponding t -channel isospin amplitudes.

$$A'_{\text{CEX}} = -\sqrt{2} A'_\rho \quad , \quad (2.2.33)$$

$$B_{\text{CEX}} = -\sqrt{2} B_\rho \quad , \quad (2.2.34)$$

The imaginary parts of the A'_ρ and B_ρ in the forward direction are related to the difference between π^-p and π^+p total cross-section. Following Igi, we use them as inputs,

$$\text{Im } A'_\rho(s, t = 0) = 2.14 \text{ s}^{1/2} \text{ mb}$$

$$\text{Im } B_\rho(s, t = 0) = 43.7 \text{ s}^{-1/2} \text{ mb GeV} \quad .$$

These yield,

$$\beta_\rho = 20.16 \text{ mb GeV} \quad , \quad (2.2.35)$$

and

$$(2 - \frac{3}{2} p) \beta_f = \gamma_\rho = 71.80 \text{ mb} \quad (2.2.36)$$

Case I: When the baryon trajectories are degenerate, no further parameters need be determined. For baryon trajectories we use

$$\alpha_{\text{eff}}(0) = -0.256.$$

Case II(a): We need all the four parameters. The remaining parameters can be determined by using information on backward scattering data. The set of parameters as determined by Igi are,

$$\begin{aligned} \beta_p &= 20.16 \text{ mb GeV} & \beta_f &= 25.7 \text{ mb} & p &= -0.526 \\ p' &= .852 & \alpha_{N_\alpha}(0) &= -0.256 & \alpha_{\Delta_\delta}(0) &= 0.18 \\ \alpha_{N_\xi}(0) &= -0.55 & & & & \end{aligned} \quad (2.2.37)$$

Case II(b): An alternative procedure to determine the parameters p, p' and β_f is to use the information on the residues of the f -Regge pole parameters derived from finite energy sum rules FESR.⁴⁹ We use following results for this purpose:

$$\text{Im}A'_f(s, t=0) = 14.6 s^{1/2} \text{ mb} \quad , \quad (2.2.38)$$

$$\text{Im}B_f(s, t=0) = 54.1 s^{-1/2} \text{ mb GeV} \quad , \quad (2.2.39)$$

Using eqns. (2.2.38) and (2.2.39) together with eqn. (2.2.36), we get the parameters as,

$$\beta_f = 44.5 \text{ mb} \quad , \quad p = 0.226 \text{ and } p' = .22 \quad (2.2.40)$$

2.3 Fenster and Wali Model:

We have mentioned earlier since the baryon trajectories appear as linear functions of s rather than that of $W(=\sqrt{s})$, baryon parity doublets are unavoidable. However, by using more subsidiary Veneziano terms, it is possible to eliminate, first few baryon poles of wrong parity on each trajectory, by a judicious choice of the coefficients. Fenster and Wali⁴⁵

have used this idea to write the Veneziano amplitude for πN scattering.

$$\begin{aligned}
 \frac{1}{4\pi} B^{(-)} = & \beta_1^{(-)} B_N^{+}(\frac{1}{2}, 1) + \beta_2^{-} B_{\Delta}^{+}(\frac{1}{2}, 1) + \beta_3^{-} C_N^{+}(\frac{3}{2}, 2) \\
 & + \beta_4^{-} C_{\Delta}^{+}(\frac{3}{2}, 2) + \phi_1^{-} B_{N\Delta}^{+}(\frac{1}{2}, \frac{1}{2}) + \phi_2^{-} C_{N\Delta}^{+}(\frac{3}{2}, \frac{3}{2}) \\
 & + \phi_3^{-} B_N(\frac{1}{2}, \frac{1}{2}) + \phi_4^{-} C_N(\frac{3}{2}, \frac{3}{2}) + \phi_5^{-} B_{\Delta}(\frac{1}{2}, \frac{1}{2}) \\
 & + \phi_6^{-} C_{\Delta}(\frac{3}{2}, \frac{3}{2}) \quad (2.3.1)
 \end{aligned}$$

$$\begin{aligned}
 \frac{1}{4\pi} A^{(-)} = & \mu_1^{-} C_N^{-}(\frac{3}{2}, 1) + \mu_2^{-} C_{\Delta}^{-}(\frac{3}{2}, 1) + \mu_3^{-} C_N^{-}(\frac{3}{2}, 2) \\
 & + \mu_4^{-} C_{\Delta}^{-}(\frac{3}{2}, 2) + \mu_5^{-} B_{\Delta}^{-}(\frac{1}{2}, 1) + \lambda_1^{-} C_{N\Delta}^{-}(\frac{3}{2}, \frac{3}{2}) \\
 & + \lambda_2^{-} B_{\Delta}^{-}(\frac{1}{2}, \frac{3}{2}) + \lambda_3^{-} B_{N\Delta}^{-}(\frac{1}{2}, \frac{3}{2}) \quad (2.3.2)
 \end{aligned}$$

$$\begin{aligned}
 \frac{1}{4\pi} B^{(+)} = & \beta_1^{+} B_N^{-}(\frac{1}{2}, 1) + \beta_2^{+} B_{\Delta}^{-}(\frac{1}{2}, 1) + \beta_3^{+} C_N^{-}(\frac{3}{2}, 2) \\
 & + \beta_4^{+} C_{\Delta}^{-}(\frac{3}{2}, 2) + \beta_5^{+} B_N^{-}(\frac{1}{2}, 2) + \beta_6^{+} B_{\Delta}^{-}(\frac{1}{2}, 2) \\
 & + \phi_1^{+} B_{N\Delta}^{-}(\frac{1}{2}, \frac{1}{2}) + \phi_2^{+} C_{N\Delta}^{-}(\frac{3}{2}, \frac{3}{2}) + \phi_3^{+} B_{N\Delta}^{-}(\frac{1}{2}, \frac{3}{2}) \\
 & + \phi_4^{+} B_N^{-}(\frac{1}{2}, \frac{3}{2}) + \phi_5^{+} B_{\Delta N}^{-}(\frac{1}{2}, \frac{3}{2}) \quad (2.3.3)
 \end{aligned}$$

$$\begin{aligned}
 \frac{1}{4\pi} A^{(+)} = & \mu_1^{+} C_N^{+}(\frac{3}{2}, 1) + \mu_2^{+} C_{\Delta}^{+}(\frac{3}{2}, 1) + \mu_3^{+} C_N^{+}(\frac{3}{2}, 2) + \mu_4^{+} C_{\Delta}^{+}(\frac{3}{2}, 2) \\
 & + \mu_5^{+} B_{\Delta}^{+}(\frac{1}{2}, 1) + \lambda_1^{+} C_N^{+}(\frac{3}{2}, \frac{3}{2}) + \lambda_2^{+} C_{N\Delta}^{+}(\frac{3}{2}, \frac{3}{2}) + \lambda_3^{+} C_{\Delta}^{+}(\frac{3}{2}, \frac{3}{2}) \\
 & + \lambda_4^{+} B_{\Delta}^{+}(\frac{1}{2}, \frac{1}{2}) + \lambda_5^{+} B_{\Delta N}^{+}(\frac{1}{2}, \frac{3}{2}) \quad (2.3.4)
 \end{aligned}$$

Following the notations of Fenster and Wali we define the various B and C functions that occur in the amplitude as:

$$B_X^{\pm} \left(\frac{1}{2}m, n \right) = \frac{\Gamma\left(\frac{1}{2}m - \alpha_X(s)\right) \Gamma(n - \alpha(t))}{\Gamma\left(\frac{1}{2}m + n - \alpha_X(s) - \alpha(t)\right)} \\ \pm \frac{\Gamma\left(\frac{1}{2}m - \alpha_X(u)\right) \Gamma(n - \alpha(t))}{\Gamma\left(\frac{1}{2}m + n - \alpha_X(u) - \alpha(t)\right)} \quad (2.3.5)$$

$$B_{XY}^{\pm} \left(\frac{1}{2}m, \frac{1}{2}n \right) = \frac{\Gamma\left(\frac{1}{2}m - \alpha_X(s)\right) \Gamma\left(\frac{n}{2} - \alpha_Y(u)\right)}{\Gamma\left(\frac{m}{2} + \frac{n}{2} - \alpha_X(s) - \alpha_Y(u)\right)} \\ \pm \frac{\Gamma\left(\frac{1}{2}m - \alpha_X(u)\right) \Gamma\left(\frac{1}{2}n - \alpha_Y(s)\right)}{\Gamma\left(\frac{m}{2} + \frac{n}{2} - \alpha_X(u) - \alpha_Y(s)\right)} \quad (2.3.6)$$

$$B_X \left(\frac{1}{2}m, \frac{1}{2}n \right) = \frac{\Gamma\left(\frac{1}{2}m - \alpha_X(s)\right) \Gamma\left(\frac{1}{2}n - \alpha_X(u)\right)}{\Gamma(m - \alpha_X(u) - \alpha_X(s))} \quad (2.3.7)$$

Here X and Y denote the fermion trajectories N and Δ . In this model N_α and N_γ are taken to be degenerate. The C functions, where

$$C(X, Y) = \frac{\Gamma(X) \Gamma(Y)}{\Gamma(X+Y-1)}$$

are defined in a similar fashion. The t-channel trajectories are taken to be degenerate as in Igi's case.

The amplitude reproduces low energy data well upto 1.6 GeV. All parity doublets in this region are eliminated and the resonance parameters for Δ_6 (1236) and N_7 (1518) are reproduced. The various parameters that occur in the scattering amplitude are determined by using the normalization at $t = 0$ of the amplitudes and the shape, for very small negative t , of the differential cross-section for charge exchange scattering data.

The predictions for polarization in the model of Igi are shown in Figs. 2 and 3. The results predicted by using FESR information as input in Igi's model and the Fenster and Wali's model are shown in Figs. 4 and 5 respectively. The predictions for the differential cross-section are shown⁵⁰ in Figs. 6 and 7.

It is worth mentioning here that the Igi's model predicts polarization which is in qualitative agreement with the experimental results, in the small $-t < .3 \text{ GeV}^2$ region. Recent data⁵¹ for polarization at higher momentum transfer values has a tendency to rise as shown in the Figs. 8 and 9. The polarization changes sign beyond $-t \geq .6 \text{ GeV}^2$. All these features of the polarization data are qualitatively reproduced in Igi's model. However, the polarization, in calculation, shows violent oscillations near the value of t where $\alpha(t) \rightarrow 0$. The model shows that polarization goes to zero as $\alpha(t) \rightarrow 0$ and has a Lorentzian form in this neighborhood. It is not clear whether experimental data will support such detailed features. However, the available information is not inconsistent with such behavior. Thus we may

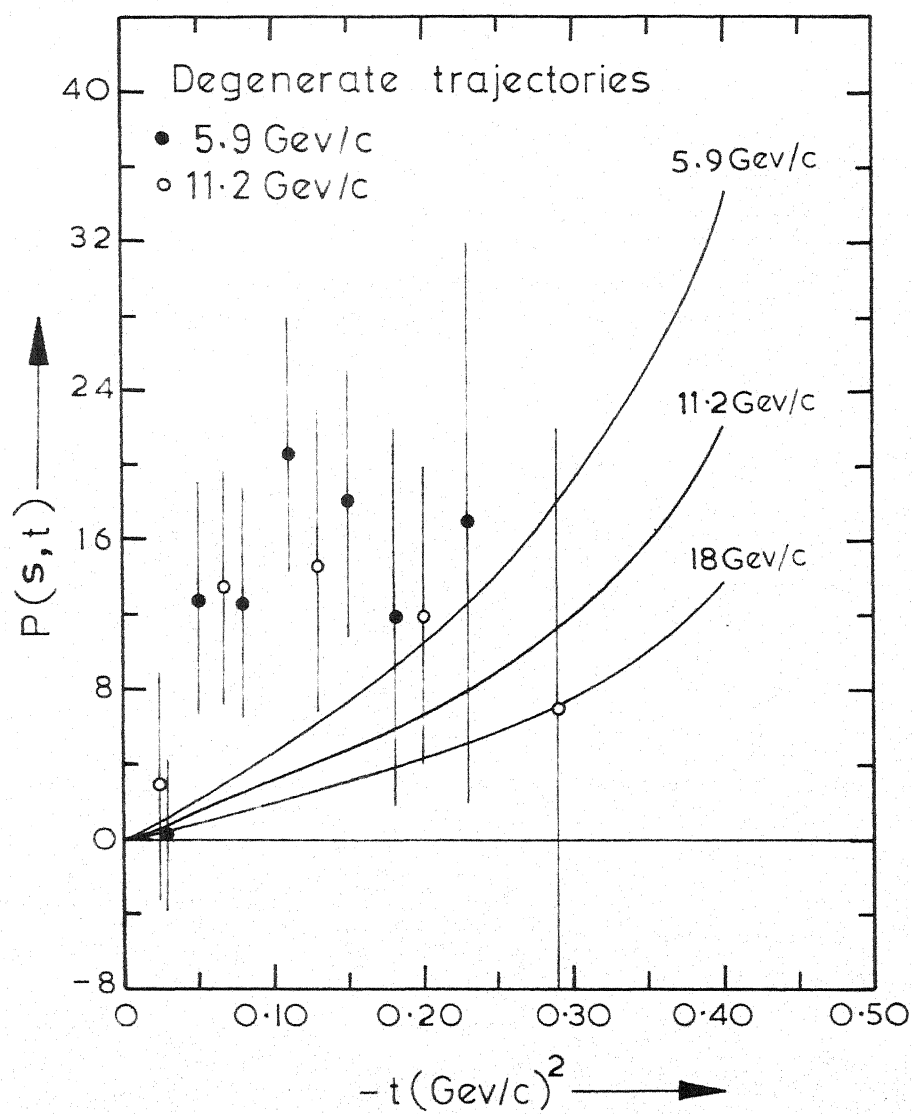


Fig. 2

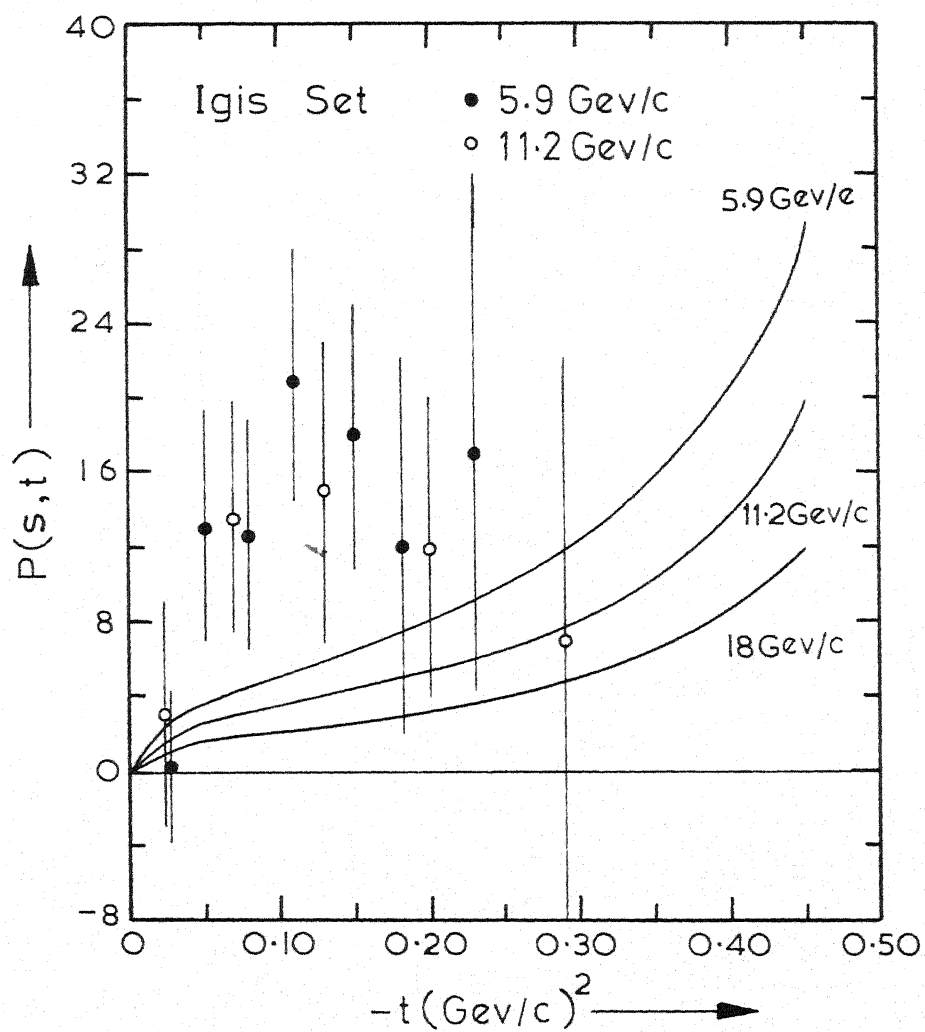


Fig. 3

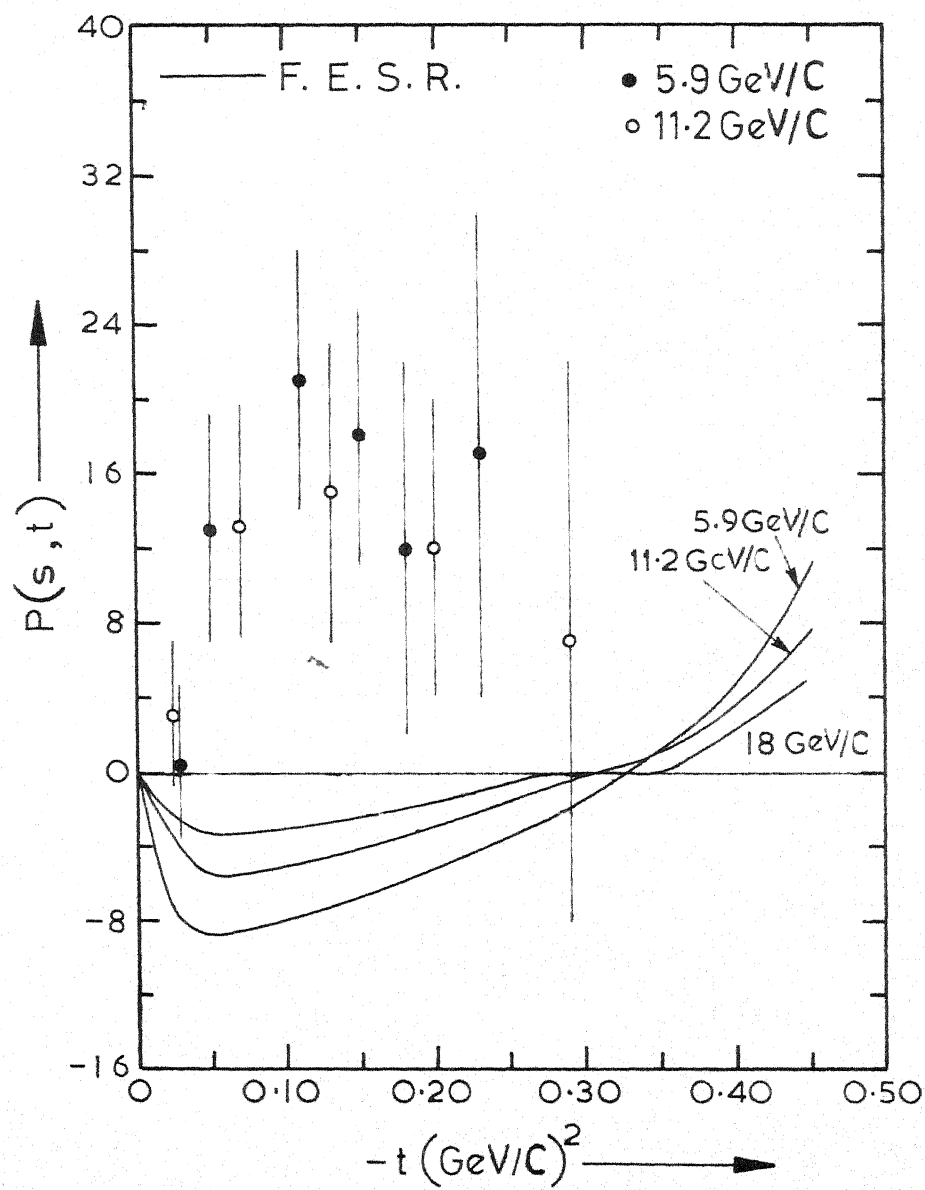


Fig. 4

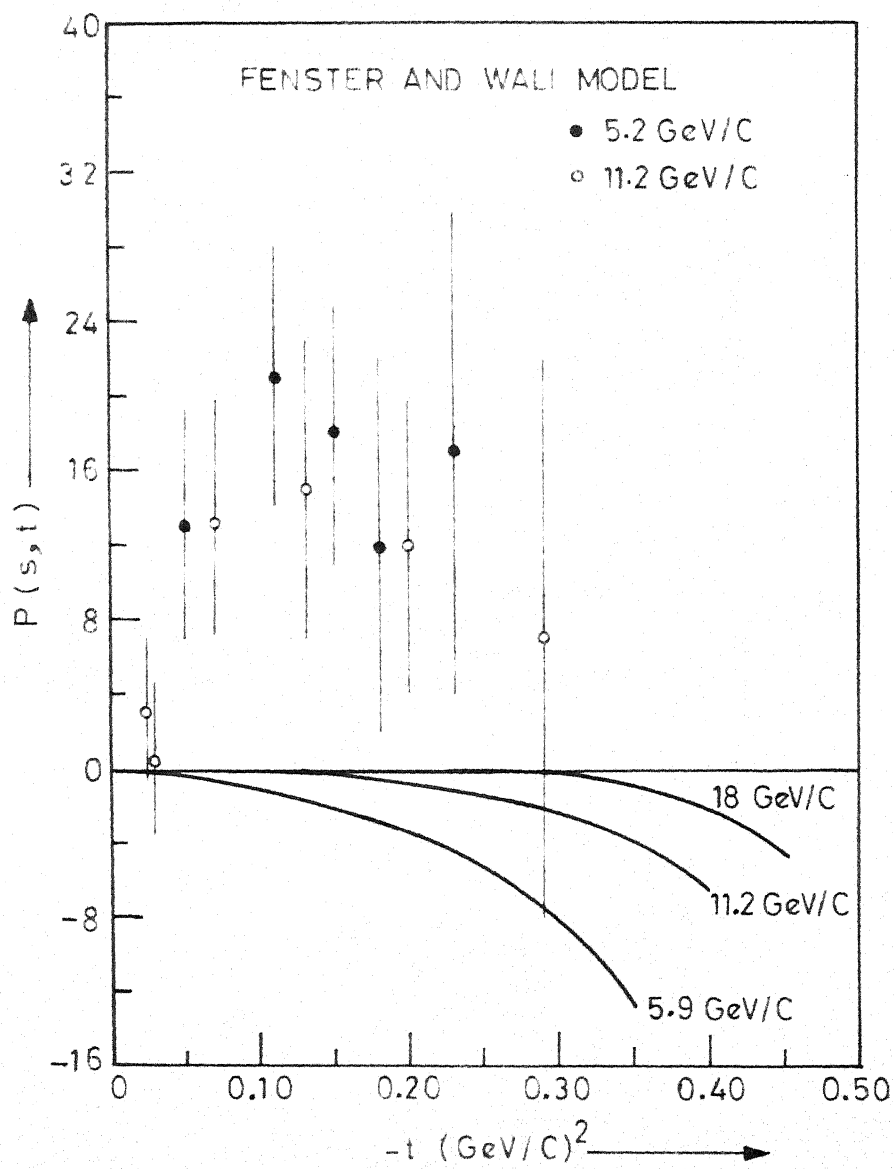


Fig. 5

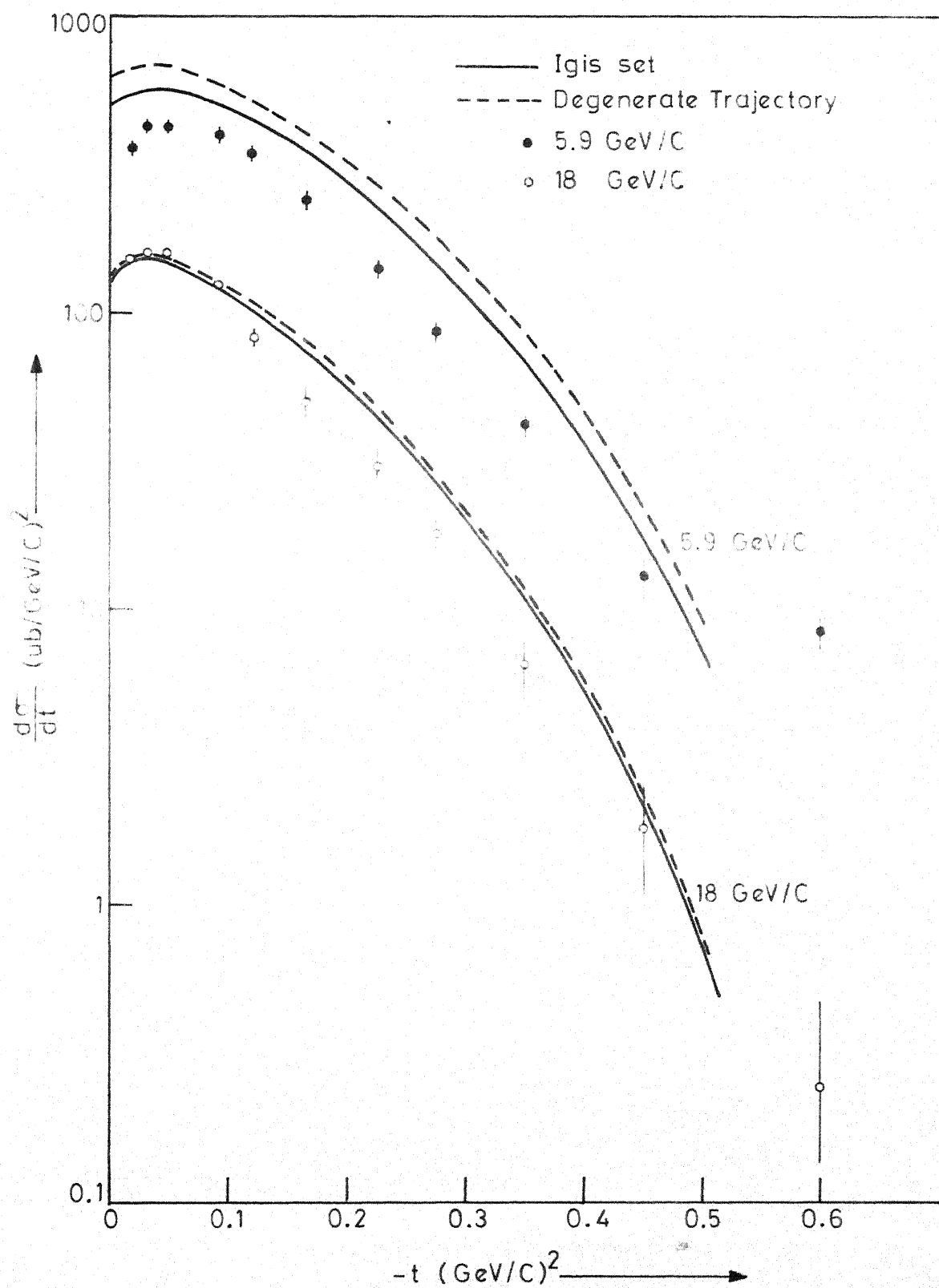


Fig. 6

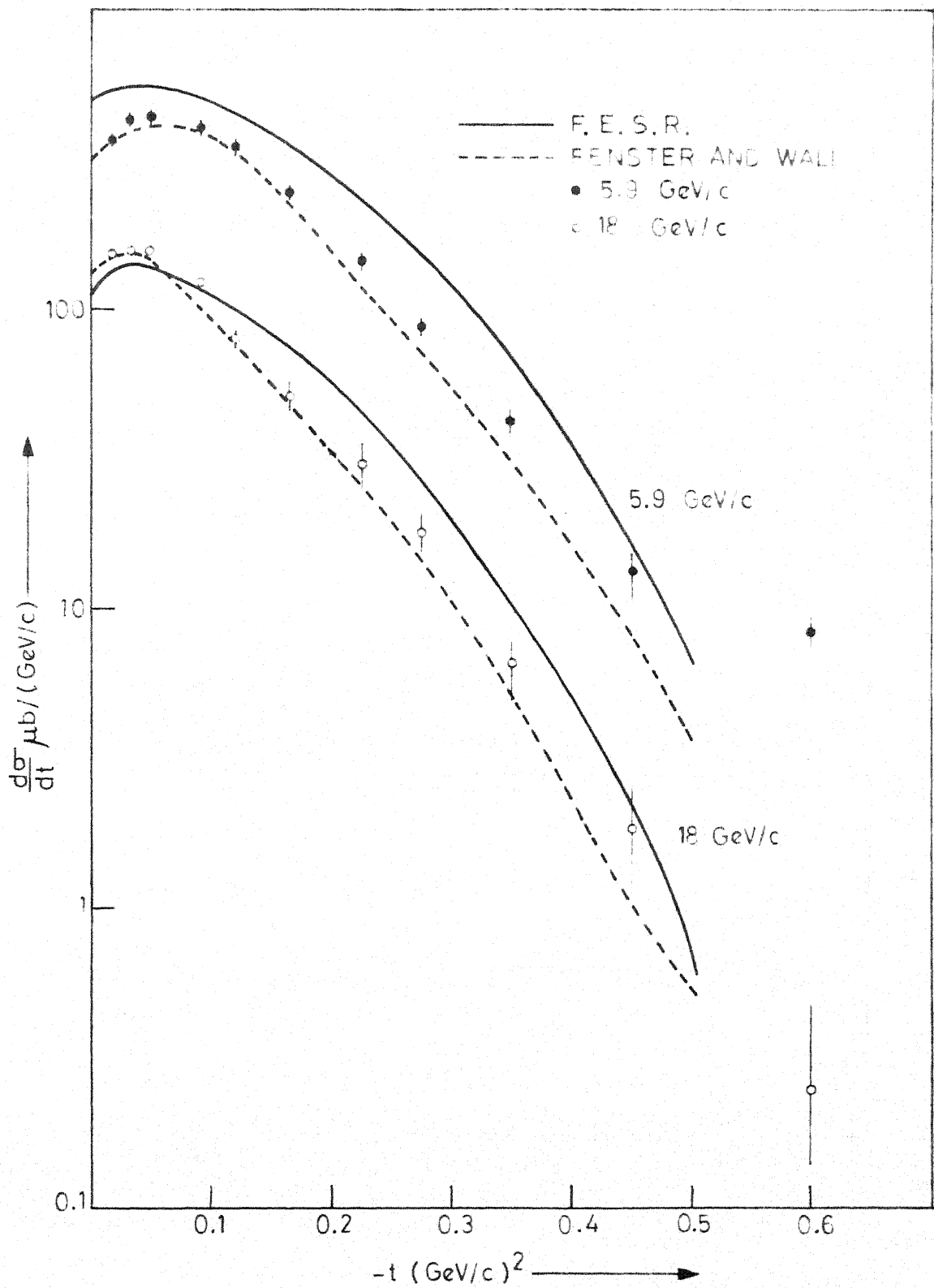


Fig.7

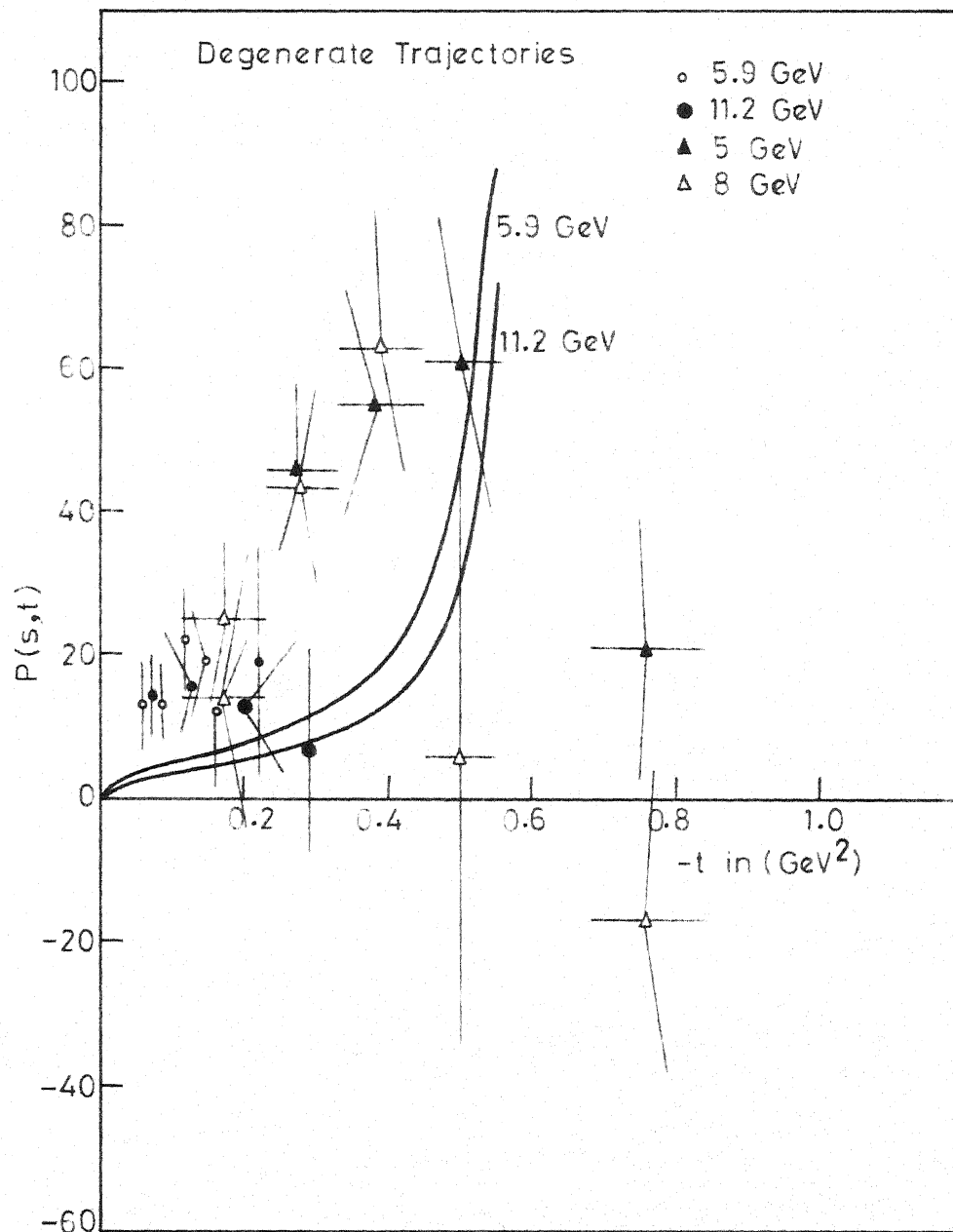


Fig. 8

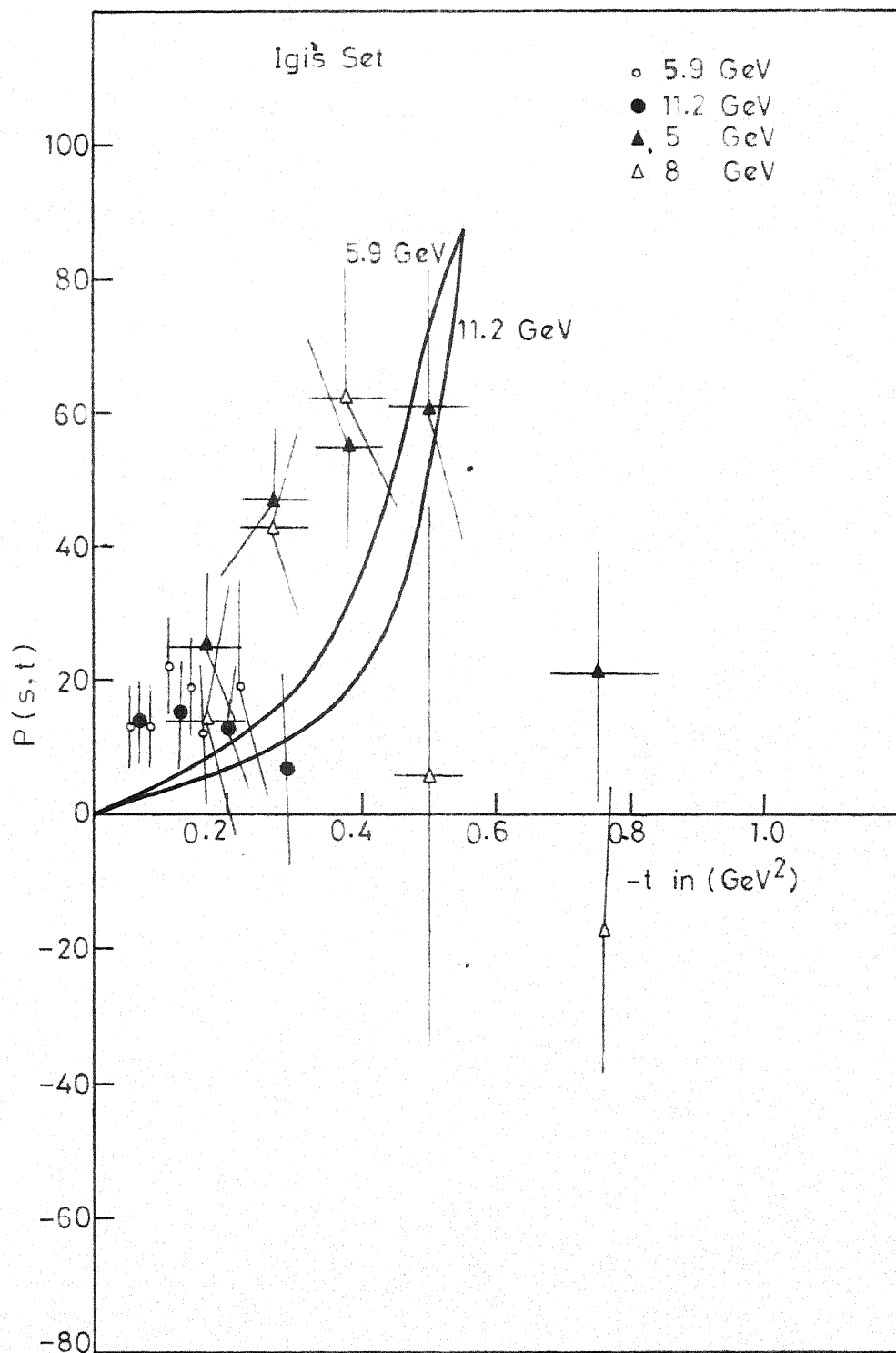


Fig. 9

conclude that the Veneziano model is able to produce a non-zero polarization which agrees qualitatively with the experimental data. Moreover, the shape of the differential cross-section can be reproduced fairly well in the low momentum transfer region using Igi's set of parameters. In case of Fenster and Wali's model though there is a better agreement with the experimental data for the differential cross-section, the polarization, as predicted, seems to have sign opposite to that of the experimental results.

2.4 η Production in πN Scattering:

In this section we study η production in πN scattering.⁵² This process is simpler to study, since from G parity considerations A_2 is the only trajectory that can be exchanged in the t-channel. In the s and u-channel only baryon trajectory with $I = 1/2$ can be exchanged.

The invariant amplitude can be written as,

$$\begin{aligned}
 A(s,t,u) = & \beta_{A_2}^1 \left[C(1-\alpha_{A_3}(t), \frac{3}{2} - \alpha_{N_\alpha}(s)) + C(1-\alpha_{A_2}(t), \frac{3}{2} - \alpha_{N_\alpha}(u)) \right. \\
 & + C(\frac{3}{2} - \alpha_{N_\alpha}(s), \frac{3}{2} - \alpha_{N_\alpha}(u)) \left. \right] + \beta_{A_2}^2 \left[C(1-\alpha_{A_2}(t), \frac{3}{2} - \alpha_{N_\gamma}(s)) \right. \\
 & + C(1-\alpha_{A_2}(t), \frac{3}{2} - \alpha_{N_\gamma}(u)) - C(\frac{3}{2} - \alpha_{N_\gamma}(s), \frac{3}{2} - \alpha_{N_\gamma}(u)) \left. \right]
 \end{aligned}$$

(2.4.1)

$$\begin{aligned}
B(s,t,u) = & \beta_{A_2}^3 \left[B(1-\alpha_{A_2}(t), \frac{1}{2} - \alpha_{N_\alpha}(s)) - B(1-\alpha_{A_2}(t), \frac{1}{2} - \alpha_{N_\alpha}(u)) \right. \\
& + B(\frac{1}{2} - \alpha_{N_\alpha}(s), \frac{1}{2} - \alpha_{N_\alpha}(u)) \left. \right] + \beta_{A_2}^4 \left[B(1-\alpha_{A_2}(t), \right. \\
& \frac{1}{2} - \alpha_{N_\gamma}(s)) - B(\frac{1}{2} - \alpha_{N_\gamma}(u), 1-\alpha_{A_2}(t)) \\
& \left. - B(\frac{1}{2} - \alpha_{N_\gamma}(s), \frac{1}{2} - \alpha_{N_\gamma}(u)) \right] \quad (2.4.2)
\end{aligned}$$

The B and C functions have the same meaning as defined in Section 2.2.1.

After writing down the invariant amplitudes A and B we use Stirling approximation for B and C functions that appear in invariant amplitudes A and B. We see that the amplitudes have appropriate signature factors corresponding to A_2 pole. The set of parameters which give a fit to the differential cross-sections for pion laboratory energy 5.9 GeV, 9.8 GeV and 13.3 GeV is the following:

$$\begin{aligned}
\beta_{A_2}^1 &= -5.76 \text{ GeV}^{-1} \\
\beta_{A_2}^2 &= -5.60 \text{ GeV}^{-1} \\
\beta_{A_2}^3 &= -6.82 \text{ GeV}^{-2} \\
\beta_{A_2}^4 &= -15.02 \text{ GeV}^{-2} \quad (2.4.3)
\end{aligned}$$

$$\alpha_{N_\alpha}(s) = -0.256 + .9s$$

$$\alpha_{N_\gamma}(s) = -0.550 + .9s$$

$$\alpha_{A_2}(t) = 0.5 + .9t \quad (2.4.4)$$

The trajectories given in eqn. (2.4.4) were used as inputs. The fits to the differential cross-sections⁵⁴ are shown in Figs. 10 and 11. The prediction for polarization⁵⁵ is shown in Fig. 12.

In the case of production we have obtained a good fit to the experimental data for a differential cross-section which is characterized by a chi-square value of 8.5 against an expected 10. The polarization data is scanty. Since there are large errors in the polarization measurements we have made no attempt to include them in our fits. Our prediction for polarization is of the same order of magnitude as the experimental data but has opposite sign.

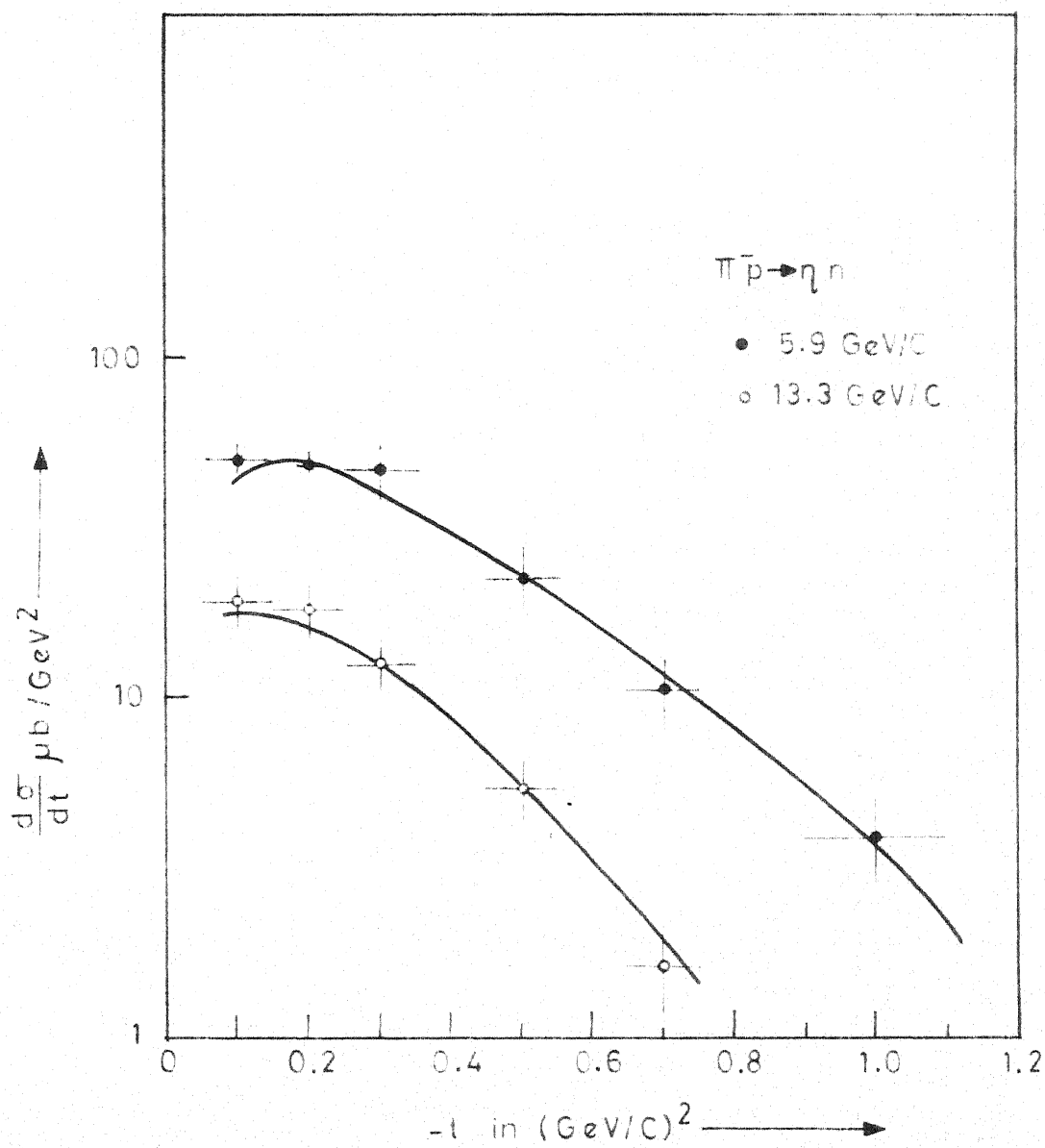


Fig.10

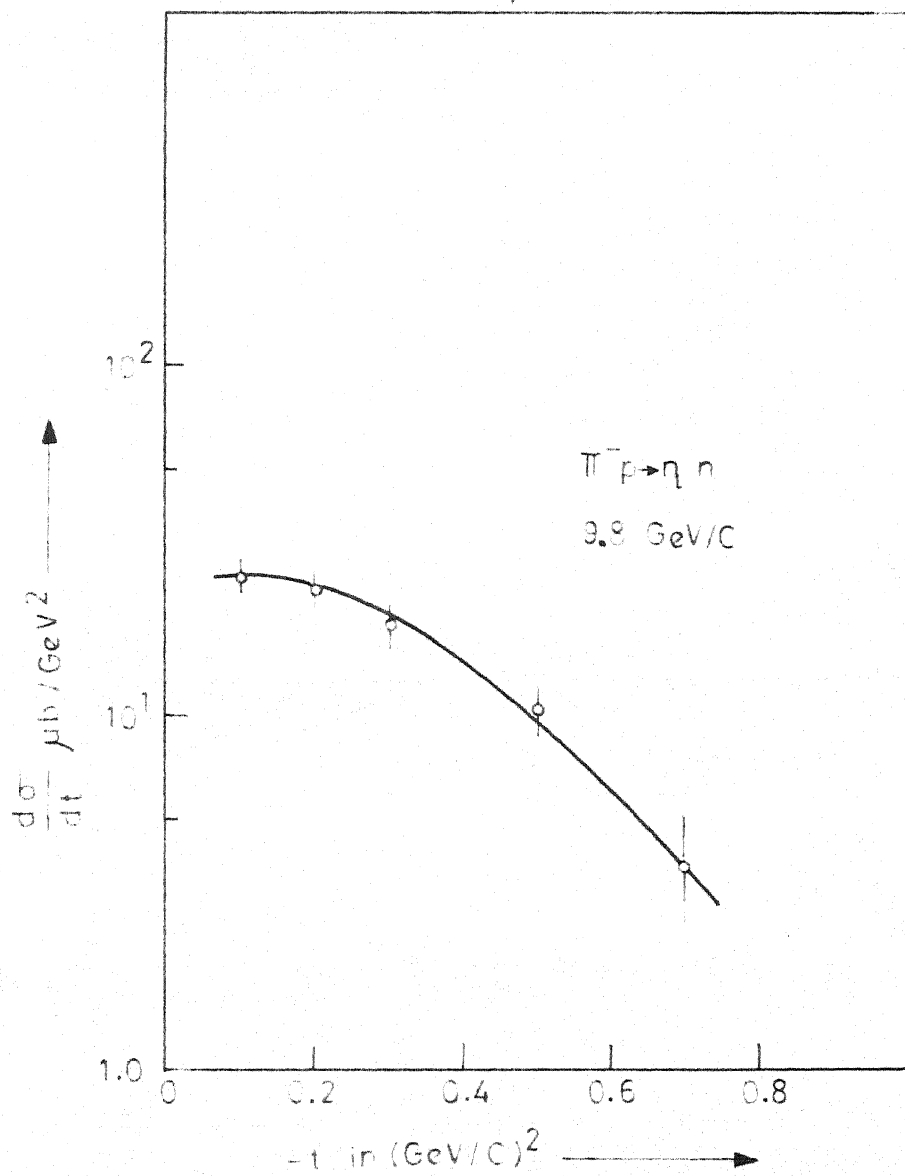


Fig. 11

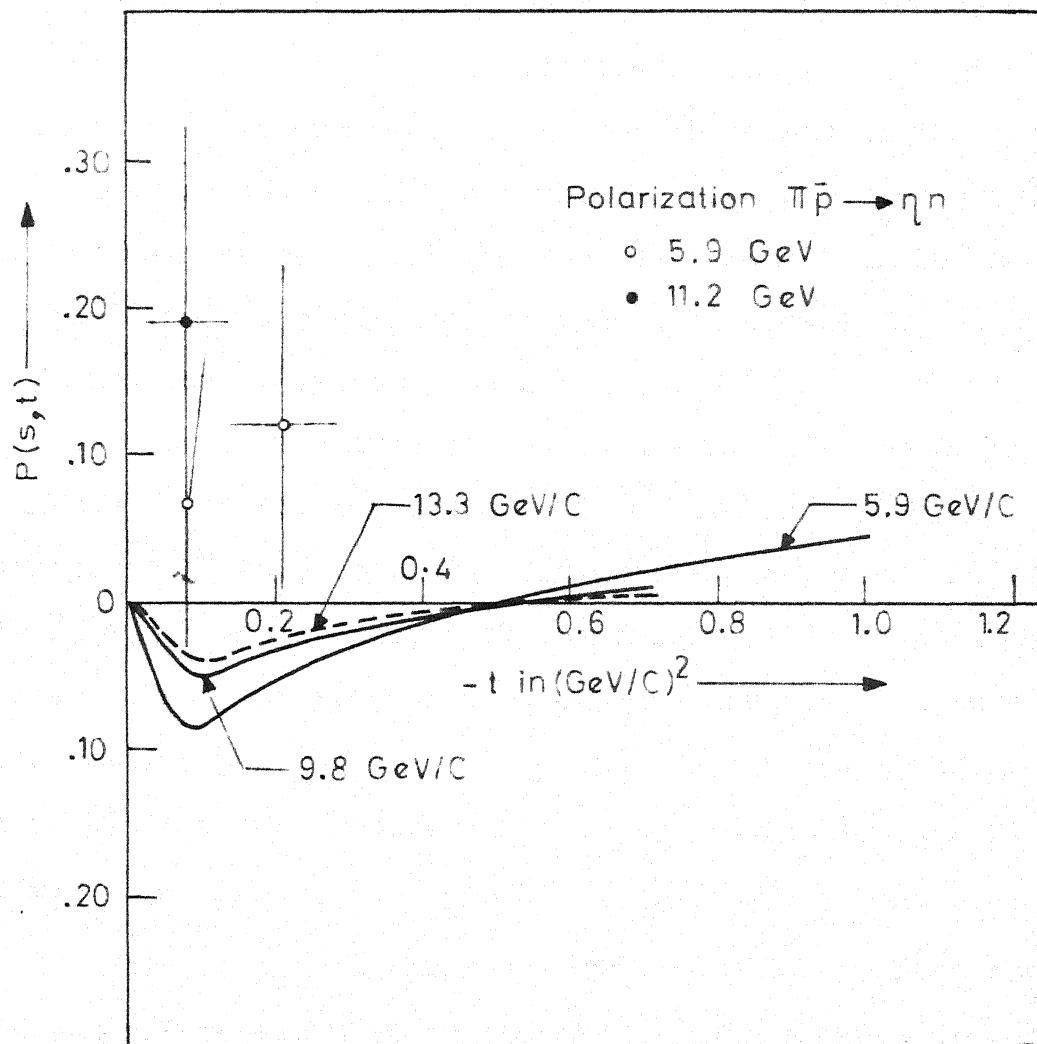


Fig. 12

CHAPTER III

We study the charge-exchange and hypercharge-exchange processes in kaon nucleon scattering in the first part of this chapter. The second part deals with the study of the charged pion photoproduction in the Veneziano model. In the preceeding chapter we have seen that the Veneziano model can be used as a good device to study the scattering phenomena in the moderately high energy region. We use the same framework to study the above mentioned process, which are also free from problems connected with Pomeranchukon. There have been several attempts⁵⁶⁻⁶⁰ to construct Veneziano like representations for the $\bar{K}N$ and KN scattering. The central philosophy behind all these works is to add a few satellite terms to eliminate a few wrong parity poles in the low energy region and at the same time obtain a description for the high energy scattering processes.

Most of the earlier attempts were to describe processes where the Pomeranchukon trajectory cannot be exchanged. However, there have been some attempts to describe elastic KN and $\bar{K}N$ scattering processes. Berger and Fox⁶⁰ have studied the KN and $\bar{K}N$ scattering problem in the frame work of the Veneziano model extensively. They have obtained fits to the charge-exchange data in $\bar{K}N$ and KN scattering in addition to the elastic

scattering data. The main problem, in describing elastic scattering process, arises due to the presence of the Pomeranchukon trajectory. These authors put the Pomeranchukon trajectory from outside in the dual amplitude. A more successful attempt has been done by Desai and Kumar⁶¹ to describe the elastic scattering processes in KN and $\bar{K}N$ scattering. They use the fact that the Pomeranchukon trajectory is rather flat and it cannot be dual to any normal trajectory. Using Freund-Harari duality, in addition to the normal trajectories, they introduce a few baryon trajectories with exotic quantum numbers. These exotic trajectories are taken to be dual to the Pomeranchukon trajectory. The fit obtained to the elastic forward and backward scattering data by these authors is quite good. However, the existence of baryon trajectories with exotic quantum numbers is rather doubtful. In the processes considered here the Pomeranchukon plays a minor role and indeed can be completely ignored if exchange degeneracy is exact. We have accordingly not considered the complications arising out of the inclusion of the Pomeranchukon trajectory.

3.2.1 Charge-Exchange Processes in $\bar{K}N$ Scattering:

We construct the Veneziano representation⁶² for $\bar{K}N$ scattering processes in this section. The s -channel gets contribution from $Y = 0$ and $I = 0$ and 1 baryon trajectories whereas the t -channel gets contribution from $I = 0$ and $I = 1$ meson trajectories f, ω and ρ, A_2 respectively.

exchange degeneracy of the meson trajectories to write

$$\alpha_{\rho}(t) = \alpha_{A_2}(t) \text{ and } \alpha_{\omega}(t) = \alpha_f(t).$$

The invariant amplitudes A and B can be written corresponding to definite isospin in the t-channel. The invariant amplitudes corresponding to $I = 0(1)$ are denoted by the subscript ρ (f).

$$\begin{aligned} A_f(s, t, u) = & \beta_{f, Y_0}^1 \left[C(1 - \alpha_f(t), \frac{3}{2} - \alpha_{Y_0}(s)) + C(1 - \alpha_f(t), \right. \\ & \left. \frac{3}{2} - \alpha_{Y_0}(u)) \right] + \beta_{f, Y_1}^1 \left[C(1 - \alpha_f(t), \frac{3}{2} - \alpha_{Y_1}(s)) \right. \\ & \left. + C(1 - \alpha_f(t), \frac{3}{2} - \alpha_{Y_1}(u)) \right] \end{aligned} \quad (3.2.1)$$

$$\begin{aligned} B_f(s, t, u) = & \beta_{f, Y_0}^2 \left[B(1 - \alpha_f(t), \frac{1}{2} - \alpha_{Y_0}(s)) - B(1 - \alpha_f(t), \right. \\ & \left. \frac{1}{2} - \alpha_{Y_0}(u)) \right] + \beta_{f, Y_1}^2 \left[B(1 - \alpha_f(t), \frac{1}{2} - \alpha_{Y_1}(s)) \right. \\ & \left. - B(1 - \alpha_f(t), \frac{1}{2} - \alpha_{Y_1}(u)) \right] \end{aligned} \quad (3.2.2)$$

$$\begin{aligned} A_{\rho}(s, t, u) = & \beta_{\rho, Y_0}^1 \left[C(1 - \alpha_{\rho}(t), \frac{3}{2} - \alpha_{Y_0}(s)) - C(1 - \alpha_{\rho}(t), \right. \\ & \left. \frac{3}{2} - \alpha_{Y_0}(u)) \right] + \beta_{\rho, Y_1}^1 \left[C(1 - \alpha_{\rho}(t), \frac{3}{2} - \alpha_{Y_1}(s)) \right. \\ & \left. - C(1 - \alpha_{\rho}(t), \frac{3}{2} - \alpha_{Y_1}(u)) \right] \end{aligned} \quad (3.2.3)$$

$$\begin{aligned} B_{\rho}(s, t, u) = & \beta_{\rho, Y_0}^2 \left[B(1 - \alpha_{\rho}(t), \frac{1}{2} - \alpha_{Y_0}(s)) + B(1 - \alpha_{\rho}(t), \right. \\ & \left. \frac{1}{2} - \alpha_{Y_0}(u)) \right] + \beta_{\rho, Y_1}^2 \left[B(1 - \alpha_{\rho}(t), \frac{1}{2} - \alpha_{Y_1}(s)) \right. \\ & \left. + B(1 - \alpha_{\rho}(t), \frac{1}{2} - \alpha_{Y_1}(u)) \right] \end{aligned} \quad (3.2.4)$$

Eqns. (3.2.1) to (3.2.4) satisfy the required crossing properties at this stage. Further constraints on the residue functions can be imposed by constructing amplitudes corresponding to definite isospin in the s-channel and demanding absence of $I = 0$ ($I = 1$) baryon poles from s-channel amplitudes with isospin $1(0)$. As a consequence of above requirement we get,

$$\alpha_f(t) = \alpha_{\rho}(t) \quad , \quad (3.3.5)$$

$$\begin{aligned} \beta_{f,Y_1}^1 &= -3 \beta_{\rho,Y_1}^1 \quad , \quad 3 \beta_{f,Y_1}^2 = - \beta_{f,Y_1}^2 \\ \beta_{\rho,Y_0}^1 &= \beta_{f,Y_0}^1 \quad \text{and} \quad \beta_{\rho,Y_0}^2 = \beta_{f,Y_0}^2 \end{aligned} \quad (3.2.6)$$

Moreover, in order to eliminate wrong isospin leading baryon poles we need slopes of all trajectories to be the same and use following set of trajectories.

$$\begin{aligned} \alpha_{Y_0}(s) &= -0.65 + .9s \\ \alpha_{Y_1}(s) &= 0.30 + .9s \end{aligned} \quad (3.2.7)$$

3.2.2 Hypercharge-Exchange Processes:

In this section we study two hypercharge exchange processes^{62,63}

- (i) $K^- N \rightarrow \pi \Sigma$
- (ii) $K^- N \rightarrow \pi^- \Lambda$

We consider various meson and baryon trajectories that can be exchanged in different channels for the process (i).

Eqns. (3.2.1) to (3.2.4) satisfy the required crossing properties at this stage. Further constraints on the residue functions can be imposed by constructing amplitudes corresponding to definite isospin in the s-channel and demanding absence of $I = 0$ ($I = 1$) baryon poles from s-channel amplitudes with isospin $1(0)$. As a consequence of above requirement we get,

$$\alpha_f(t) = \alpha_\rho(t) \quad , \quad (3.3.5)$$

$$\begin{aligned} \beta_{f,Y_1}^1 &= -3 \beta_{\rho,Y_1}^1 \quad , \quad 3 \beta_{f,Y_1}^2 = - \beta_{f,Y_1}^2 \\ \beta_{\rho,Y_0}^1 &= \beta_{f,Y_0}^1 \quad \text{and} \quad \beta_{\rho,Y_0}^2 = \beta_{f,Y_0}^2 \end{aligned} \quad (3.2.6)$$

Moreover, in order to eliminate wrong isospin leading baryon poles we need slopes of all trajectories to be the same and use following set of trajectories.

$$\begin{aligned} \alpha_{Y_0}(s) &= -0.65 + .9s \\ \alpha_{Y_1}(s) &= 0.30 + .9s \end{aligned} \quad (3.2.7)$$

3.2.2 Hypercharge-Exchange Processes:

In this section we study two hypercharge exchange processes^{62,63}

- (i) $K^- N \rightarrow \pi \Sigma$
- (ii) $K^- N \rightarrow \pi^- \Lambda$

We consider various meson and baryon trajectories that can be exchanged in different channels for the process (i).

- a) In the s-channel, baryon trajectories having quantum number $S = -1$ and $I = 0$ and 1 are exchanged. We retain Λ (octet) and Y_0^* (SU(3) singlet) in the $I = 0$ channel and Σ (octet) and Y_1^* (decimet) trajectories in the $I = 1$ channel.
- b) Meson trajectories having quantum numbers $I = 1/2, 3/2$ and $S = -1$ are exchanged in the t-channel. However, there is very little experimental evidence about existence of $I = 3/2$ $S = -1$ meson trajectory. Therefore we retain only $I = 1/2$ trajectory corresponding to K^* and K^{**} . We take them to be the same using the exchange degeneracy for meson trajectories.
- c) u-channel gets contributions from N_α , N_γ and Δ_δ trajectories.

The invariant amplitudes written below, correspond to definite isospin in the s-channel.

$$\begin{aligned}
 A^{I_S=0}(s,t,u) = & \beta_1^0 \left[C(1-\alpha_{K^*}(t), \frac{3}{2} - \alpha_{Y_0^*}(s)) - C(1-\alpha_{K^*}(t), \right. \\
 & \left. \frac{3}{2} - \alpha_{N_\alpha}(u)) - C(\frac{3}{2} - \alpha_{Y_0^*}(s), \frac{3}{2} - \alpha_{N_\alpha}(u)) \right] \\
 & + \beta_2^0 \left[C(1-\alpha_{K^*}(t), \frac{3}{2} - \alpha_\Lambda(s)) - C(1-\alpha_{K^*}(t), \right. \\
 & \left. \frac{3}{2} - \alpha_{N_\gamma}(u)) + C(\frac{3}{2} - \alpha_\Lambda(s), \frac{3}{2} - \alpha_{N_\gamma}(u)) \right] \\
 & + \beta_3^0 \left[C(1-\alpha_{K^*}(t), \frac{3}{2} - \alpha_\Lambda(s)) - C(1-\alpha_{K^*}(t), \right. \\
 & \left. \frac{3}{2} - \alpha_{\Delta_\delta}(u)) + C(\frac{3}{2} - \alpha_\Lambda(s), \frac{3}{2} - \alpha_{\Delta_\delta}(u)) \right]
 \end{aligned}
 \tag{3.2.8}$$

$$\begin{aligned}
A^{I_S=1}(s,t,u) = & \beta_1^1 \left[C(1-\alpha_{K^*}(t), \frac{3}{2} - \alpha_{Y_1^*}(s)) - C(1-\alpha_{K^*}(t), \right. \\
& \left. \frac{3}{2} - \alpha_{N_\alpha}(u)) - C(\frac{3}{2} - \alpha_{Y_1^*}(s), \frac{3}{2} - \alpha_{N_\alpha}(u)) \right] \\
& + \beta_2^1 \left[C(1-\alpha_{K^*}(t), \frac{3}{2} - \alpha_\Sigma(s)) - C(1-\alpha_{K^*}(t), \right. \\
& \left. \frac{3}{2} - \alpha_{N_\gamma}(u)) - C(\frac{3}{2} - \alpha_\Sigma(s), \frac{3}{2} - \alpha_{N_\gamma}(u)) \right] \\
& + \beta_3^1 \left[C(1-\alpha_{K^*}(t), \frac{3}{2} - \alpha_\Sigma(s)) - C(1-\alpha_{K^*}(t), \right. \\
& \left. \frac{3}{2} - \alpha_{\Delta_\delta}(u)) + C(\frac{3}{2} - \alpha_\Sigma(s), \frac{3}{2} - \alpha_{\Delta_\delta}(u)) \right]
\end{aligned}
\tag{3.2.9}$$

$$\begin{aligned}
B^{I_S=0}(s,t,u) = & \gamma_1^0 \left[B(1-\alpha_{K^*}(t), \frac{1}{2} - \alpha_{Y_0^*}(s)), B(1-\alpha_{K^*}(t), \right. \\
& \left. \frac{1}{2} - \alpha_{N_\alpha}(u)) + B(\frac{1}{2} - \alpha_{Y_0^*}(s), \frac{1}{2} - \alpha_{N_\alpha}(u)) \right] \\
& + \gamma_2^0 \left[B(1-\alpha_{K^*}(t), \frac{1}{2} - \alpha_\wedge(s)) + B(1-\alpha_{K^*}(t), \right. \\
& \left. \frac{1}{2} - \alpha_{N_\gamma}(u)) - B(\frac{1}{2} - \alpha_\wedge(s), \frac{1}{2} - \alpha_{N_\gamma}(u)) \right] \\
& + \gamma_3^0 \left[B(1-\alpha_{K^*}(t), \frac{1}{2} - \alpha_\wedge(s)) + B(1-\alpha_{K^*}(t), \right. \\
& \left. \frac{1}{2} - \alpha_{\Delta_\delta}(u)) - B(\frac{1}{2} - \alpha_\wedge(s), \frac{1}{2} - \alpha_{\Delta_\delta}(u)) \right]
\end{aligned}
\tag{3.2.10}$$

$$\begin{aligned}
B^{I_S=1}(s,t,u) = & \gamma_1^1 \left[B(1-\alpha_K^*(t), \frac{1}{2} - \alpha_{Y_1}^*(s)) + B(1-\alpha_K^*(t), \right. \\
& \left. \frac{1}{2} - \alpha_{N_\alpha}(u)) + B(\frac{1}{2} - \alpha_{Y_1}^*(s), \frac{1}{2} - \alpha_{N_\alpha}(u)) \right] \\
& + \gamma_2^1 \left[B(1-\alpha_K^*(t), \frac{1}{2} - \alpha_\Sigma(s)) + B(1-\alpha_K^*(t), \right. \\
& \left. \frac{1}{2} - \alpha_{N_\gamma}(u)) - B(\frac{1}{2} - \alpha_\Sigma(s), \frac{1}{2} - \alpha_{N_\gamma}(u)) \right] \\
& + \gamma_3^1 \left[B(1-\alpha_K^*(t), \frac{1}{2} - \alpha_\Sigma(s)) + B(1-\alpha_K^*(t), \right. \\
& \left. \frac{1}{2} - \alpha_{\Delta_\delta}(u)) - B(\frac{1}{2} - \alpha_\Sigma(s), \frac{1}{2} - \alpha_{\Delta_\delta}(u)) \right]
\end{aligned}
\tag{3.2.11}$$

As emphasized earlier, the Veneziano representation for the scattering amplitude as written in eqn. (3.2.8) to (3.2.11) are not unique. One can write down many more terms with the same asymptotic behavior. However our effort is to describe the scattering processes with a relatively small number of parameters. Therefore, we choose this representation. Now we can impose the constraints due to isospin crossing in order to obtain relations among the parameters to eliminate wrong isospin baryon poles in the u-channel.

The relations are,

$$\beta_3^1 = -\frac{1}{\sqrt{6}} \beta_3^0 \tag{3.2.12}$$

$$(i) \quad \beta_1^1 = (2/3)^{1/2} \beta_1^0, (ii) \quad \beta_2^1 = (2/3)^{1/2} \beta_2^0 \tag{3.2.13}$$

$$\gamma_3^1 = -\frac{1}{\sqrt{6}} \gamma_1^0 \tag{3.2.14}$$

$$(i) \quad \gamma_1^1 = (2/3)^{1/2} \gamma_1^0, \quad (ii) \quad \gamma_2^1 = (2/3)^{1/2} \gamma_2^0 \quad (3.2.15)$$

The amplitude for $K^-n \rightarrow \pi^- \Lambda$ is assumed to couple only with Y_1^* trajectory in s-channel.

$$A(s,t,u) = \beta^1 \left[C(1-\alpha_{K^*}(t), \frac{3}{2} - \alpha_{Y_1^*}(s)) - C(1-\alpha_{K^*}(t), \frac{3}{2} - \alpha_N(u)) - C(\frac{3}{2} - \alpha_{Y_1^*}(s), \frac{3}{2} - \alpha_N(u)) \right] \quad (3.2.16)$$

$$B(s,t,u) = \beta^2 \left[B(1-\alpha_{K^*}(t), \frac{1}{2} - \alpha_{Y_1^*}(s)) + B(1-\alpha_{K^*}(s), \frac{1}{2} - \alpha_N(u)) + B(\frac{1}{2} - \alpha_{Y_1^*}(s), \frac{1}{2} - \alpha_N(u)) \right] \quad (3.2.17)$$

The fits to the differential cross-sections of the process⁶⁴ $K^-p \rightarrow \bar{K}^0 n$ are shown in Fig. 13. The fit is characterized by a chi-square value of 21.3 against an expected 20. The process $K^+n \rightarrow K^0 p$ can be related to $K^-p \rightarrow \bar{K}^0 n$ through s-u crossing. The s - u crossing together with $\rho - A_2$ exchange degeneracy⁶⁵ predict that the cross-sections for $K^-p \rightarrow \bar{K}^0 n$ and $K^+n \rightarrow K^0 p$ at a given energy will be same. We have obtained the cross-section for the process $K^+n \rightarrow K^0 p$, as shown in Fig.14 at kaon laboratory energy corresponding to⁶⁵ 12 GeV. It is interesting to note here that the predicted cross-section is in good agreement with the experimental results, except the broad shoulder⁶⁶ at $t = -0.3$ to -0.5 GeV^2 which cannot be reproduced from our model. We also predict the polarization for $K^-p \rightarrow \bar{K}^0 n$ as shown in Fig. 15. Though there is as yet⁶⁷, no published result for polarization in K^-N charge exchange

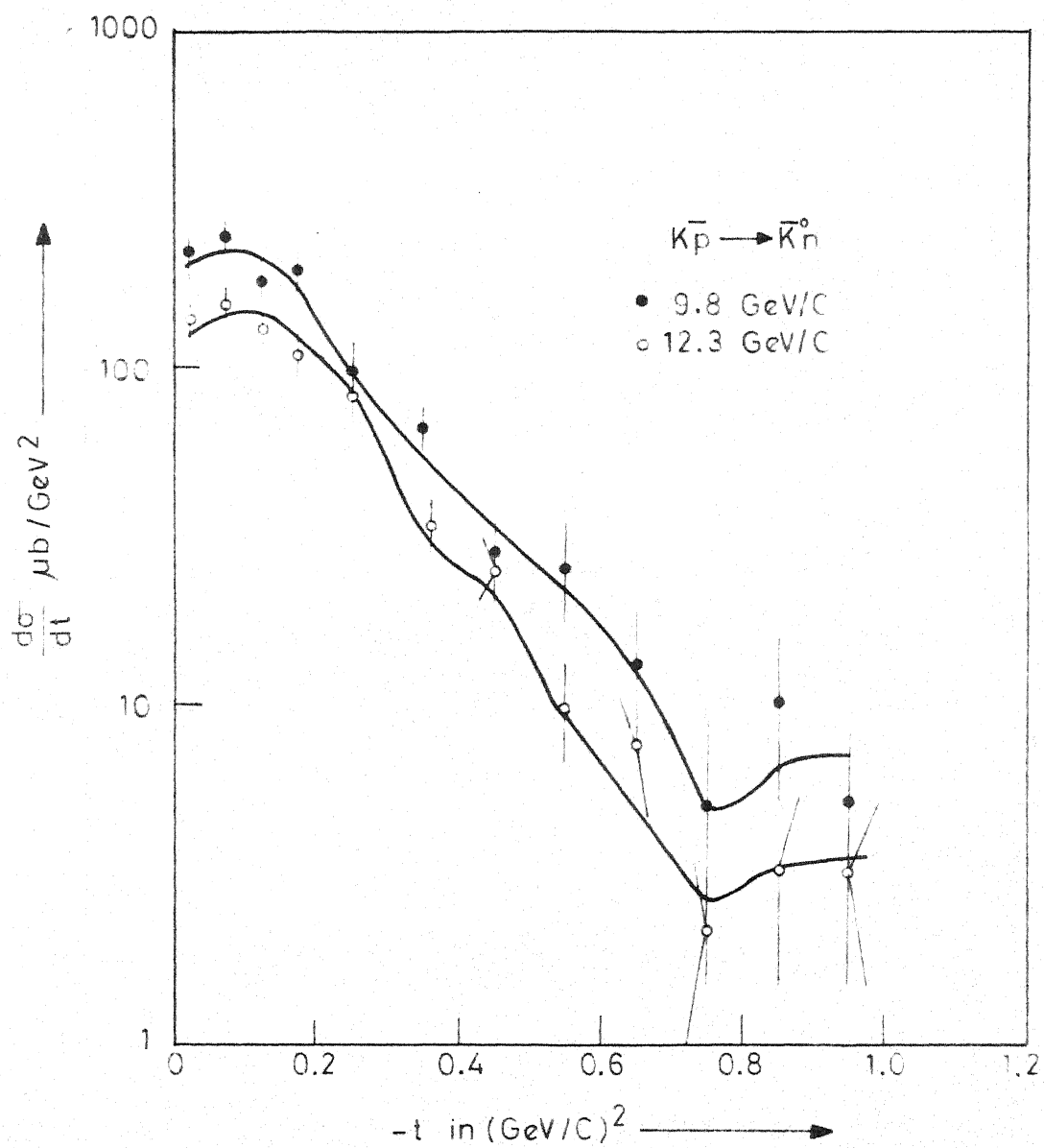


Fig.13

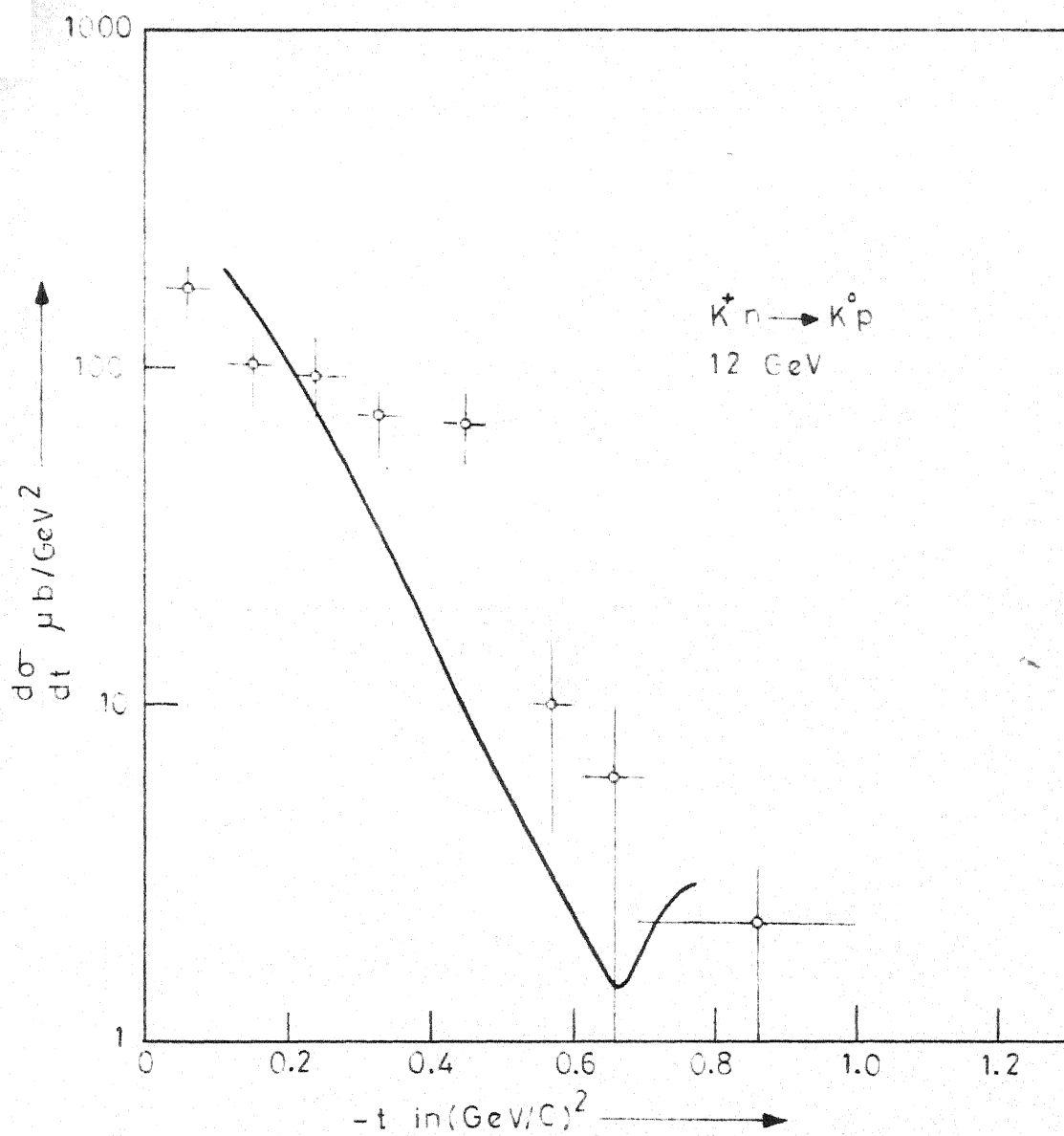


Fig.14

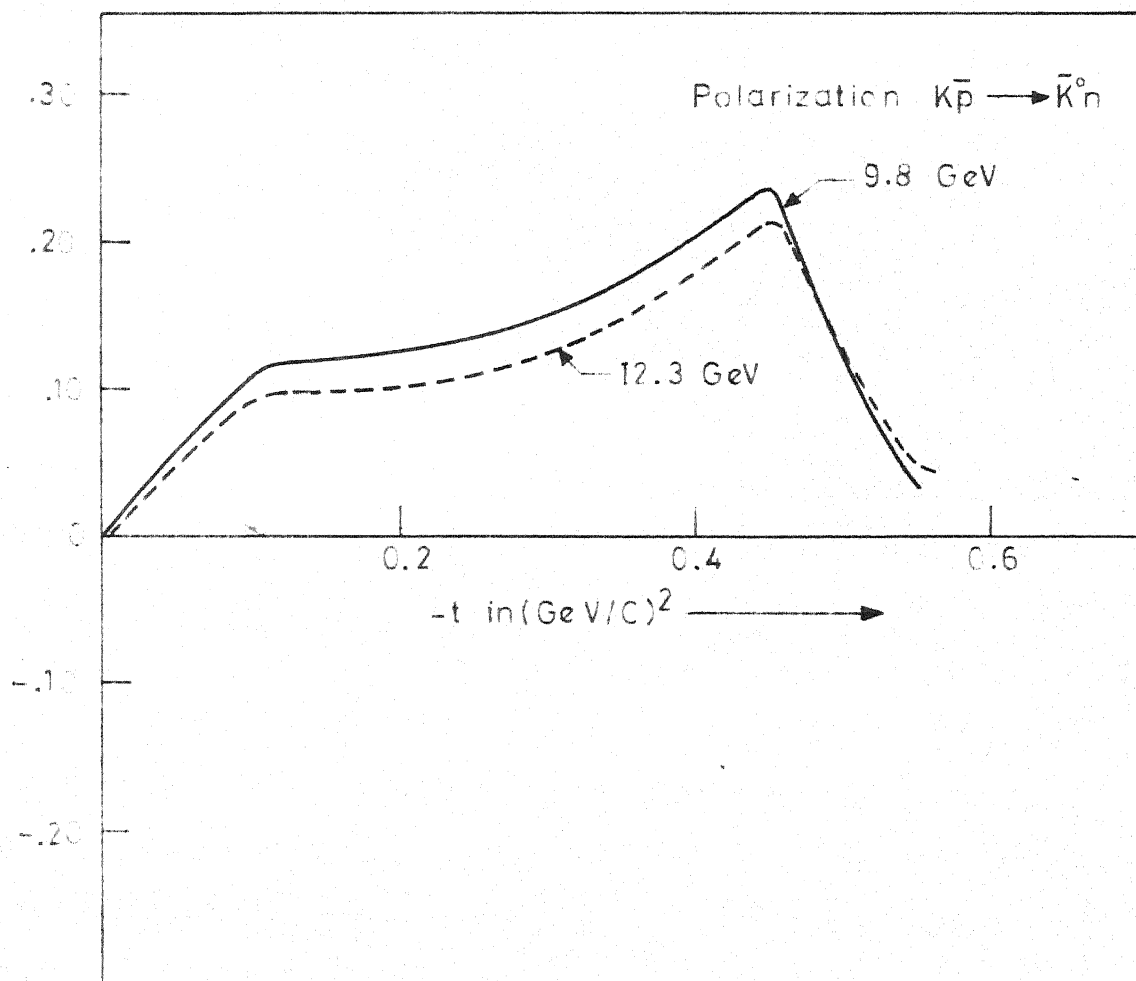


Fig. 15

scattering, there is indication that the polarization in this process has the same trend as predicted by our model.

The parameters that are used to obtain the fits to the differential cross-section are the following:

$$\begin{aligned} \beta_{\rho, Y_0}^1 &= -13.52 \text{ GeV}^{-1} & , & \quad \beta_{\rho, Y_1}^1 = -19.28 \text{ GeV}^{-1} \\ \beta_{\rho, Y_0}^2 &= 5.76 \text{ GeV}^{-2} & \text{ and } & \quad \beta_{\rho, Y_1}^2 = -68.96 \text{ GeV}^{-2} \end{aligned} \quad (3.2.18)$$

Fits to the differential cross-section for $K^-p \rightarrow \pi^- \Sigma^+$ ⁶⁸ and $K^-n \rightarrow \pi^- \Lambda$ ⁶⁹ are shown in Figs. 16 and 17 respectively. The chi-square for the two processes are 12 and 19 respectively against expected values of 7 and 11. The available polarization data⁶⁹ for $K^-n \rightarrow \pi^- \Lambda$ has been compared with our predictions (See Fig. 18). In view of large errors involved in polarization measurements we have not made any attempt to obtain a simultaneous fit to the polarization and cross-section data. However, our predictions for polarization are in qualitative agreement with the experimental results. A more interesting feature is observed in $K^-N \rightarrow \pi \Sigma$ scattering process. This process can be related to the reaction $\pi N \rightarrow K \Sigma$ through s - u crossing. We observe our predictions for the polarization⁷⁰ in the reaction $\pi^+p \rightarrow K^+\Sigma^+$ are consistent with the experimental data in the low momentum transfer region (Sec. Fig. 19). ($-t < .4 \text{ GeV}^2$). The polarization for $\pi^+p \rightarrow K^+\Sigma^+$ is calculated by using the same set of parameters that give fit to the differential cross-section

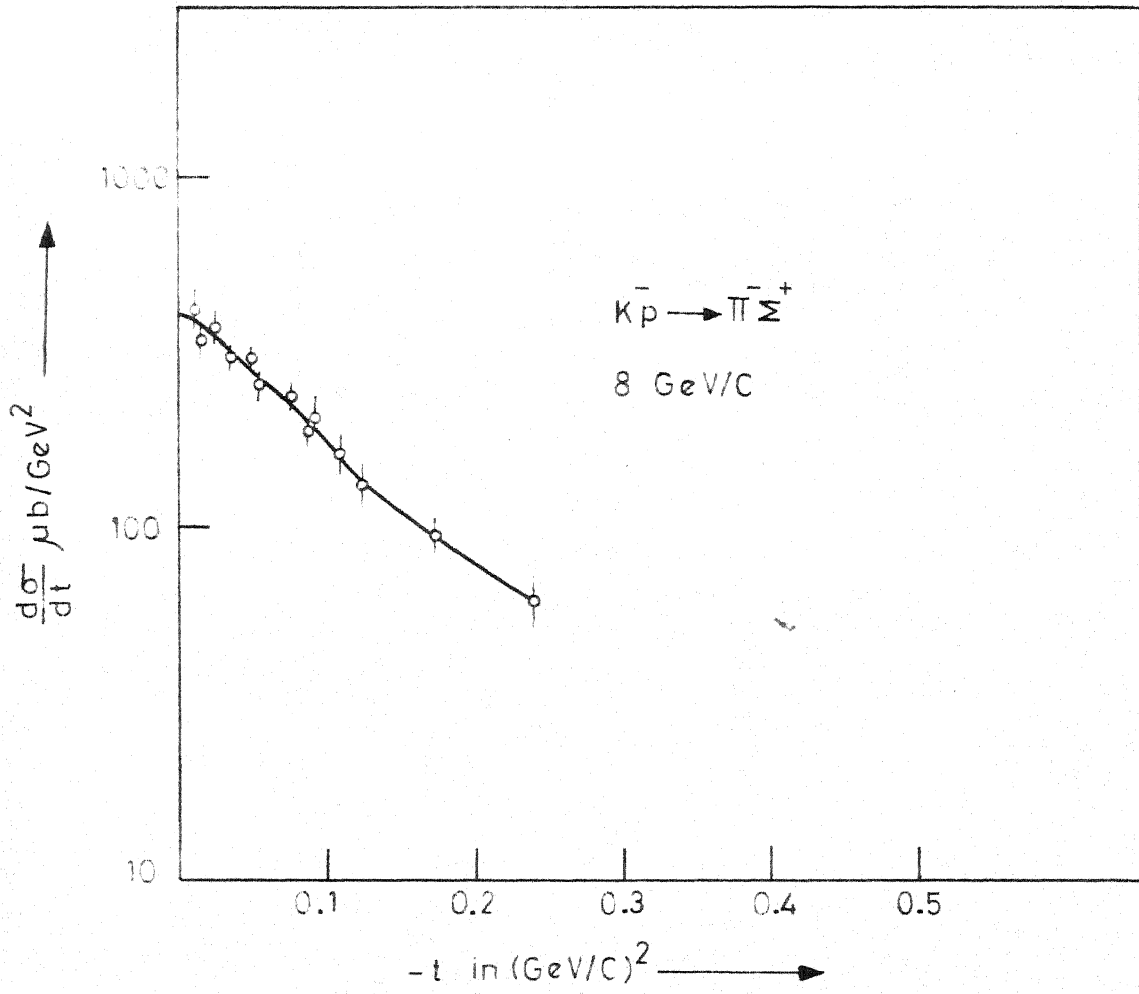


Fig.16

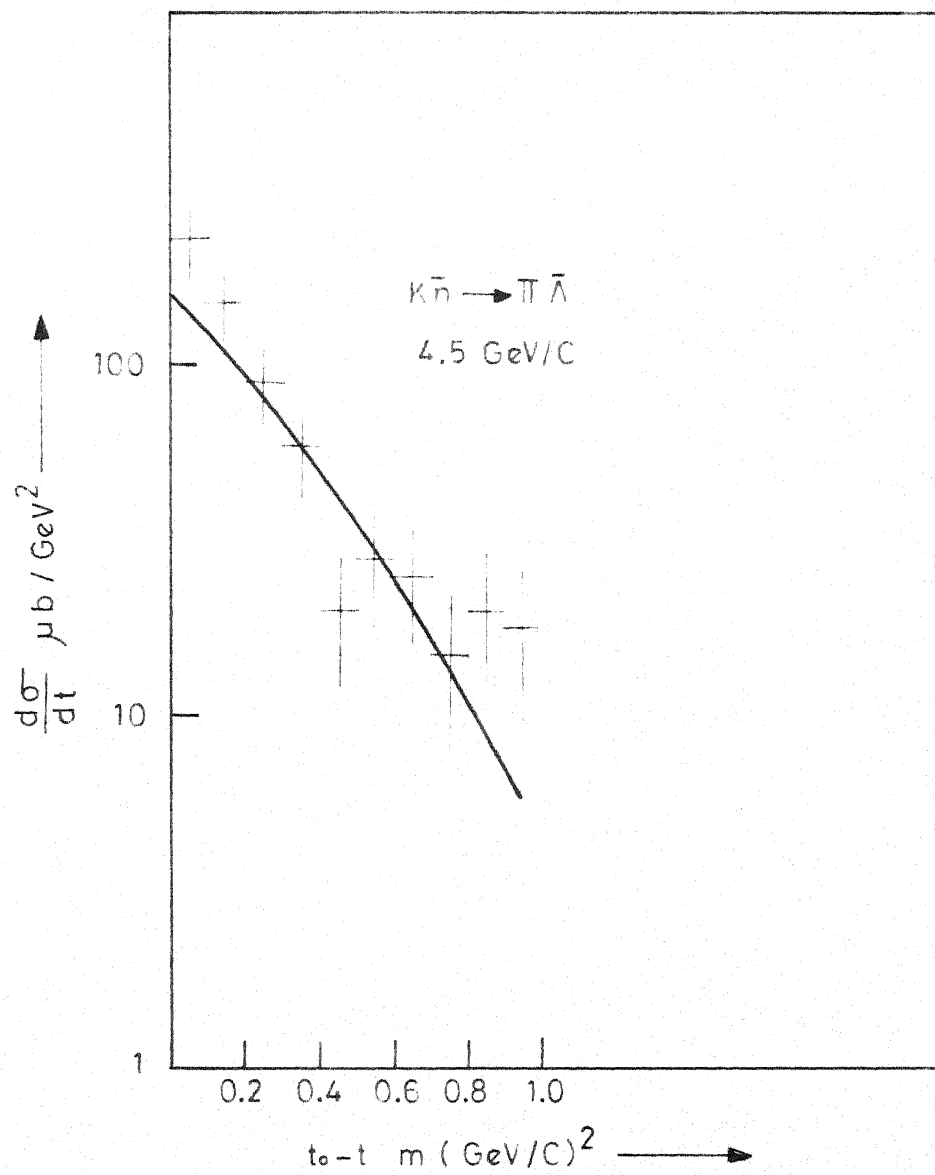


Fig.17

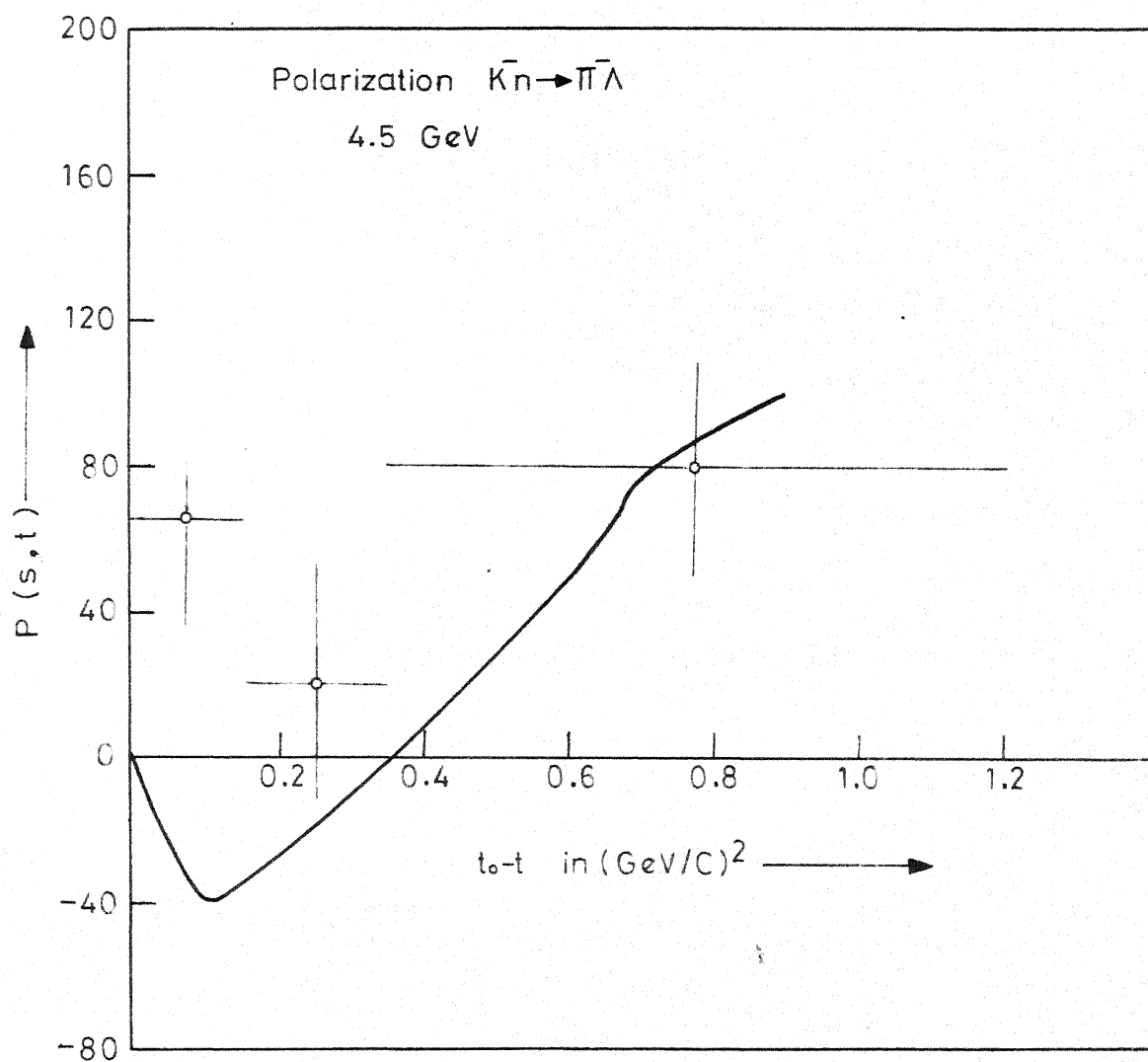


Fig. 18

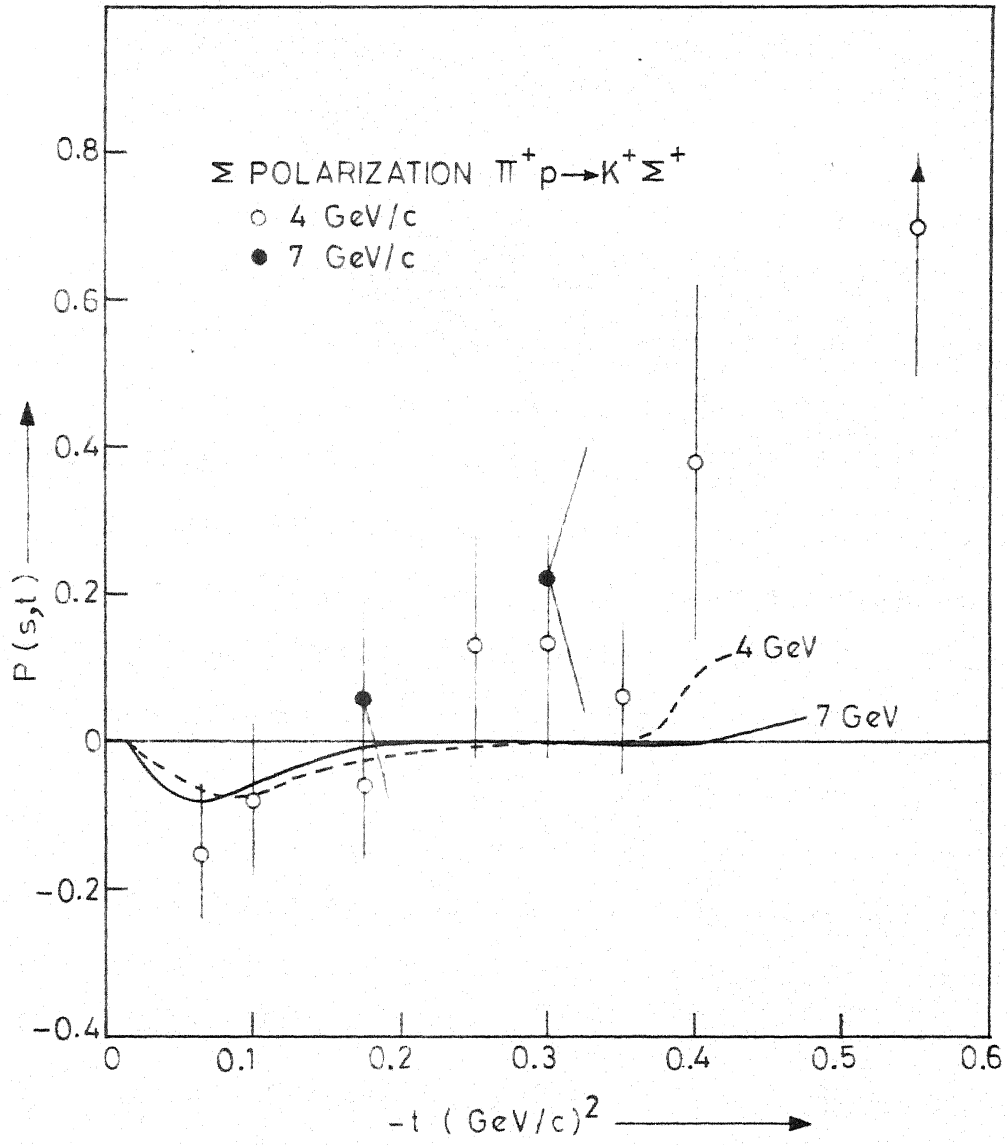


Fig. 19

for the process $K^-p \rightarrow \pi^- \Sigma^+$. We mention here that when attempts were made to predict the differential cross-sections for the process $\pi^+p \rightarrow K^+ \Sigma^+$ with the same set of parameters the results were not in good agreement with the experimental data. One of the explanations given for this result is that the exchange degeneracy of K^* and K^{**} trajectories might not be true. Such arguments have been presented earlier from the Regge pole theory. In fact, Lie and Louice⁷¹ have studied this problem extensively for the charge-exchange and hypercharge exchange-processes. They have concluded that though $\rho - A_2$ exchange degeneracy is fairly good, $K^* - K^{**}$ exchange degeneracy might be broken. The possibility of non exchange degeneracy of $K^* - K^{**}$ was concluded by these authors⁷¹ from the study of hypercharge-exchange processes like $K^-p \rightarrow \pi^- \Lambda$, $\pi^-p \rightarrow K^- \Lambda$, $\pi^+p \rightarrow K^+ \Sigma^+$ and $K^-p \rightarrow \pi^- \Sigma^+$. However, the Chew-Frautschi plot for mesons indicates that K^* and K^{**} are exchange degenerate. Recently there has been an attempt to explain the difference between the differential cross-sections for $K^-n \rightarrow \pi^- \Lambda$ and $\pi^+n \rightarrow K^+ \Lambda$, in a Regge pole and Regge cut model⁷². In this work the $K^* - K^{**}$ exchange degeneracy is kept in tact. One needs additional exchange degenerate daughters $K'^* - K'^{**}$ trajectories in addition to the Regge cuts to explain the data satisfactorily. In our model though the exchange degenerate $K^* - K^{**}$ do not give a good fit to the process $\pi^+p \rightarrow K^+ \Sigma^+$, the discrepancy is not too much. This, we feel, is because there are already daughters of K^* and K^{**} contained in our model. However,

one cannot expect to describe all the finer aspects of the data in a simple model like ours.

The set of parameters that were used to obtain fits to the $KN \rightarrow \pi\Sigma$ and $KN \rightarrow \pi\Lambda$ are the following.

$$(i) \quad \beta_1^0 = 1938.8 \text{ GeV}^{-1}, \quad \beta_2^0 = -1544.1 \text{ GeV}^{-1} \quad \text{and} \\ \beta_3^0 = -63.11 \text{ GeV}^{-1} \quad (3.2.19)$$

$$(ii) \quad \gamma_1^0 = 2118.5 \text{ GeV}^{-2}, \quad \gamma_2^0 = 1442.7 \text{ GeV}^{-2} \\ \gamma_3^0 = 59.32 \text{ GeV}^{-2} \quad (3.2.20)$$

$$(iii) \quad \beta_0^1 = 0.2 \text{ GeV}^{-1}, \quad \beta^2 = -26.24 \text{ GeV}^{-2} \quad (3.2.21)$$

We take $\alpha_{Y_0^*}(s) = \alpha_\Lambda(s)$ and $\alpha_{Y_1^*}(s) = \alpha_\Sigma(s)$.

3.3 Pion Conspiracy in Charged Pion Photo-Production:

The sharp forward peak in the charged pion photo-production has been explained by the help of conspiracy between pion and its partner of opposite parity.⁷³ According to conspiracy condition several Regge poles coincide at a particular value of the momentum transfer and thereby produce a perfectly regular behavior of the amplitude at that point, although various conspiring poles - when taken separately - are singular. The finite energy sum rules also support the fact that there is conspiracy in charged pion photo production⁷⁴. We attempt here to construct a Veneziano representation

for charged pion photo-production and obtain a fit to the differential cross-section. It is indeed known that a Veneziano model with conspirator trajectories would explain the differential cross-section of the reaction. What we wish to see here is whether such a model has correct phase factors between various amplitudes in the medium high-energy region. Just as the polarization in the charge and hypercharge exchange processes gave information about the phase factors, in photo production there is an asymmetry parameter which plays a similar role. We have evaluated the asymmetry parameter and find that it does not correspond with the present experimental numbers.

3.3.1 Kinematics and Invariant Amplitudes:

The invariant amplitudes for the pion photo production can be written as follows^{75,76}

$$T = \sum_{i=1}^4 [A_i^+ g_\beta^+ + A_i^- g_\beta^- + A_i^0 g_\beta^0] M_i \quad , \quad (3.3.1)$$

where A_i 's are scalar functions of s , t and u . The gauge invariant functions M_i are given by,

$$M_1 = i \gamma_5 \gamma \cdot \epsilon \gamma \cdot k \quad , \quad (3.3.2)$$

$$M_2 = 2i \gamma_5 (P \cdot \epsilon Q \cdot K - P \cdot K Q \cdot \epsilon) \quad , \quad (3.3.3)$$

$$M_3 = \gamma_5 (\gamma \cdot \epsilon Q \cdot K - \gamma \cdot K Q \cdot \epsilon) \quad , \quad (3.3.4)$$

$$M_4 = 2 \gamma_5 (\gamma \cdot \epsilon P \cdot K - \gamma \cdot K P \cdot \epsilon - i M_N \gamma \cdot \epsilon \gamma \cdot K) \quad , \quad (3.3.5)$$

where $P = \frac{1}{2}(p_1 + p_2)$, p_1 and p_2 being four momenta of the initial and final nucleon respectively. K and Q are the four momenta of the pion and the photon respectively and ϵ is the photon polarization vector. The isotopic spin matrices have the following form,

$$g_{\beta}^{+} = \delta_{\beta 3} \quad (3.3.6)$$

$$g_{\beta}^{-} = \frac{1}{2} [\tau_{\beta}, \tau_3] \quad (3.3.7)$$

$$g_{\beta}^0 = \tau_{\beta} \quad (3.3.8)$$

In order to study the charged pion $\gamma p \rightarrow \pi^+ n$ photo-production we consider t -channel helicity amplitudes⁷³ F_i as defined below:

$$F_1(s, t) = K_1(t) [\bar{F}_{01++}^t + \bar{F}_{01--}^t], \quad K_1(t) = \frac{1}{t - m_{\pi}^2}, \quad (3.3.9)$$

$$F_2(s, t) = K_2(t) [\bar{F}_{01++}^t - \bar{F}_{01--}^t], \quad K_2(t) = \left(\frac{t}{t - 4M_N^2} \right)^{1/2}, \quad (3.3.10)$$

$$F_3(s, t) = K_3(t) [\bar{F}_{01+-}^t + \bar{F}_{01-+}^t], \quad K_3(t) = \frac{t^{1/2}}{t - m_{\pi}^2}, \quad (3.3.11)$$

$$F_4(s, t) = K_4(t) [\bar{F}_{01+-}^t - \bar{F}_{01-+}^t], \quad K_4(t) = \frac{1}{(t - m_{\pi}^2)(t - 4M_N^2)} \quad (3.3.12)$$

Here 0, 1 represent the helicities of the pion and the photon and +(-) denote the two helicities of the nucleon and anti-nucleon. F_i 's as defined in eqns. (3.3.9) to (3.3.12) are free of kinematical singularities. The amplitudes F_1 and F_3 receive

contributions from normal parity trajectories such as ρ and A_2 . The pion contributes only to F_2 , whereas A_1 trajectory contributes to F_4 . The invariant amplitudes, A_i 's defined above, are related to F_i 's in the following manner.

$$A_1 = -(tF_1 + 2M_N F_3)/(t - 4M_N^2), \quad (3.3.13)$$

$$A_2 = \frac{F_1}{t - 4M_N^2} + \frac{F_2}{t(t - m_\pi^2)} + \frac{2M_N F_3}{t(t - 4M_N^2)}, \quad (3.3.14)$$

$$A_3 = -F_4, \quad (3.3.15)$$

$$A_4 = -\frac{(2M_N F_1 + F_3)}{(t - 4M_N^2)}. \quad (3.3.16)$$

In order that the amplitudes A_i be regular at $t = 0$ and $t = 4M_N^2$, the F_i 's must be related at these points. The pion pole in the invariant amplitude is a consequence of gauge invariance. The amplitude A_2 , at $t = 4M_N^2$, will be regular if the condition $2M_N F_1(4M_N^2) + F_3(4M_N^2) = 0$ is satisfied which is a threshold condition. However, the condition at $t = 0$ is more interesting. We get the condition,

$$F_2(0) = -\frac{m_\pi^2}{2M_N} F_3(0) \quad (3.3.17)$$

Since F_2 and F_3 receive contributions from different trajectories, if only a single trajectory contributes then we are forced to conclude that $F_2(0) = F_3(0) = 0$. This will imply that at high energies the cross-section will vanish at $t = 0$. But the existence of a sharp forward peak cannot be explained through

this mechanism if the residue functions are assumed to have a smooth t -behavior.

In order to satisfy eqn. (3.3.17) without forcing both the sides to vanish, one needs to postulate conspiring trajectories. The sharp forward peak suggests a pion exchange, so a conspiring pion is required. The pion trajectory contributes in the following manner at high energies.

$$F_2(s,t) = \beta_\pi(t) \alpha_\pi(t) \xi_\pi(t) (s/s_0)^{\alpha_\pi(t)-1}, \quad (3.3.18)$$

$$\text{where } \xi_c = \frac{1+e^{-i\pi\alpha_i(t)}}{\sin \pi\alpha_i(t)} \quad (3.3.19)$$

and s_0 is the usual scale factor taken to be 1 GeV^2 .

A Regge pole contributing to F_3 has the form

$$F_3(s,t) = \beta_c(t) \alpha_c(t) \xi_c(t) (s/s_0)^{\alpha_c(t)-1} \quad (3.3.20)$$

Then in order to satisfy eqn. (3.3.17) for all s we need $\beta_\pi(0) = - (m_\pi^2/2M_N) \beta_c(0)$ and $\alpha_c(0) = \alpha_\pi(0)$. This means pion and its conspirator must be degenerate at $t = 0$. Moreover, the conspirator must have opposite parity to the pion, but all other quantum numbers the same.

We now proceed to write a Veneziano representation for the process $\gamma p \rightarrow \pi^+ n$. We take N_α and N_γ to be degenerate⁷⁷ and write the amplitude as follows:

$$\begin{aligned}
F_1(s, t, u) = & \lambda_1 \left[B(1 - \alpha_\rho(t), \frac{1}{2} - \alpha_N(s)) + B(1 - \alpha_\rho(t), \right. \\
& \left. \frac{1}{2} - \alpha_N(u)) + B(\frac{1}{2} - \alpha_N(s), \frac{1}{2} - \alpha_N(u)) \right] \\
& + \mu_1 \left[B(1 - \alpha_\rho(t), \frac{1}{2} - \alpha_{\Delta_\delta}(s)) + B(1 - \alpha_\rho(t), \right. \\
& \left. \frac{1}{2} - \alpha_{\Delta_\delta}(u)) + B(\frac{1}{2} - \alpha_{\Delta_\delta}(s), \frac{1}{2} - \alpha_{\Delta_\delta}(u)) \right] \quad (3.3.21)
\end{aligned}$$

$$\begin{aligned}
F_2(s, t, u) = & -eg\alpha'^2(t-m_\pi^2) \frac{(-\alpha_\pi(t)) (\frac{1}{2} - \alpha_N(s))}{(\frac{3}{2} - \alpha_\pi(t) - \alpha_N(s))} \\
& + \lambda_2 \left[B(1 - \alpha_\pi(t), \frac{1}{2} - \alpha_N(s)) - B(1 - \alpha_\pi(t), \right. \\
& \left. \frac{1}{2} - \alpha_{\Delta_\delta}(u)) + B(\frac{1}{2} - \alpha_N(s), \frac{1}{2} - \alpha_{\Delta_\delta}(u)) \right] \\
& + \mu_2 \left[B(1 - \alpha_\pi(t), \frac{1}{2} - \alpha_{\Delta_\delta}(s)) - B(1 - \alpha_\pi(t), \right. \\
& \left. \frac{1}{2} - \alpha_N(u)) + B(\frac{1}{2} - \alpha_{\Delta_\delta}(s), \frac{1}{2} - \alpha_N(u)) \right] \quad (3.3.22)
\end{aligned}$$

$$\begin{aligned}
F_3(s, t, u) = & \text{pion conspirator} + \lambda_3 \left[B(1 - \alpha_{A_2}(t), \frac{1}{2} - \alpha_N(s)) \right. \\
& \left. - B(1 - \alpha_{A_2}(t), \frac{1}{2} - \alpha_{\Delta_\delta}(u)) + B(\frac{1}{2} - \alpha_N(s), \frac{1}{2} - \alpha_{\Delta_\delta}(u)) \right] \\
& + \mu_3 \left[B(1 - \alpha_{A_2}(t), \frac{1}{2} - \alpha_{\Delta_\delta}(s)) - B(1 - \alpha_{A_2}(t), \right. \\
& \left. \frac{1}{2} - \alpha_N(u)) + B(\frac{1}{2} - \alpha_{\Delta_\delta}(s), \frac{1}{2} - \alpha_N(u)) \right] \quad (3.3.23)
\end{aligned}$$

$$\begin{aligned}
F_4(s, t, u) = & \lambda_4 \left[B(1 - \alpha_{A_1}(t), \frac{1}{2} - \alpha_N(s)) + B(1 - \alpha_{A_1}(t), \right. \\
& \left. \frac{1}{2} - \alpha_N(u)) + B(\frac{1}{2} - \alpha_N(s), \frac{1}{2} - \alpha_N(u)) \right] \\
& + \mu_4 \left[B(1 - \alpha_{A_1}(t), \frac{1}{2} - \alpha_{\Delta_\delta}(s)) + B(1 - \alpha_{A_1}(t), \right. \\
& \left. \frac{1}{2} - \alpha_{\Delta_\delta}(u)) + B(\frac{1}{2} - \alpha_{\Delta_\delta}(s), \frac{1}{2} - \alpha_{\Delta_\delta}(u)) \right] \quad (3.3.24)
\end{aligned}$$

And the B functions appearing in the above equations have their usual meaning.

The first term in eqn. (3.3.22) is the pion pole term as required by gauge invariance and $g^2/4\pi = 14.9$, $e^2/4\pi = 1/137$ and α' is the common slope of all trajectories taken to be 0.9 GeV^{-2} . We choose $\alpha_\pi(t) = \alpha_{A_1}(t)$ and $\alpha_{A_2}(t) = \alpha_\rho(t)$ as implied by exchange degeneracy.

There have been many attempts to construct the Veneziano representation for pion photoproduction⁷⁸⁻⁸³. Ahmad and Fayyazuddin and Riazuddin⁸¹, and Ahmad and Fayyuzuddin⁸³ have constructed the Veneziano representation with a pion conspirator. These authors have more number of parameters in their model compared to that of ours. The parameters are fixed up by using information on low energy parameters of the baryon resonances. However they were not able to reproduce the structure of $(1/2)(s-M_N^2)^2 \left[\frac{d\sigma}{dt} (\gamma p \rightarrow \pi^+ n) + \frac{d\sigma}{dt} (\gamma n \rightarrow \pi^- p) \right]$ in the near forward direction at high energies. We have obtained a good fit to the high energy differential cross-section⁸⁴ data at photon laboratory energies 5 GeV, 8 GeV and 11 GeV as shown in Fig. 20. There has been experiments to determine the asymmetry parameters in the process $\gamma + p \rightarrow \pi^+ n$. In this experiment beams of high-energy linearly polarized photons have allowed measurements of the production asymmetry by photons with states of polarization parallel and perpendicular to the plane of production. The asymmetry parameter⁸⁵ for production of pions

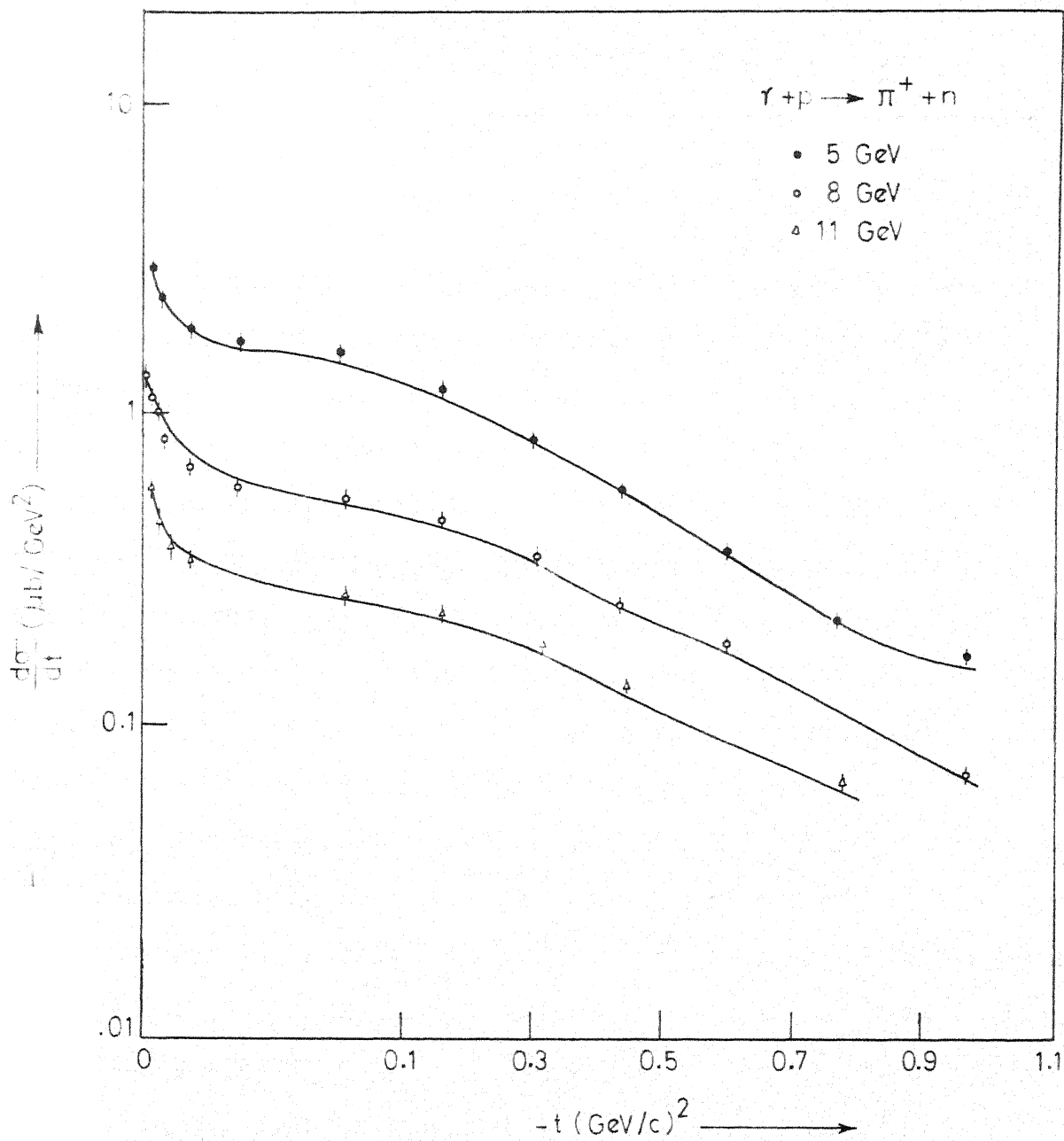


Fig. 20

with two states of proton polarization for the process $\gamma p \rightarrow \pi^+ n$ has been measured. The asymmetry parameter, in the high energy limit, can be written as

$$\Sigma(t) = \frac{-2(-t)^{1/2} \operatorname{Im} [\bar{A}_1^* A_4 + A_3^* (A_1 + tA_2)]}{32\pi \frac{d\sigma}{dt}} \quad (3.3.25)$$

The first term in the numerator corresponds to an out-of phase interference between natural parity exchanges in the t -channel while second term in the numerator contains interference between unnatural -parity exchanges. The fact that π and A_1 are exchange degenerate implies that A_3 and $A_1 + tA_2$ have the same phase and hence we expect the asymmetry parameter to be rather small for small values of t . We have calculated the asymmetry parameter in our model with the set of parameters that were used to fit the differential cross-section. But the results do not agree with the experimental data (See Fig. 21). We have also tried to obtain a simultaneous fit to the differential cross-section and the asymmetry parameter. The fit continues to be poor, with a chi square value of 55.3 against an expected 37. It is however to be noted that the data on asymmetry parameter are still meagre and not very accurate.

The set of parameters that was used to obtain the fit to the differential cross-section is given by,

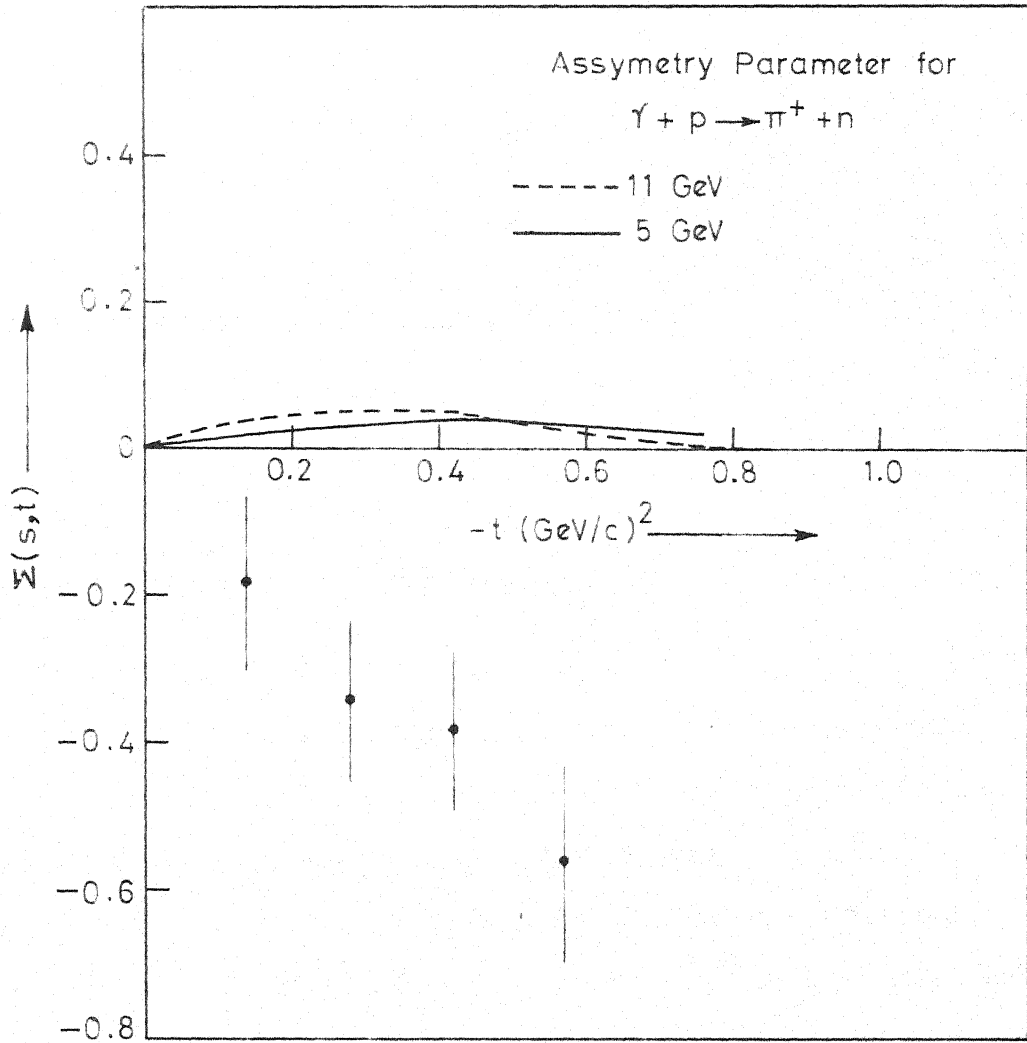


Fig. 21

$$\begin{aligned}
\lambda_1 &= 11.90 \sqrt{\mu b} \text{ GeV}^{-1} & \mu_1 &= -10.63 \sqrt{\mu b} \text{ GeV}^{-1}, \\
\lambda_2 &= .149 \sqrt{\mu b} \text{ GeV} & \mu_2 &= -.380 \sqrt{\mu b} \text{ GeV}, \\
\lambda_3 &= -21.39 \sqrt{\mu b} & \mu_3 &= 2.99 \sqrt{\mu b}, \\
\lambda_4 &= 7.99 \sqrt{\mu b} \text{ GeV}^{-2} & \mu_4 &= 2.30 \sqrt{\mu b} \text{ GeV}^{-2}.
\end{aligned}
\tag{3.3.26}$$

The trajectory functions are given by,

$$\alpha_\pi(t) = \alpha_{A_1}(t) = -0.025 + .9 t, \tag{3.3.27}$$

$$\alpha_\rho(t) = \alpha_{A_2}(t) = .5 + .9 t, \tag{3.3.28}$$

$$\alpha_N(s) = -.256 + .9s \text{ and } \alpha_{\Delta_8}(s) = .18 + .9s \tag{3.3.29}$$

Perhaps there is a need for a more sophisticated version of the Veneziano model to explain the asymmetry parameter. Indeed what we need is to include a term in the Veneziano amplitude which will produce an adequate phase difference between A_3 and $A_1 + tA_2$. Perhaps this can be done if there is a provision for Regge cut or other complicated singularities. We may speculate that inclusion of twisted loops in the dual model may contain the necessary features.

CHAPTER IV

In Chapter II and Chapter III, we have applied the Veneziano model to meson-baryon scattering processes, in the narrow resonance approximation. In this chapter we propose to study yet another application of the Veneziano model. We impose self-consistency conditions⁸⁶, on the coupling constants of the Veneziano amplitude, which follow from the unitarity of the Veneziano amplitude in the narrow resonance limit. It is well known from the optical theorem that the total cross-section for $a + b \rightarrow \text{anything}$, can be related to the imaginary part of the forward amplitude for the process $a + b \rightarrow a + b$. A similar relation can be obtained for the cross-section of the process $a + b \rightarrow c + \text{anything}$. In this case the cross-section is related to the discontinuity of the forward scattering amplitude for the process $a + b + \bar{c} \rightarrow a + b + \bar{c}$. The reaction $a + b \rightarrow c_1 + c_2 + \dots c_n + \text{anything}$, is known as an inclusive process, in which n final particles with definite momentum and quantum numbers are detected, but 'anything' is allowed to be produced in conjunction with the n -particles. The relation between the cross-section for $a + b \rightarrow c + \text{anything}$ and the discontinuity of the forward scattering amplitude of the six point function for $a + b + \bar{c} \rightarrow a + b + \bar{c}$ is obtained using a generalised unitarity relation. In deriving the bootstrap

conditions, we make use of the results of unitarity relation for the four point as well as six point amplitudes.

In the recent past, considerable attention has been focussed on the properties of the inclusive type reactions. It was conjectured by Feynman⁸⁷ and independently by Benecke⁸⁸ et al. that the inclusive cross-sections show a scaling behavior, which is independent of the energy of the incident particles. Mueller⁸⁹, then related the cross-section for the process $a + b \rightarrow c + \text{anything}$ to the discontinuity function of the forward three particle scattering amplitude of the process $a + b + \bar{c} \rightarrow a + b + \bar{c}$ as mentioned earlier. Hence, it is now possible to study the inclusive processes in different kinematical regions by examining the characteristics of the six point amplitude.

Several models⁹⁰⁻⁹⁴ have been used to understand the properties of the six point amplitude, principal among them being the multi-Regge model and Dual Resonance Model. Multi-Regge model is expected to be most useful in those kinematic regions where the total energy of the incoming particles and various sub-energies of the outgoing particles are both large. However, the experimental data in most production processes, favour the sub-energies to be not too large. Since the dual resonance model (DRM), on the contrary, incorporates the features of the high energy and the low energy resonance region in a natural way it is perhaps a better candidate for describing

multiparticle processes. Further, it should provide a unified approach to the different kinematic regions of the reactions.

Di Giacomo, Fubini, Sertorio and Veneziano⁹⁵ and Gordon and Veneziano⁹² have suggested that in the frame work of DRM, there exist self-consistency conditions on the coupling constants, as a consequence of unitarity applied to the four point and six point amplitudes. Whereas the finite energy sum rules (FESR), which reflect the principle of duality, are conditions, homogeneous in coupling constants and hence, would not be a bootstrap scheme, Veneziano^{96,97}, and Gordon and Veneziano⁹² showed how DRM had some features of a fully unitary amplitude and obtained a nonlinear equation for determining the coupling constants.

The technique makes use of the fact that the total cross-section for $a + b \rightarrow X$ is related to the absorptive part of the forward scattering amplitude and that the inclusive cross-section $a + b \rightarrow c + \text{anything}$ is given by the discontinuity across a cut in the amplitude for $a + b + \bar{c} \rightarrow a + b + \bar{c}$. In DRM the factorization of the amplitude requires the six point amplitude to be of the order of g^4 while the four point amplitude is proportional to g^2 . If one now integrates the inclusive cross-section and equates it to the total cross-section, an inhomogeneous equation in g^2 would result. This can easily be shown to give g^2 as an integral of inclusive cross-section over its kinematical range.

We have considered such an outline seriously and obtained some meson coupling constants using their masses as inputs. Exchange degeneracy is used, wherever appropriate. No attempt has been made to incorporate SU(3) or other symmetry considerations.

4.2 Single Particle Distributions and Total Cross-Section:

4.2.1 Total Cross-Section for Two Particle Scattering:

The Veneziano representation for $T_{ab \rightarrow a'b'}$ is,

$$T_{ab \rightarrow a'b'} = \frac{-2\gamma^2 \Gamma(-\alpha(t)) \Gamma(-\alpha(s))}{\Gamma(-\alpha(t)-\alpha(s))} \quad +s \rightarrow u \quad (4.2.1)$$

where $\alpha(s) = \alpha(0) + \alpha's$.

Then through optical theorem the total cross-section for $a+b \rightarrow \text{anything}$ is given by,

$$\sigma_t \underset{s \rightarrow \infty}{\sim} \frac{2\gamma^2 \pi \alpha' (\alpha(s))^{\alpha(0)-1}}{\Gamma(1 + \alpha(0))} \quad (4.2.2)$$

From Harari-Freund^{19,20} duality we know that the total cross-section can be broken up into two parts: (i) Pomeron part and (ii) Reggeon part. The former is related to the background in the direct channel and the latter is associated with the resonances in the direct channel. In the dual multi loop theory, the scattering amplitude for $a + b \rightarrow \text{anything}$ is broken up into two parts: those which contain resonances in the direct channel and those which do not. When there is no single

resonance in the direct channel $a + b$ may form two resonances and then they decay into final states. The total cross-section is obtained by squaring the amplitude and integrating over the phase space. The case when $a + b$ do form a single resonance the total cross-section is related to the imaginary part of the forward scattering amplitude for the elastic process $a + b \rightarrow a + b$. As mentioned in Ref. 92, the other contribution, to the total cross-section, comes from squaring the amplitude of Fig. 22b gives rise to twisted non planar dual loops as shown in Fig. 23. These, by virtue of their having vacuum quantum numbers in the t -channel, are associated with the Pomeron contribution and as such bring in diffraction together with non-resonating background. We shall not be concerned with either this contribution or with that coming from the interference between amplitudes of Fig. 22a and Fig. 22b, following the arguments of Gordon and Veneziano.

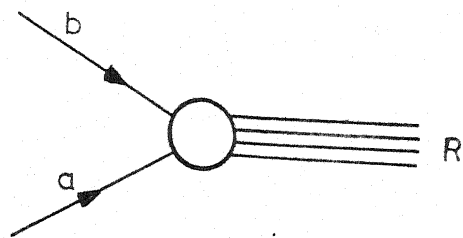
4.2.2 Kinematics of Single Particle Distribution:

We consider the inclusive reaction,

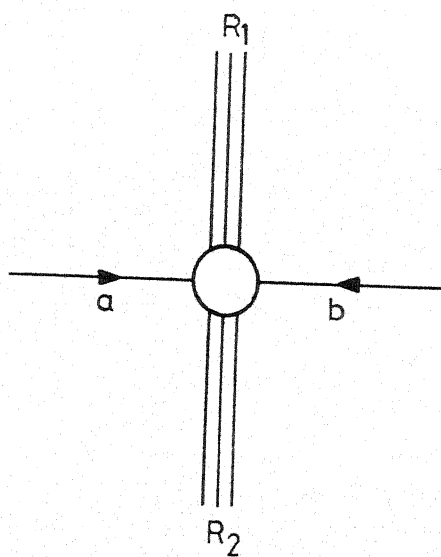
$$a + b \rightarrow c + \text{anything} \quad (4.2.3)$$

We define following invariants in terms of which the differential cross-section for this process, can be expressed.

$$\begin{aligned} s &= (p_a + p_b)^2, \quad t = (p_b - p_c)^2 \text{ and} \\ M^2 &= (p_a + p_b - p_c)^2 \end{aligned} \quad (4.2.4)$$



(a)



(b)

Fig. 22

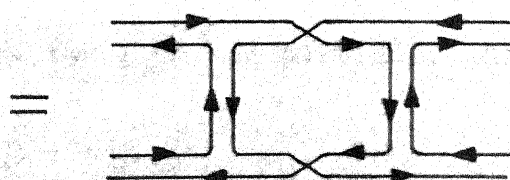
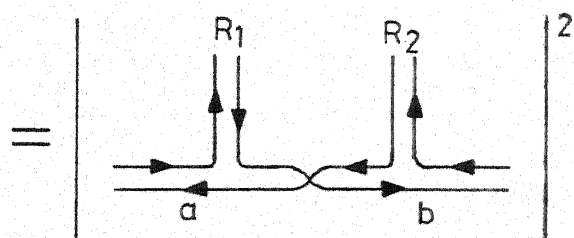
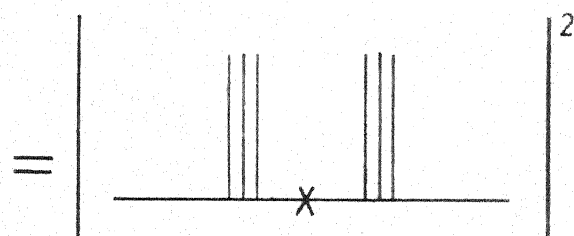
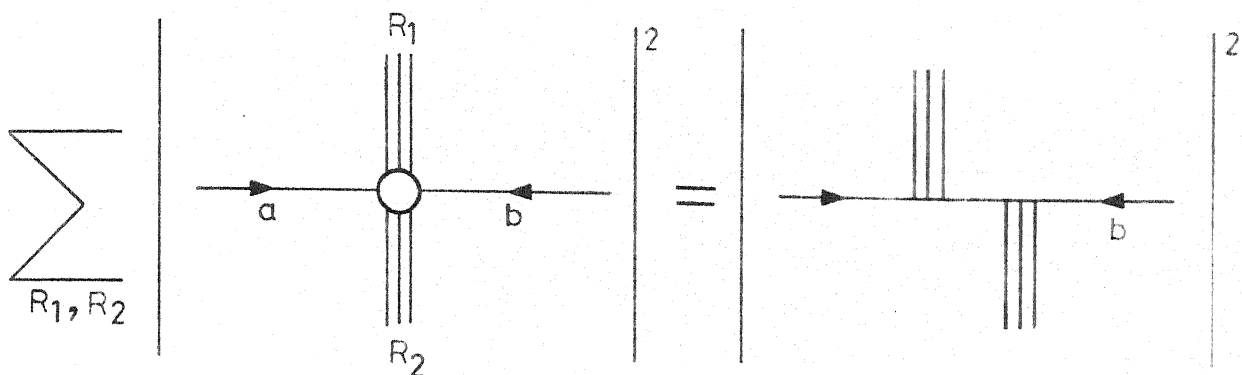
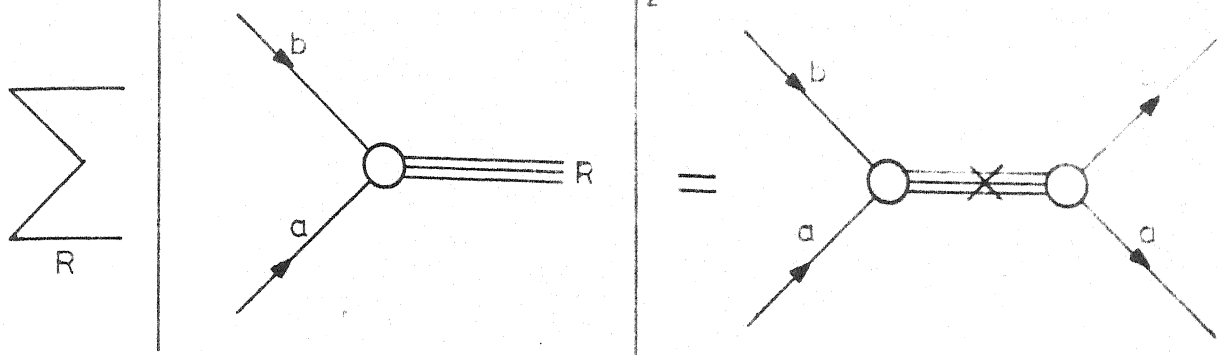


Fig. 23

Feynman⁸⁷ has used following set of variables,

$$s = (p_a + p_b)^2, \quad |p_c^\perp|, \quad x = \frac{2p_c^{\parallel}}{\sqrt{s}}, \quad (4.2.5)$$

where p_c^\perp and p_c^{\parallel} are the transverse and longitudinal momenta of the outgoing particle in the centre of mass frame.

The invariant variables defined in eqns. (4.2.4) and (4.2.5) are related as follows in the limit when $s \rightarrow \infty$, and masses of all external particles are equal.

$$t = -\frac{1}{x} (m^2(1-x)^2 + p_c^{\perp 2}) + O\left(\frac{1}{s}\right) \quad \text{for } x > 0$$

$$\bar{y} = \frac{M^2}{s} = (1 - \bar{x}) + O\left(\frac{1}{s}\right)$$

$$\bar{x} = \left(x^2 + \frac{p_c^{\perp 2} + m^2}{s/4}\right)^{1/2} = \frac{2E_c}{\sqrt{s}}, \quad (4.2.6)$$

where m is the mass of the external particles.

There has been extensive study⁹¹ on the behavior of the inclusive cross-section in different kinematical regions. We mention below the different kinematical regions, that are significant when incident energy is large.

(i) Pionization Region:

This is the region in which $s \rightarrow \text{large}$, $t \rightarrow \text{large}$, $u \rightarrow \text{large}$ and $\frac{tu}{s} \rightarrow \text{fixed}$. The amplitude has a double Regge behavior in this kinematical region and the cross-section depends upon the square of the transverse momentum of the detected particle. This

is also known as the central excitation region (CEX). The relevant diagram is shown in Fig. 24a. The detected particle has a finite momentum in the c.m. frame in this region.

(ii) Target Fragmentation (TEX) Region:

In this kinematical region $s \rightarrow \infty$, $t \rightarrow \text{fixed}$ and $\frac{s}{M^2} \rightarrow \text{fixed}$. The relevant Regge pole diagram is shown in the Fig. 24b. The inclusive cross-section, in this kinematical region can be written as,

$$E_c \frac{d^3 \sigma}{d^3 p_c} = \beta(0) s^{\alpha(0)-1} \sigma_t^{bc} \quad (4.2.7)$$

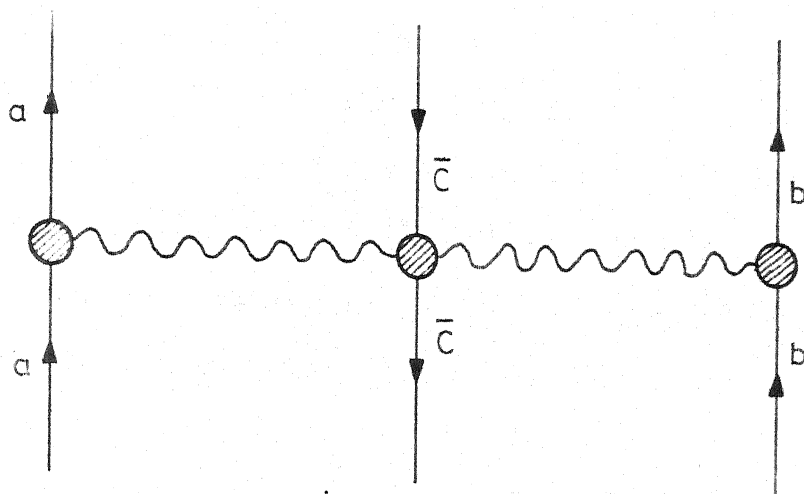
In this kinematic region the detected particle has finite momentum in the rest frame of the target.

A similar kinematical region exists for u fixed $\frac{s}{M^2}$ fixed and $s \rightarrow \infty$. This region is known as projectile fragmentation (PEX) region. In the PEX region the observed particle has finite momentum in the rest frame of the projectile.

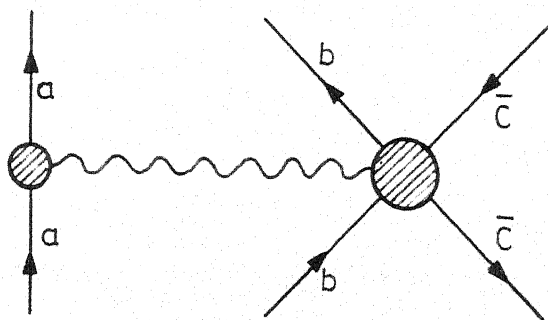
(iii) Tripple Regge Region:

This limit is approached when $s \rightarrow \text{large}$, $M^2 \rightarrow \text{large}$, $t \rightarrow \text{fixed}$ and $\frac{s}{M^2} \rightarrow \text{large}$. The inclusive cross-section has a simple closed form in this region.

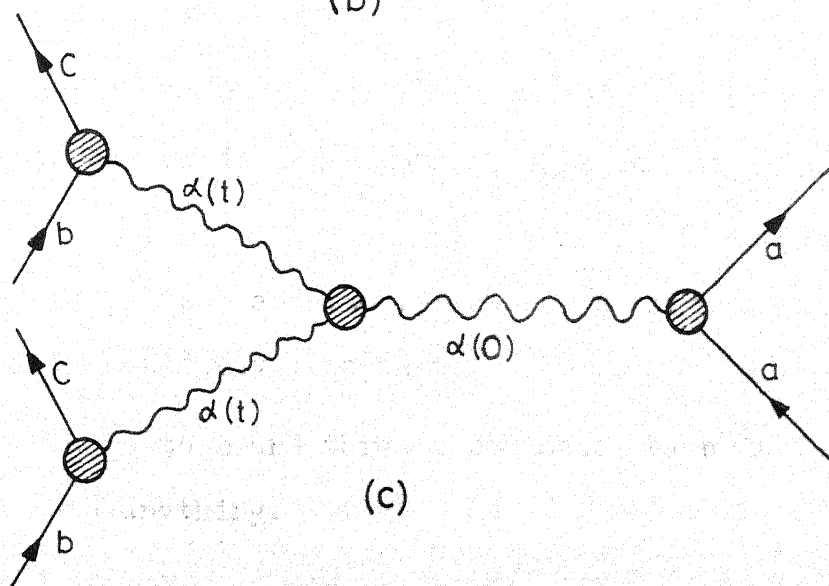
$$E_c \frac{d \sigma}{dt dM^2} \sim \frac{1}{s} \left(\frac{s}{M^2} \right)^{2\alpha(t)} \gamma_{bcR}(t) (M^2)^{\alpha(0)}, \quad (4.2.8)$$



(a)



(b)



(c)

Fig. 24

where $\gamma_{bcR}(t)$ is the residue function. We have discussed the behavior of the inclusive cross-section in different kinematical region. The relevant diagram is shown in Fig. 24c.

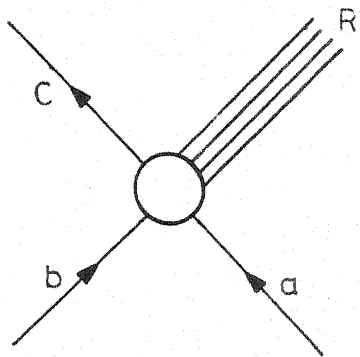
In the dual resonance model the tripple Regge region is one of the regions which can be evaluated exactly in the limit $\frac{M^2}{s} = \rho \rightarrow 0$.

Scaling⁸⁷ is a statement about the limit of the above mentioned inclusive cross-section when $s \rightarrow \infty$ and both $|p_c^\perp|$ and x are kept fixed. In terms of our variables (s , t and ρ) scaling means,

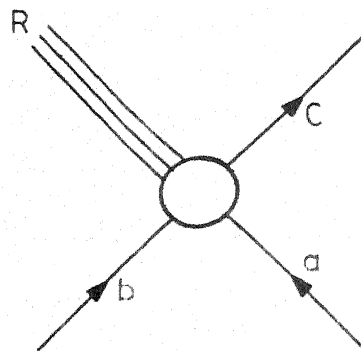
$$\lim_{\substack{s \rightarrow \infty \\ \rho, t \text{ fixed}}} \frac{d\sigma}{\sigma_t} = \frac{d^3 p_c}{E_c} G(\rho, t) \quad (4.2.9)$$

The scattering amplitude for the process $a + b \rightarrow c + \text{anything}$ gets contribution from different set of diagrams. They can be classified as follows:

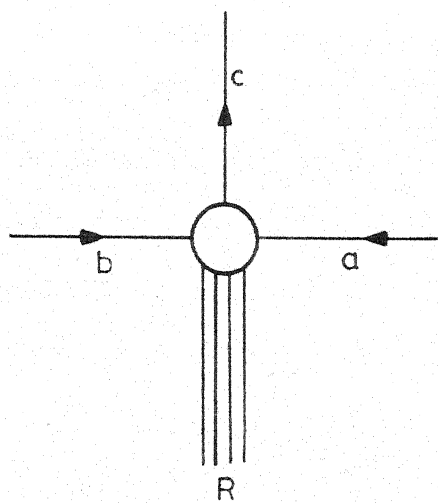
- (i) $a + b$ can go to c and a resonance which decays into anything. This can happen in three ways as shown in Fig. 25a to Fig. 25c.
- (ii) $a + b$ can go to c and two resonances R_1 and R_2 and then R_1 and R_2 can decay into anything.
- (iii) $a + b$ can go to c and three resonances which subsequently decay into anything.



(a)



(b)



(c)

Fig. 25

The processes described in (ii) and (iii) give rise to nonplanar loops. We consider diagrams corresponding to Fig. 25a to 25c, only, since other diagrams will give rise to the Pomeranchukon exchange.

4.2.3 The Total Cross-Section and Inclusive Cross-Section:

In all our calculations we have not included Pomeranchukon trajectory due to the well known difficulties present in treating Pomeranchukon in dual resonance model. Therefore, the inclusive cross-section, we shall obtain, is due to the non-Pomeranchukon trajectories alone. In calculating the total cross-section from inclusive cross-section we shall get contribution due to the Reggeon part only. The cross-section obtained in this manner is equated with the Reggeon part of the total cross-section obtained using optical theorem. Justification for such equality has been put forward by Tye and Veneziano⁹⁸ recently. Tye and Veneziano obtained following results:

$$\sum_X \sigma(a+b \rightarrow X) \equiv \sigma_t \xrightarrow{s \rightarrow \infty} c_{ab} + \bar{c}_{ab} s^{\alpha(0)-1}, \quad (4.2.10)$$

$$\sum_X \sigma(a+b \rightarrow c+X) = \frac{d\sigma_{ab}}{dp_c} \xrightarrow{s \rightarrow \infty} f_{ab}^c(x, p_c) + f_{ab}^{-c}(x, p_c, s). \quad (4.2.11)$$

In equations (4.2.10) and (4.2.11) \bar{c}_{ab} and f_{ab}^{-c} get contributions from non-Pomeranchukon trajectories. Then they⁹⁸ obtain following relations:

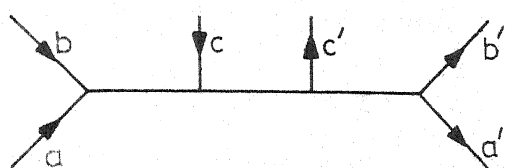
$$2c_{ab} = \sum_c \int dp_c^\perp dx_c f_{ab}^c(x_c, p_c^\perp) \quad (4.2.12)$$

$$2\bar{c}_{ab} s^{\alpha(0)-1} = \sum_c \int dp_c^\perp dx_c f_{ab}^{-c}(x_c, p_c^\perp, s) \quad (4.2.13)$$

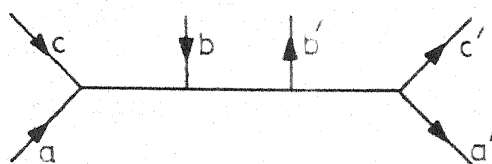
Therefore, the total cross-section obtained by integrating over d^3p_c in inclusive cross-section can be equated with the non-Pomeranchukon part of the total cross-section obtained from the optical theorem. Hopefully this justifies our retaining only amplitudes corresponding to Fig. 22a and Fig. 25a to 25c in setting up the bootstrap equation.

We have not computed diagram corresponding to Fig. 25c and interference of this diagram with Fig. 25a and Fig. 25b. Since its contribution is small (See Chapter V). Significant contribution of this diagram is related to the Pomeranchukon part. Therefore, in calculating the discontinuity functions, we have only to consider the amplitude corresponding to Fig. 26a - d.

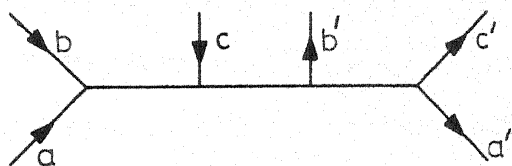
We are aware of the several shortcomings of the DRM. For example, there is no simple way of handling baryons, whose introduction give rise to the appearance of unwanted poles of wrong parity. Similarly, when the pseudoscalar mesons are introduced they cause some problems in, factorisation of the multi Veneziano amplitudes. There are problems connected with the ghost states lying on the secondary trajectories. Indeed,



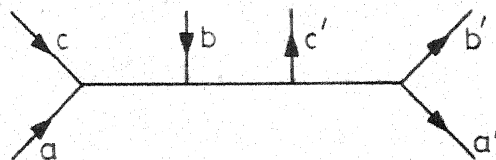
(a)



(b)



(c)



(d)

Fig. 26

there are standard, though not fully satisfactory, procedures to overcome these difficulties. We can only hope that such procedures are sufficient to get a first order approximation in solution of the bootstrap problem.

We have chosen for the study the reactions (i) $\pi^- K^+ \rightarrow \pi^- K^+$ and the inclusive reaction $\pi^- K^+ \rightarrow \pi^0 + \text{anything}$ and (ii) $\pi^+ \eta \rightarrow \pi^+ \eta$ and the inclusive reaction $\pi^+ \eta \rightarrow \pi^+ + \text{anything}$. In both cases, there is a single amplitude that participates. In the first process exchange degenerates K^* and K^{**} trajectories in the s-channel and ρ and f in t-channel are exchanged. In the second process A_2 trajectory is exchanged in the s-channel and f in the t-channel are allowed. In order to account for Pomeranchukon exchange, more complicated version of the DRM which includes 'twisted nonplanar loops' is required. We have not considered them here, primarily for the sake of simplicity, but also with the hope that the bootstrap equations could be factored into two parts, one with only Pomeranchukon exchange and the other which involves regular Regge trajectories as discussed above.

In constructing the six-point dual amplitude, we use the method prescribed by Panchapakesan. The amplitude has appropriate factors to remove the unwanted ghosts and tachyon states from the parent trajectory and satisfies factorization for states on the parent trajectories. Since we are interested only in the qualitative features of the nonlinear bootstrap we do not attempt to remove the difficulties present in the multi Veneziano model for pseudoscalar mesons.

4.2.4 The Process $\pi^- K^+ \rightarrow \pi^- K^+$ and the Inclusive Reaction $\pi^- K^+ \rightarrow \pi^0 + \text{anything}$:

We follow the method prescribed by Kawarabayashi, Kitakado and Yabuki²³ to write the amplitude for the process $\pi^- K^+ \rightarrow \pi^- K^+$. There are f and ρ trajectories exchanged in the t -channel. The s -channel and u -channel get contributions from K^* and K^{**} trajectories. We take $\alpha_{K^*} = \alpha_{K^{**}}$ and $\alpha_f = \alpha_\rho = \alpha$ using exchange degeneracy.

We write the amplitudes corresponding to definite isospin in t -channel

$$\begin{aligned}
 A^{I_t=1} &= -2\gamma^2 \left[\frac{\Gamma(1-\alpha(t)) \Gamma(1-\alpha_{K^*}(s))}{\Gamma(1-\alpha(t)-\alpha_{K^*}(s))} - \frac{\Gamma(1-\alpha(t)) \Gamma(1-\alpha_{K^*}(u))}{\Gamma(1-\alpha(t)-\alpha_{K^*}(u))} \right], \\
 A^{I_t=0} &= -2\gamma^2 \left[\frac{\Gamma(1-\alpha(t)) \Gamma(1-\alpha_{K^*}(s))}{\Gamma(1-\alpha(t)-\alpha_{K^*}(s))} - \frac{\Gamma(1-\alpha(t)) \Gamma(1-\alpha_{K^*}(u))}{\Gamma(1-\alpha(t)-\alpha_{K^*}(u))} \right]
 \end{aligned}
 \tag{4.2.14}$$

From optical theorem we get,

$$\begin{aligned}
 \sigma_t^{\pi^- K^+ \rightarrow \pi^- K^+} &= \frac{\text{Im } A^{\pi^- K^+ \rightarrow \pi^- K^+}(s, t=0)}{s} \\
 &= \frac{2}{3s} \text{Im} \left[\frac{1}{\sqrt{6}} A^{I_t=0} + A^{I_t=1} \right]
 \end{aligned}
 \tag{4.2.15}$$

where $\gamma^2 = G^2_{\pi K K^*}$, $\alpha(0) = .5$ and $\alpha' = 1 \text{ GeV}^{-2}$ is the common slope of all trajectories as required by the Veneziano model.

In the equation (4.2.15), we have written the contribution due to the non-Pomeranchukon trajectories to the total cross-section.

Now we construct six point functions for the process $\pi^- K^+ \rightarrow \pi^0$ anything in the following manner, keeping only trajectories which have highest intercept in each channel. The amplitudes corresponding to Fig. 26a-26d are written down separately as B_6^a , B_6^b , B_6^c and B_6^d respectively.

$$\begin{aligned}
 B_6^a = & G^4 \int_0^1 \int_0^1 \int_0^1 dx_1 dx_2 dx_3 x_1^{-\alpha_{K^*}(s)-1} x_2^{-\alpha_{K^*}(M^2)-1} x_3^{-\alpha_{K^*}(\bar{s})-1} \\
 & \times (1-x_1)^{-\alpha(t)-1} (1-x_2)^{-\alpha(0)-1} (1-x_3)^{-\alpha(t)-1} \\
 & \times (1-x_1 x_2)^{2\alpha(0)+\alpha't} (1-x_2 x_3)^{2\alpha(0)+\alpha't} (1-x_1 x_2 x_3)^{-2\alpha(0)} F_1(x, p)
 \end{aligned}
 \tag{4.2.16}$$

$$\begin{aligned}
 \text{where } F_1(x, p) = & [\alpha_{K^*}(s)(1-x_1) + \alpha(t)x_1] [\alpha_{K^*}(\bar{s})(1-x_3) \\
 & + \alpha(t)x_3] \alpha_{K^*}(M^2)(1-x_2)
 \end{aligned}$$

is multiplied to kill ghosts on the leading trajectory at $\alpha(t) = 0$.

$$s = \text{Re } s + i\epsilon, \quad \bar{s} = \text{Re } s - i\epsilon \quad \text{and} \quad G^4 = G^4_{\pi K K^*} G^2_{K^* K^* \pi}$$

Similarly,

$$B_6^b = G^4 \int_0^1 \int_0^1 \int_0^1 dx_1 dx_2 dx_3 x_1^{-\alpha_K^*(u)-1} x_2^{-\alpha_K^*(M^2)-1} x_3^{-\alpha_K^*(\bar{u})-1} \\ \times (1-x_1)^{-\alpha(t)-1} (1-x_2)^{-\alpha(0)-1} (1-x_3)^{-\alpha(t)-1} \\ \times (1-x_1 x_2)^{2\alpha(0)+\alpha't} (1-x_2 x_3)^{2\alpha(0)+\alpha't} (1-x_1 x_2 x_3)^{-2\alpha(0)} F_2(x, p), \quad (4.2.17)$$

$$B_6^c = G^4 \int_0^1 \int_0^1 \int_0^1 dx_1 dx_2 dx_3 x_1^{-\alpha_K^*(s)-1} x_2^{-\alpha_K^*(M^2)-1} x_3^{-\alpha_K^*(\bar{u})-1} \\ \times (1-x_1)^{-\alpha(t)-1} (1-x_2)^{-\alpha(t)-1} (1-x_3)^{-\alpha(t)-1} \\ \times (1-x_1 x_2)^{2\alpha(t)} (1-x_2 x_3)^{2\alpha(t)} (1-x_1 x_2 x_3)^{-\alpha(t)-\alpha(0)} F_3(x, p), \quad (4.2.18)$$

$$B_6^d = G^4 \int_0^1 \int_0^1 \int_0^1 dx_1 dx_2 dx_3 x_1^{-\alpha_K^*(u)-1} x_2^{-\alpha_K^*(M^2)-1} x_3^{-\alpha_K^*(\bar{s})-1} \\ \times (1-x_1)^{-\alpha(t)-1} (1-x_2)^{-\alpha(t)-1} (1-x_3)^{-\alpha(t)-1} \\ \times (1-x_1 x_2)^{2\alpha(t)} (1-x_2 x_3)^{2\alpha(t)} (1-x_1 x_2 x_3)^{-\alpha(t)-\alpha(0)} F_4(x, p), \quad (4.2.19)$$

with,

$$F_2(x, p) = [\alpha_K^*(u)(1-x_1) + \alpha(t)x_1] \\ \times [\alpha_K^*(\bar{u})(1-x_3) + \alpha(t)x_3] [\alpha_K^*(M^2)(1-x_2)] ,$$

$$F_3(x, p) = [\alpha_K^*(s)(1-x_1) + \alpha(t)x_1] [\alpha_K^*(M^2)(1-x_2) \\ + \alpha(t)x_2] [\alpha_K^*(\bar{u})(1-x_3) + \alpha(t)x_3] ,$$

$$F_4(x,p) = [x_1 \alpha(t) + \alpha_K^*(u)(1-x_1)] [x_2 \alpha(t) + \alpha_K^*(1-x_2)] \\ [\alpha_K^*(s)(1-x_3) + \alpha(t)x_3] \quad , \quad (4.2.20)$$

and $u = \text{Re } u + i\epsilon$, $\bar{u} = \text{Re } u - i\epsilon$. Here and every where

$$\alpha_f(z) = \alpha_\rho(z) = \alpha_{A_2}(z) = .5 + z = \alpha(z).$$

To calculate the inclusive cross-section we have to take discontinuity across the ρ cut of the above mentioned amplitude.

4.2.5 $\pi\eta \rightarrow \pi\eta$ and the Inclusive Reaction $\pi\eta \rightarrow \pi + \text{anything}$:

In the process $\pi\eta \rightarrow \pi\eta$, A_2 is exchanged in the s and u channel and f is exchanged in the t-channel. We write the amplitude as follows:

$$A = -2g^2 \pi \eta A_2 \left[-\frac{\Gamma(1-\alpha(t)) \Gamma(1-\alpha(s))}{\Gamma(1-\alpha(t) - \alpha(s))} + \frac{\Gamma(1-\alpha(t)) \Gamma(1-\alpha(u))}{\Gamma(1-\alpha(t) - \alpha(u))} \right. \\ \left. + \frac{\Gamma(1-\alpha(u)) \Gamma(1-\alpha(s))}{\Gamma(1-\alpha(s) - \alpha(s))} \right] \quad (4.2.21)$$

And the total cross-section due to the non-Pomeranchukon part in the limit $s \rightarrow \infty$ is:

$$\sigma_t = 2g^2 \pi \eta A_2 \frac{\pi \alpha'(\alpha_{A_2}(s))^{\alpha_f(0)-1}}{\Gamma(\alpha(0))} \quad (4.2.22)$$

The six point functions whose discontinuities are related to the inclusive cross-section of the process $\pi\eta \rightarrow \pi + \text{anything}$ are the following:

$$\begin{aligned}
B_6'^a &= G'^4 \int_0^1 \int_0^1 \int_0^1 dx_1 dx_2 dx_3 x_1^{-\alpha(s)-1} x_2^{-\alpha(M^2)-1} x_3^{-\alpha(\bar{s})-1} \\
&\quad (1-x_1)^{-\alpha(t)-1} (1-x_2)^{-\alpha(0)-1} (1-x_3)^{-\alpha(t)-1} (1-x_1 x_2)^{2\alpha(0)+\alpha't} \\
&\quad (1-x_2 x_3)^{2\alpha(0)+\alpha't} (1-x_1 x_2 x_3)^{-2\alpha(0)} F_1'(x, p) \quad , \quad (4.2.23)
\end{aligned}$$

$$\begin{aligned}
B_6'^b &= G'^4 \int_0^1 \int_0^1 \int_0^1 dx_1 dx_2 dx_3 x_1^{-\alpha(u)-1} x_2^{-\alpha(M^2)-1} x_3^{-\alpha(\bar{u})-1} \\
&\quad (1-x_1)^{-\alpha(t)-1} (1-x_2)^{-\alpha(0)-1} (1-x_1 x_2)^{2\alpha(0)+\alpha't} \\
&\quad (1-x_2 x_3)^{2\alpha(0)+\alpha't} (1-x_1 x_2 x_3)^{-2\alpha(0)} F_2'(x, p) \quad , \quad (4.2.24)
\end{aligned}$$

$$\begin{aligned}
B_6'^c &= G'^4 \int_0^1 \int_0^1 \int_0^1 dx_1 dx_2 dx_3 x_1^{-\alpha(s)-1} x_2^{-\alpha(M^2)-1} x_3^{-\alpha(\bar{u})-1} \\
&\quad (1-x_1)^{-\alpha(t)-1} (1-x_2)^{-\alpha(t)-1} (1-x_3)^{-\alpha(t)-1} (1-x_1 x_2)^{2\alpha(t)} \\
&\quad (1-x_2 x_3)^{2\alpha(t)} (1-x_1 x_2 x_3)^{-\alpha(t)-\alpha(0)} F_3'(x, p) \quad , \quad (4.2.25)
\end{aligned}$$

$$\begin{aligned}
B_6'^d &= G'^4 \int_0^1 \int_0^1 \int_0^1 dx_1 dx_2 dx_3 x_1^{-\alpha(u)-1} x_2^{-\alpha(M^2)-1} x_3^{-\alpha(\bar{s})-1} \\
&\quad (1-x_1)^{-\alpha(t)-1} (1-x_2)^{-\alpha(t)-1} (1-x_3)^{-\alpha(t)-1} (1-x_1 x_2)^{2\alpha(t)} \\
&\quad (1-x_2 x_3)^{2\alpha(t)} (1-x_1 x_2 x_3)^{-\alpha(t)-\alpha(0)} F_4'(x, p) \quad , \quad (4.2.26)
\end{aligned}$$

where, $F_1' = (\alpha(s)(1-x_1)+\alpha(t)x_1)(\alpha(\bar{s})(1-x_3)+\alpha(t)x_3)\alpha(M^2)(1-x_2)$,

$F_2' = (\alpha(s)(1-x_1)+\alpha(t)x_1)(\alpha(\bar{s})(1-x_3)+\alpha(t)x_3)\alpha(M^2)(1-x_2)$,

$F_3' = (\alpha(s)(1-x_1)+\alpha(t)x_1)(\alpha(M^2)(1-x_2)+\alpha(t)x_2)(\alpha(\bar{u})$

$(1-x_3)+\alpha(t)x_3)$,

$$F'_4 = (x_1 \alpha(t) + \alpha(u)(1-x_1))(x_2 \alpha(t) + \alpha(M^2)(1-x_2))(\alpha(\bar{s})(1-x_3) + \alpha(t)x_3) \quad (4.2.27)$$

$$G'^4 = g_{\pi\gamma A_2}^2 g_{A_2 \rho \pi}^2$$

Now we proceed to calculate the discontinuity functions of the six point functions defined above.

4.3 Discontinuity Functions:

In this section, we shall calculate the discontinuity function of the six point amplitude in different asymptotic limits.

We begin with the explicit evaluation of the discontinuity function for the amplitude B_6^a in the limit when $s \rightarrow \infty$ $M^2 \rightarrow$ large, $\frac{M^2}{s} = \rho \rightarrow 0$ and t is fixed and small (Tripple Regge limit).

First of all we make a change of variable using methods of Bardakçi and Rucgg¹⁰⁰. We define,

$$x_1 = e^{\frac{-U}{-\alpha_K^*(s)-1}} \quad x_2 = e^{\frac{-W}{-\alpha_K^*(M^2)-1}} \quad x_3 = e^{\frac{-V}{-\alpha_K^*(\bar{s})-1}}$$

$$\begin{aligned} B_6^a &= \alpha_K^*(M^2) \alpha_K^*(s) \alpha_K^*(\bar{s}) (-\alpha_K^*(s)-1)^{\alpha(t)-1} (-\alpha_K^*(\bar{s})-1)^{\alpha(t)-1} \\ &\times (-\alpha_K^*(M^2)-1)^{\alpha(0)-2\alpha(t)-1} \int_0^\infty \int_0^\infty \int_0^\infty dU dV dW e^{-(U+V+W)} \\ &\times (UV)^{-\alpha(t)} W^{-\alpha(0)} (F(U')F(V'))^{-\alpha(t)} (F(W'))^{-\alpha(0)} \\ &\times (\rho_{U+W})^{2\alpha(0)+\alpha't} (\bar{\rho}_{V+W})^{2\alpha(0)+\alpha't} F(U'+W')^{2\alpha(0)+\alpha't} \end{aligned}$$

$$\begin{aligned}
& \times F(V'+W')^{2\alpha(0)+\alpha't} (U\rho_U+\bar{\rho}_V+W)^{-2\alpha(0)} F(U'+V'+W')^{-2\alpha(0)} \\
& + \alpha_{K^*}(s) \alpha(t) \alpha_{K^*}(M^2) (-\alpha_{K^*}(s)-1)^{\alpha(t)-1} (1-\alpha_{K^*}(\bar{s})-1)^{\alpha(t)} \\
& \times (-\alpha_{K^*}(M^2)-1)^{\alpha(0)-2\alpha(t)-1} \int_0^\infty \int_0^\infty \int_0^\infty dU dV dW e^{-(U''+V''+W'')} \\
& \times e^{-V' U^{-\alpha(t)} V^{-\alpha(t)-1} W^{-\alpha(0)} F(U')^{-\alpha(t)} F(V')^{-\alpha(t)-1}} \\
& \times F(W')^{-\alpha(0)} (\rho_{U+W})^{2\alpha(0)+\alpha't} (\bar{\rho}_{V+W})^{2\alpha(0)+\alpha't} \\
& \times (\rho_U+\bar{\rho}_{V+W})^{-2\alpha(0)} (F(U'+W')F(V'+W'))^{2\alpha(0)+\alpha't} \\
& \times (F(U'+V'+W'))^{-2\alpha(0)} + \alpha_{K^*}(M^2) \alpha_{K^*}(\bar{s}) \alpha(t) (-\alpha_{K^*}(s)-1)^{\alpha(t)} \\
& \times (-\alpha_{K^*}(\bar{s})-1)^{\alpha(t)-1} (-\alpha_{K^*}(M^2)-1)^{\alpha(0)-2\alpha(t)-1} \int_0^\infty \int_0^\infty \int_0^\infty \\
& \times dU dV dW e^{-(U''+V''+W'')} e^{-U' U^{-\alpha(t)-1} V^{-\alpha(t)} W^{-\alpha(0)}} \\
& \times F(U')^{-\alpha(t)-1} V^{-\alpha(t)} W^{-\alpha(0)} F(U')^{-\alpha(t)-1} F(V')^{-\alpha(t)} \\
& \times F(W')^{-\alpha(0)} ((\rho_{U+W})(\bar{\rho}_{V+W}))^{2\alpha(0)+\alpha't} (F(U'+W'))^{2\alpha(0)+\alpha't} \\
& \times F(V'+W')^{2\alpha(0)+\alpha't} (\rho_U+\bar{\rho}_{V+W})^{-2\alpha(0)} F(U'+V'+W')^{-2\alpha(0)} \\
& + \alpha_{K^*}(M^2) \alpha(t) \alpha(t) (-\alpha_{K^*}(s)-1)^{\alpha(t)} (-\alpha_{K^*}(\bar{s})-1)^{\alpha(t)} \\
& \times (-\alpha_{K^*}(M^2)-1)^{\alpha(0)-2\alpha(t)-1} \int_0^\infty \int_0^\infty \int_0^\infty dU dV dW e^{-(U''+V''+W'')} \\
& \times e^{-(U'+V')} (UV)^{-\alpha(t)-1} W^{-\alpha(0)} (F(U')F(V'))^{-\alpha(t)-1} \\
& \times F(W')^{-\alpha(0)} ((\rho_{U+W})(\bar{\rho}_{V+W}))^{2\alpha(0)+\alpha't} (F(U'+W')F(V'+W'))^{2\alpha(0)+\alpha't} \\
& \times (\rho_U+\bar{\rho}_{V+W})^{-2\alpha(0)} F(U'+V'+W')^{-2\alpha(0)}
\end{aligned}$$

where,

$$U' = \frac{U}{-\alpha_K^*(s)-1}, \quad V' = \frac{V}{-\alpha_K^*(\bar{s})-1}, \quad W' = \frac{W}{-\alpha_K^*(M^2)-1} \quad (4.3.2)$$

$$U'' = U + U', \quad V'' = V + V', \quad W'' = W + W' \quad (4.3.3)$$

$$F(x) = \frac{1}{x} (1-e^{-x}), \quad \rho = \frac{\alpha(M^2)}{\alpha(s)}, \quad \bar{\rho} = \frac{\alpha(M^2)}{\alpha(\bar{s})} \quad (4.3.4)$$

The other amplitudes can be written as follows:

$$\begin{aligned} B_6^b &= \alpha_K^*(M^2) \alpha_K^*(u) \alpha_K^*(\bar{u}) (-\alpha_K^*(u)-1)^{\alpha(t)-1} (-\alpha_K^*(\bar{u})-1)^{\alpha(t)-1} \\ &\times (-\alpha_K^*(M^2)-1)^{\alpha(0)-2\alpha(t)-1} \int_0^\infty \int_0^\infty \int_0^\infty dU dV dW e^{-(U''+V''+W'')} (UV)^{-\alpha(t)} \\ &\times W^{-\alpha(0)} (F(U')F(V'))^{-\alpha(t)} (F(W'))^{-\alpha(0)} ((U\rho'+W)(V\bar{\rho}+W))^{2\alpha(0)+\alpha't} \\ &\times (F(U'+W'))^{2\alpha(0)+\alpha't} (U\rho'+V\bar{\rho}+W)^{-2\alpha(0)} \\ &\times (F(U'+V'+W'))^{-2\alpha(0)} + \alpha_K^*(M^2) \alpha_K^*(u) \alpha(t) (-\alpha_K^*(u)-1)^{\alpha(t)-1} \\ &\times (-\alpha_K^*(\bar{u})-1)^{\alpha(t)} (-\alpha_K^*(M^2)-1)^{\alpha(0)-2\alpha(t)-1} \int_0^\infty \int_0^\infty \int_0^\infty dU dV dW \\ &\times e^{-(U''+V''+W'')} e^{-V'} U^{-\alpha(t)} V^{-\alpha(t)-1} W^{-\alpha(0)} F(U')^{-\alpha(t)} F(V')^{-\alpha(t)-1} \\ &\times F(W)^{-\alpha(0)} ((U\rho'+W)(V\bar{\rho}+W))^{2\alpha(0)+\alpha't} (F(U'+W'))^{2\alpha(0)+\alpha't} \\ &\times F(V'+W')^{2\alpha(0)+\alpha't} (U\rho'+V\bar{\rho}+W)^{-2\alpha(0)} F(U'+V'+W')^{-2\alpha(0)} \\ &+ \alpha_K^*(M^2) \alpha(t) \alpha_K^*(\bar{u}) (-\alpha_K^*(\bar{u})-1)^{\alpha(t)-1} (-\alpha_K^*(u)-1)^{\alpha(t)} \end{aligned}$$

$$\begin{aligned}
& \times (-\alpha_{K*}(M^2)-1)^{\alpha(0)-2\alpha(t)-1} \int_0^\infty \int_0^\infty \int_0^\infty dU dV dW e^{-(U''+V''+W'')} e^{-U'} \\
& \times U^{-\alpha(t)-1} V^{-\alpha(t)} W^{-\alpha(0)} F(U')^{-\alpha(t)-1} F(V')^{-\alpha(t)} F(W')^{-\alpha(0)} \\
& ((U\rho'+W)(V\bar{\rho}'+W))^{2\alpha(0)+\alpha't} (F(U'+W')F(V'+W'))^{2\alpha(0)+\alpha't} \\
& (U\rho'+V\bar{\rho}'+W)^{-2\alpha(0)} (F(U'+V'+W'))^{-2\alpha(0)} + \alpha_{K*}(M^2)\alpha(t)\alpha(t) \\
& \times (-\alpha_{K*}(u)-1)^{\alpha(t)} (-\alpha_{K*}(\bar{u})-1)^{\alpha(t)} (-\alpha_{K*}(M^2)-1)^{\alpha(0)-2\alpha(t)-1} \\
& \times \int_0^\infty \int_0^\infty \int_0^\infty dU dV dW e^{-(U''+V''+W'')} e^{-(U'+V')} (UV)^{-\alpha(t)-1} W^{-\alpha(0)} \\
& \times (F(U')F(V'))^{-\alpha(t)-1} F(W')^{-\alpha(0)} ((U\rho'+W)(V\bar{\rho}'+W))^{2\alpha(0)+\alpha't} \\
& \times (F(U'+W')F(V'+W'))^{2\alpha(0)+\alpha't} (U\rho'+V\bar{\rho}'+W)^{-2\alpha(0)} \\
& \times (F(U'+W'+V'))^{-2\alpha(0)} \quad (4.3.5)
\end{aligned}$$

It is understood that the change of variable for x_1, x_2, x_3 is made in terms of the Mandelstam variable u . And $\rho' = \frac{M^2}{u}$, $\bar{\rho}' = \frac{M^2}{\bar{u}}$.

$$\begin{aligned}
B_6^C &= \alpha_{K*}(s)\alpha_{K*}(M^2)\alpha_{K*}(\bar{u})(-\alpha_{K*}(s)-1)^{\alpha(t)-1}(-\alpha_{K*}(\bar{u})-1)^{\alpha(t)-1} \\
& \times (-\alpha_{K*}(M^2)-1)^{\alpha(0)-2\alpha(t)-1} \int_0^\infty \int_0^\infty \int_0^\infty dU dV dW e^{-(U''+V''+W'')} \\
& \times (UVW)^{-\alpha(t)} (FU')F(V')F(W')^{-\alpha(t)} (\rho'_{U+W})^{2\alpha(t)} (\bar{\rho}'_{V+W})^{2\alpha(t)} \\
& (F(U'+W')F(V'+W'))^{2\alpha(t)} (\rho'_{U+W}\bar{\rho}'_{V+W})^{-\alpha(0)-\alpha(t)}
\end{aligned}$$

$$\begin{aligned}
& (\rho_{U+W} \bar{\rho}'_{V+W})^{-\alpha(0)-\alpha(t)} F(U'+V'+W')^{-\alpha(0)-\alpha(t)} + \alpha_K^*(s) \alpha(t) \\
& \times \alpha_K^*(\bar{u}) (-\alpha_K^*(s)-1)^{\alpha(t)-1} (-\alpha_K^*(\bar{u})-1)^{\alpha(t)-1} \\
& \times (-\alpha_K^*(M^2)-1)^{\alpha(0)-2\alpha(t)} \int_0^\infty \int_0^\infty \int_0^\infty dU dV dW e^{-(U''+V''+W'')} \\
& \times e^{-W'} (UV)^{-\alpha(t)} (F(U')F(V'))^{-\alpha(t)} W^{-\alpha(t)-1} (F(W'))^{-\alpha(t)-1} \\
& \times ((\rho_{U+W})(\bar{\rho}'_{V+W}))^{2\alpha(t)} (F(U'+W')F(V'+W'))^{2\alpha(t)} \\
& \times (\rho_{U+W} \bar{\rho}'_{V+W})^{-\alpha(0)-\alpha(t)} F(U'+V'+W')^{-\alpha(0)-\alpha(t)} + \alpha_K^*(s) \alpha(t) \\
& \times \alpha(t) (-\alpha_K^*(s)-1)^{\alpha(t)-1} (-\alpha_K^*(\bar{u})-1)^{\alpha(t)} (-\alpha_K^*(M^2)-1)^{\alpha(0)-2\alpha(t)} \\
& \times \int_0^\infty \int_0^\infty \int_0^\infty dU dV dW e^{-(U''+V''+W'')} e^{-(V'+W')} (VW)^{-\alpha(t)-1} \\
& \times (F(V')F(W'))^{-\alpha(t)-1} U^{-\alpha(t)} F(U')^{-\alpha(t)} ((\rho_{U+W})(\bar{\rho}'_{V+W}))^{2\alpha(t)} \\
& \times (F(U'+W')F(V'+W'))^{2\alpha(t)} (\rho_{U+W} \bar{\rho}'_{V+W})^{-\alpha(0)-\alpha(t)} \\
& \times (F(U'+V'+W'))^{-\alpha(0)-\alpha(t)} + \alpha(t) \alpha_K^*(M^2) \alpha_K^*(\bar{u}) (-\alpha_K^*(s)-1)^{\alpha(t)} \\
& \times (-\alpha_K^*(\bar{u})-1)^{\alpha(t)-1} (-\alpha_K^*(M^2)-1)^{\alpha(0)-2\alpha(t)-1} \int_0^\infty \int_0^\infty \int_0^\infty dU dV dW \\
& e^{-(U''+V''+W'')} e^{-U'} U^{-\alpha(t)-1} F(U')^{-\alpha(t)-1} (VW)^{-\alpha(t)} \\
& (F(V')F(W'))^{-\alpha(t)} ((\rho_{U+W})(\bar{\rho}'_{V+W}))^{2\alpha(t)} (F(U'+W')F(V'+W'))^{2\alpha(t)} \\
& (U \rho_{U+W} \bar{\rho}'_{V+W})^{-\alpha(0)-\alpha(t)} F(U'+V'+W')^{-\alpha(0)-\alpha(t)} + \alpha(t) \alpha(t) \alpha(t)
\end{aligned}$$

$$\begin{aligned}
& \times (-\alpha_{K^*}(s)-1)^{\alpha(t)} (-\alpha_{K^*}(\bar{u})-1)^{\alpha(t)} (-\alpha_{K^*}(M^2)-1)^{\alpha(0)-2\alpha(t)} \\
& \times \int_0^\infty \int_0^\infty \int_0^\infty dU dV dW e^{-\frac{1}{2}(U''+V''+W'')} e^{-\frac{1}{2}(U'+V'+W')} (UVW)^{-\alpha(t)-1} \\
& \times (F(U')F(V')F(W'))^{-\alpha(t)-1} ((\rho_{U+W})(\bar{\rho}'_{V+W}))^{2\alpha(t)} (F(U'+W'))^{2\alpha(t)} \\
& \times F(V'+W')^{2\alpha(t)} (U\rho+\bar{\rho}'_{V+W})^{-\alpha(0)-\alpha(t)} F(U'+V'+W')^{-\alpha(0)-\alpha(t)} \\
& + \alpha(t)\alpha(t)\alpha_{K^*}(M^2)(-\alpha_{K^*}(s)-1)^{\alpha(t)} (-\alpha_{K^*}(\bar{u})-1)^{\alpha(t)} \\
& \times (-\alpha_{K^*}(M^2)-1)^{\alpha(0)-2\alpha(t)-1} \int_0^\infty \int_0^\infty \int_0^\infty dU dV dW e^{-\frac{1}{2}(U''+V''+W'')} \\
& \times e^{-\frac{1}{2}(U'+V')} (UV)^{-\alpha(t)-1} (F(U')F(V'))^{-\alpha(t)-1} \frac{1}{W} F(W')^{-\alpha(t)} \\
& \times ((\rho_{U+W})(\bar{\rho}'_{V+W}))^{2\alpha(t)} (F(U'+W')F(V'+W'))^{2\alpha(t)} (U\rho+\bar{\rho}'_{V+W})^{-\alpha(0)-\alpha(t)} \\
& \times (U\rho+\bar{\rho}'_{V+W})^{-\alpha(0)-\alpha(t)} F(U'+V'+W')^{-\alpha(0)-\alpha(t)} + \alpha(t)\alpha(t), \\
& \times \alpha_{K^*}(\bar{u})(-\alpha_{K^*}(s)-1)^{\alpha(t)} (-\alpha_{K^*}(\bar{u})-1)^{\alpha(t)-1} (-\alpha_{K^*}(M^2)-1)^{\alpha(0)-2\alpha(t)} \\
& \times \int_0^\infty \int_0^\infty \int_0^\infty dU dV dW e^{-\frac{1}{2}(U''+V''+W'')} e^{-\frac{1}{2}(W'+U')} (UW)^{-\alpha(t)-1} \frac{1}{V} F(V')^{-\alpha(t)} \\
& \times (F(U')F(W'))^{-\alpha(t)-1} F(V')^{-\alpha(t)} ((\rho_{U+W})(\bar{\rho}'_{V+W}))^{2\alpha(t)} \\
& \times (F(U'+W')F(V'+W'))^{2\alpha(t)} (U\rho+V\bar{\rho}'_{V+W})^{-\alpha(0)-\alpha(t)} \\
& F(U'+V'+W')^{-\alpha(0)-\alpha(t)}
\end{aligned}$$

(4.3.6)

$$\begin{aligned}
B_6^d = & \alpha_{K^*}(\bar{s}) \alpha_{K^*}(u) \alpha_{K^*}(M^2) (-\alpha_{K^*}(u)-1)^{\alpha(t)-1} \\
& \times (-\alpha_{K^*}(\bar{s})-1)^{\alpha(t)-1} (-\alpha_{K^*}(M^2)-1)^{\alpha(0)-2\alpha(t)-1} \int_0^\infty \int_0^\infty \int_0^\infty \\
& \times dU dV dW e^{-\frac{1}{2}(U'+V'+W')} (UVW)^{-\alpha(t)} (F(U')F(V')F(W'))^{-\alpha(t)} \\
& \times ((\bar{\rho}'_{U+W})(\bar{\rho}'_{V+W}))^{2\alpha(t)} (F(U'+W')F(V'+W'))^{2\alpha(t)} \\
& \times (\bar{\rho}'_{U+W} \bar{\rho}'_{V+W})^{-\alpha(0)-\alpha(t)} F(U'+V'+W')^{-\alpha(0)-\alpha(t)} \\
& + \alpha_{K^*}(u) \alpha_{K^*}(M^2) \alpha(t) (-\alpha_{K^*}(u)-1)^{\alpha(t)-1} (-\alpha_{K^*}(\bar{s})-1)^{\alpha(t)} \\
& \times (-\alpha_{K^*}(M^2)-1)^{\alpha(0)-2\alpha(t)-1} \int_0^\infty \int_0^\infty \int_0^\infty dU dV dW e^{-\frac{1}{2}(U'+V'+W')} e^{-V'} \\
& \times (UW)^{-\alpha(t)} (F(U')F(W'))^{-\alpha(t)} V^{-\alpha(t)-1} F(V')^{-\alpha(t)-1} \\
& \times ((\bar{\rho}'_{U+W})(\bar{\rho}'_{V+W}))^{2\alpha(t)} (F(U'+W')F(V'+W'))^{2\alpha(t)} \\
& \times (U \bar{\rho}'_{U+W} \bar{\rho}'_{V+W})^{-\alpha(0)-\alpha(t)} F(U'+V'+W')^{-\alpha(0)-\alpha(t)} \\
& + \alpha_{K^*}(u) \alpha(t) \alpha_{K^*}(\bar{s}) (-\alpha_{K^*}(u)-1)^{\alpha(t)-1} (-\alpha_{K^*}(\bar{s})-1)^{\alpha(t)-1} \\
& \times (-\alpha_{K^*}(M^2)-1)^{\alpha(0)-2\alpha(t)} \int_0^\infty \int_0^\infty \int_0^\infty dU dV dW e^{-\frac{1}{2}(U'+V'+W')} e^{-W'} \\
& \times (UV)^{-\alpha(t)} (F(U')F(V'))^{-\alpha(t)} W^{-\alpha(t)-1} F(W')^{-\alpha(t)-1} \\
& \times ((\bar{\rho}'_{U+W})(\bar{\rho}'_{V+W}))^{2\alpha(t)} (F(U'+W')F(V'+W'))^{2\alpha(t)} \\
& \times (U \bar{\rho}'_{U+W} \bar{\rho}'_{V+W})^{-\alpha(0)-\alpha(t)} F(U'+V'+W')^{-\alpha(0)-\alpha(t)}
\end{aligned}$$

$$\begin{aligned}
& + \alpha(t) \alpha(t) \alpha_K^*(u) (-\alpha_K^*(u) - 1)^{\alpha(t) - 1} (-\alpha_K^*(\bar{s}) - 1)^{\alpha(t)} \\
& \times (-\alpha_K^*(M^2) - 1)^{\alpha(0) - 2\alpha(t)} \int_0^\infty \int_0^\infty \int_0^\infty dU dV dW e^{-\frac{1}{2}(U'+V'+W')} e^{-\frac{1}{2}(V'+W')} \\
& (VW)^{-\alpha(t) - 1} (F(V')F(W'))^{-\alpha(t) - 1} U^{-\alpha(t)} F(U')^{-\alpha(t)} \\
& \times ((\xi'_{U+W})(\bar{\xi}_{V+W}))^{2\alpha(t)} (F(U'+W')F(V'+W'))^{2\alpha(t)} \\
& \times (\xi'_{U+W} \bar{\xi}_{V+W})^{-\alpha(0) - \alpha(t)} F(U'+V'+W')^{-\alpha(0) - \alpha(t)} \\
& + \alpha(t) \alpha_K^*(M^2) \alpha_K^*(\bar{s}) (-\alpha_K^*(u) - 1)^{\alpha(t)} (-\alpha_K^*(\bar{s}) - 1)^{\alpha(t) - 1} \\
& \times (-\alpha_K^*(M^2) - 1)^{\alpha(0) - 2\alpha(t)} \int_0^\infty \int_0^\infty \int_0^\infty dU dV dW e^{-\frac{1}{2}(U'+V'+W')} e^{-\frac{1}{2}(U'+V')} \\
& \times (UV)^{-\alpha(t) - 1} (F(U')F(V'))^{-\alpha(t) - 1} W^{-\alpha(t)} F(W')^{-\alpha(t)} \\
& \times ((\xi'_{U+W})(\bar{\xi}_{V+W}))^{2\alpha(t)} (F(U'+W')F(V'+W'))^{2\alpha(t)} \\
& \times (\xi'_{U+W} \bar{\xi}_{V+W})^{-\alpha(0) - \alpha(t)} F(U'+V'+W')^{-\alpha(0) - \alpha(t)} + \alpha(t) \alpha(t) \\
& \times \alpha_K^*(M^2) (-\alpha_K^*(u) - 1)^{\alpha(t)} (-\alpha_K^*(\bar{s}) - 1)^{\alpha(t)} \\
& \times (-\alpha_K^*(M^2) - 1)^{\alpha(0) - 2\alpha(t) - 1} \int_0^\infty \int_0^\infty \int_0^\infty dU dV dW e^{-\frac{1}{2}(U'+V'+W')} e^{-\frac{1}{2}(U'+V')} \\
& \times (UV)^{-\alpha(t) - 1} (F(U')F(V'))^{-\alpha(t) - 1} W^{-\alpha(t)} F(W')^{-\alpha(t)} \\
& \times ((\xi'_{U+W})(\bar{\xi}_{V+W}))^{2\alpha(t)} (F(U'+W')F(V'+W'))^{2\alpha(t)} \\
& \times (\xi'_{U+W} \bar{\xi}_{V+W})^{-\alpha(0) - \alpha(t)} F(U'+V'+W')^{-\alpha(0) - \alpha(t)}
\end{aligned}$$

$$\begin{aligned}
& +\alpha(t)\alpha(t)\alpha(t)\alpha_K^*(\bar{s})(-\alpha_K^*(u)-1)^{\alpha(t)}(-\alpha_K^*(\bar{s})-1)^{\alpha(t)-1} \\
& \times (-\alpha_K^*(M^2)-1)^{\alpha(0)-2\alpha(t)} \int_0^\infty \int_0^\infty \int_0^\infty dUdVdW e^{-(U'+V'+W')} e^{-(U'+W')} \\
& \times (UW)^{-\alpha(t)-1} (F(U')F(W'))^{-\alpha(t)-1} V^{-\alpha(t)} F(V)^{-\alpha(t)} \\
& \times ((\rho'_{U+W})(\bar{\rho}_{V+W}))^{2\alpha(t)} (F(U'+W')F(V'+W'))^{2\alpha(t)} \\
& \times (\rho'_{U+W+\bar{\rho}_V})^{-\alpha(0)-\alpha(t)} F(U'+V'+W')^{-\alpha(0)-\alpha(t)} \\
& +\alpha(t)\alpha(t)\alpha(t)\alpha(t)(-\alpha_K^*(u)-1)^{\alpha(t)}(-\alpha_K^*(\bar{s})-1)^{\alpha(t)} \\
& \times (-\alpha_K^*(M^2)-1)^{\alpha(0)-2\alpha(t)} \int_0^\infty \int_0^\infty \int_0^\infty dUdVdW e^{-(U'+V'+W')} e^{-(U'+V'+W')} \\
& \times (UVW)^{-\alpha(t)-1} (F(U')F(V')F(W'))^{-\alpha(t)-1} ((\rho'_{U+W})(\bar{\rho}_{V+W}))^{2\alpha(t)} \\
& \times (F(U'+W')F(V'+W'))^{2\alpha(t)} (U\rho'_{+V}\bar{\rho}_{+W})^{-\alpha(0)-\alpha(t)} \\
& F(U'+V'+W')^{-\alpha(0)-\alpha(t)}
\end{aligned}
\tag{4.3.7}$$

Now following the arguments of Bardakci and Ruegg we can take the limit $s \rightarrow -\infty$ and $M^2 \rightarrow -\infty$ inside the integral and obtain the asymptotic behavior of the amplitude. Then we can analytically continue the amplitude to positive quadrant of the complex s and complex M^2 plane. In the limit $\rho \rightarrow 0$ the discontinuity function for B_6^a is given by,

$$\begin{aligned}
\text{Disc}_{M^2} \frac{1}{2\pi i} B_6^a &= \frac{1}{\pi} \left[\Gamma^2(1-\alpha(t)) \Gamma(-2\alpha(t)) \Gamma(-\alpha(t)) \right. \\
&\quad \times \left. \Gamma(1-\alpha(t)) + \alpha^2(t) \Gamma^2(-\alpha(t)) \right] \\
&\quad \sin \pi (\alpha(0) - 2\alpha(t)) \rho^{\alpha(0)-2\alpha(t)} \\
&\quad (\alpha_{K*}(s))^{\alpha(0)} \Gamma(1+\alpha(0)+2\alpha't) \quad (4.3.8)
\end{aligned}$$

$$\begin{aligned}
\text{Disc}_{M^2} \frac{1}{2\pi i} B_6^b &= \frac{1}{\pi} \left[\Gamma^2(1-\alpha(t)) \Gamma(-2\alpha(t)) \Gamma(-\alpha(t)) \right. \\
&\quad \left. \Gamma(1-\alpha(t)) + \alpha^2(t) \Gamma^2(-\alpha(t)) \right] \\
&\quad \times \sin \pi (\alpha(0) - 2\alpha(t)) (1-\rho)^{2\alpha(t)} \\
&\quad \times \rho^{\alpha(0)-2\alpha(t)} (\alpha_{K*}(s))^{\alpha(0)} \\
&\quad \times \Gamma(1+\alpha(0)+2\alpha't) \quad (4.3.9)
\end{aligned}$$

$$\begin{aligned}
\text{Disc}_{M^2} \frac{1}{2\pi i} (B_6^c + B_6^d) &= 2 \cos \pi \alpha(0) (\alpha_{K*}(s))^{\alpha(0)} (1-\rho)^{\alpha(t)} \\
&\quad \rho^{\alpha(0)-2\alpha(t)} \sin \pi (\alpha(0) - 2\alpha(t)) \\
&\quad \left[\Gamma^2(1-\alpha(t)) \Gamma(1+\alpha(0)+2\alpha't) \Gamma(-\alpha(t)) \right. \\
&\quad \times \Gamma(1-\alpha(t)) \Gamma(-\alpha(t)) \Gamma(1+\alpha(0)+2\alpha't) \\
&\quad \times \Gamma(-\alpha(t)) \Gamma^2(1-\alpha(t)) \Gamma(\alpha(0)+2\alpha't) \\
&\quad \times \alpha^2(t) \Gamma(-\alpha(t)) \Gamma(1-\alpha(t)) \\
&\quad \times \left. \Gamma(\alpha(0)+2\alpha't) \Gamma(-\alpha(t)) \Gamma(1-\alpha(t)) \right]
\end{aligned}$$

$$\begin{aligned}
& \times \Gamma(-\alpha(t)) \Gamma(1+\alpha(0)+2\alpha't)-\alpha^3(t) \\
& \Gamma(-\alpha(t)) \Gamma(\alpha(0)+2\alpha't)+\alpha^2(t) \Gamma^2(-\alpha(t)) \\
& \Gamma(1+\alpha(0)+2\alpha't)+\alpha^2(t) \Gamma(-\alpha(t)) \\
& \Gamma(1-\alpha(t)) \Gamma(\alpha(0)+2\alpha't); \quad (4.3.10)
\end{aligned}$$

The discontinuity functions given in the eqn. (4.3.8)-(4.3.10) are strictly valid for $\rho \rightarrow 0$ in the dual resonance models. Now we consider a different kinematic region where $s \rightarrow \infty$, $t \rightarrow \infty$, $M^2 \rightarrow \infty$ and $\theta_{c.m.}$ is not infinitesimal. We calculate the discontinuity function in this region. The functions are determined in the following manner: (i) We first take the limit $s \rightarrow \infty$ and (ii) the limit $t \rightarrow \infty$ and $M^2 \rightarrow \infty$. Keeping in mind the fact that $\alpha(0) = 1/2$, we get the discontinuity function as,

$$B_6^a = 4G^4 e^{-\alpha_K^*(s) \log(\alpha_K^*(s)(\alpha_K^*(s)+\alpha(t)))} \Phi(s, \cos \theta) \quad (4.3.11)$$

where $\Phi(s, \cos \theta)$ is a polynomial in s and $\cos \theta$. Because of the $\alpha(s)$ factor in the exponential this gives a negligible contribution for large s values.

$$\begin{aligned}
\text{Disc}_{M^2} \frac{1}{2\pi i} B_6^b &= 4G^4 (\exp[-\alpha_K^*(s)(1-\rho)(1-\cos \theta) \log \frac{2}{1-\cos \theta} \\
&+ (1+\cos \theta) \log \frac{2}{1+\cos \theta}] + [\alpha_K^*(s)(1-\rho)(1-\cos \theta) \\
&- \alpha(0)] \log(1/(1-\cos \theta))) / \pi. \quad (4.3.12)
\end{aligned}$$

where $\cos \theta = \hat{p}_a \cdot \hat{p}_c$, \hat{p}_a and \hat{p}_c being unit vectors in the CM frame. In the above equation we have retained only leading terms.

The discontinuity functions for nonzero ρ assume a very complicated form, as it has been observed by Gordon and Veneziano, in the case of scalar particles. In the presence of pseudoscalar mesons they become even more complicated. It is also not possible to obtain any closed form for the discontinuity functions for non-zero ρ value.

In view of the above mentioned difficulties we assume that the discontinuity functions as given in eqns. (4.3.8)-(4.3.10) can be extrapolated to a region where ρ is nonzero. This corresponds to extrapolating from the tripple Regge region to the target fragmentation region. But it will be a very drastic assumption to use the equations (4.3.8) to (4.3.10) all the way upto $\rho = 1$. Therefore, we use the form (4.3.12) for large ρ and t values. We mention here that the eqn. (4.3.10) gives vanishing contribution since there is a factor $\cos \pi \alpha(0)$ and $\alpha(0) = 1/2$ in our case. Therefore, we are left with only two functions given by eqns. (4.3.8) and (4.3.9). There is some experimental indication that the tripple Regge parameterization is valid in substantial part of fragmentation region.¹⁰¹

In order to obtain the inclusive cross-section we divide the discontinuity function by appropriate flux factor.

$$\frac{d\sigma}{dt dM^2} = \frac{\alpha'^2}{4\pi\alpha(s)} \text{Disc } B_6(s, \rho, t) \quad (4.3.13)$$

To obtain the total cross-section we integrate eqn. (4.3.13) over dM^2 and dt . Then σ_t is given by¹⁰²

$$\sigma_t = \frac{G^4 \alpha'^2}{4\alpha(s)} \int_0^1 d\rho \int_{t_{\min}}^{t_{\max}} dt f(\rho, t, s) \quad (4.3.14)$$

where,

$$f(\rho, t, s) = \text{Disc} \frac{1}{M^2} B_6(s, \rho, t).$$

The integral (4.3.13) was performed by a computer analysis. The actual computation was done in the following manner.

The discontinuity functions defined in eqns. (4.3.8)-(4.3.10) and in (4.3.12) are computed for different values of ρ and t in the computer and are compared at each value of ρ and t . Then the values of t and ρ for which the two discontinuity functions (4.3.8)-(4.3.10) and (4.3.12) coincide are taken, say, they match at $t = t_1$ is carried out by taking the discontinuity functions defined in eqns. (4.3.8)-(4.3.10) and the integration from $\rho = \rho_1$ to $\rho = 1$ and $t_{\min} = t_1$ to $t = t_{\max}$ is carried out by taking the discontinuity functions as defined in eqn. (4.3.12). The total cross-section obtained in this manner is equated with the expression obtained for total cross-section from optical theorem.

$$\begin{aligned}
& \frac{4}{3} \left(\frac{1}{\sqrt{6}} + 1 \right) \frac{G^2 \pi_{KK^*} \pi_{K^*K} (\alpha_{K^*}(s))^{\alpha(0)-1}}{\Gamma(\alpha(0))} \\
& = \frac{\alpha'^2 G^2 \pi_{KK^*} G^2_{K^*K} \pi}{4\pi \alpha_{K^*}(s)} \int_0^1 d\rho \int_{t_{\min}}^{t_{\max}} dt f(s, \rho, t)
\end{aligned} \tag{4.3.15}$$

And we get,

$$\begin{aligned}
G^2_{K^*K} \pi_{K^*K} & = \frac{2}{3} \frac{(1 + \frac{1}{\sqrt{6}}) 8\pi^2 (\alpha_{K^*}(s))^{\alpha(0)}}{\alpha' \Gamma(\alpha(0)) \int_0^1 d\rho \int_{t_{\min}}^{t_{\max}} dt f(s, \rho, t)} \tag{4.3} \\
& \tag{4.3.16}
\end{aligned}$$

A similar expression can be derived for $\pi\eta \rightarrow \pi\eta$ and $\pi\eta \rightarrow \pi + \text{anything}$ in a straight-forward manner (See Appendix A). Also it is worth mentioning that the coupling constants occurring here are dimensionless. Therefore, this fact must be kept in mind while comparing these coupling constants with the experimental results.

4.4 Results:

We summarise, in this section, the results on the computation of the eqn. (4.3.16) and the analogous equation for $\pi\eta$ processes.

(i) On comparing the cross-section $\pi^- K^+ \rightarrow \pi^0 + \text{anything}$ and $\pi^- K^+ \rightarrow \text{anything}$ we obtain the dimensionless quantity $\frac{G_{K^*K^*\pi}^2}{4\pi} = 1.99$ and this has to be compared with $\frac{m_\rho^2 g_{K^*K^*\pi}^2}{4\pi}$ as calculated from other models.

a) $\frac{m_\rho^2 g_{K^*K^*\pi}^2}{4\pi}$ computed from the Super-Convergence Relations by Adamello, Rubinstein, Veneziano and Virasoro¹⁰³ turns out to be 3.7.

b) The predictions of the pole model for $\omega \rightarrow \pi\gamma$ gives $\frac{m_\rho^2 g_{\omega\rho\pi}^2}{4\pi} = 13 \pm 5$ which through $SU(3)$ ¹⁰⁴ can be related to $\frac{m_\rho^2 g_{K^*K^*\pi}^2}{4\pi} = 3.25 \pm 1.25$.

Our results are in qualitative agreement with the results of these models.

(ii) Similar results obtained from the reactions $\pi + \eta \rightarrow \text{anything}$ and $\pi + \eta \rightarrow \pi + \text{anything}$ yields:

$\frac{G_{A_2\rho\pi}^2}{4\alpha'^2} = 101.68 \text{ GeV}^{-4}$, which must be compared with the coupling constant $g_{A_2\rho\pi}^2$ which can be computed from $A_2 \rightarrow \rho\pi$ decay width¹⁰⁵. We get $g_{A_2\rho\pi}^2 = 313.4 \text{ GeV}^{-4}$.

Thus the coupling constants obtained through this bootstrap scheme, share qualitative agreement with the experimental results. In view of the drastic simplifying assumption we have made throughout a more quantitative agreement could not be expected at this stage and must await further refinements of the Dual Resonance theory.

In arriving at these results, we have not included the contributions of the diagram 25c, (which corresponds to PEX region or projectile fragmentation limit). This is prompted by two main reasons. (i) An explicit estimate shows that the contribution is too small to alter the general conclusions (ii) the inclusion of Fig. 25c, makes the problem computationally more difficult without adding anything in principle. In view of our interest mainly in qualitative features, we admit this approximation to facilitate the computation.

CHAPTER V

We seek to summarise and discuss our results and suggest possible improvements of our model in this chapter. It is a well known experimental fact that the cross-sections for charge-exchange and hypercharge-exchange processes decrease as energy increases since the Pomeranchukon trajectory cannot be exchanged in these processes. We feel that the dynamical nature of the vector and tensor meson trajectories is rather well understood in the frame work of duality, whereas the dynamical origin of the Pomeranchukon is not known so well. Therefore, it is of interest to study the charge and hypercharge exchange reactions, where the vector and tensor meson trajectories are exchanged, in a model which exhibits the principle of duality. Moreover, there is vast amount of experimental data in the intermediate and medium high energy region for these processes. We have studied such processes in a Veneziano like model.

In the first chapter we have studied processes in which a single Regge pole can be exchanged in the t -channel. In case of πN charge-exchange process, we have tried to understand the polarization phenomena in a qualitative manner. We have calculated polarization for πN CEX in different models and have compared the results with the experimental data. A single Regge pole exchange model for πN CEX gives vanishing

polarization, though it describes the differential cross-sections fairly well. We sought to explain the polarization phenomena through the non-asymptotic-terms of the Veneziano amplitude. It is expected that a simple model like that of Igi's cannot give a quantitative description of the polarization phenomena. Nevertheless it is interesting to note that a simple model, like the one we have considered, gives a fairly good description of the polarization data. Of the various parametrizations, we have considered the best agreement with the polarization data are obtained in two sets. First when we consider all baryon trajectories to be degenerate and a second set of parameters are obtained by the use of backward scattering data. Our calculations show 20 percent polarization in the low momentum transfer region ($0 < -t < 0.3$) and predict an increasing magnitude of polarization at higher momentum transfers. The data on polarization that has become available recently show such a trend at higher momentum transfers ($.3 < -t < .55$) indicating a substantial agreement between our predictions and the experimental data. In addition both the models predict a negative polarization for $\alpha(t) < 0$ and indeed polarization has a violent oscillation when $\alpha(t)$ changes sign. Presently available data do not contradict such a possibility. Our prediction for polarization, calculated using information on FESR, has a wrong sign compared to the experimental data though it is of the same order of magnitude. The predictions of Fenster and Wali model

also turns out to **give** a wrong sign for the polarization. We have also calculated the πN CEX differential cross-sections. It is important to note that the differential cross-section is not changed significantly when we keep the background terms. We observe here that the Veneziano model provides a background term to produce a nonzero polarization in πN CEX scattering, which agrees qualitatively with the experimental data. However, the results depend sensitively upon the details of the parametrizations of the amplitude. Therefore, this information alone cannot be used to test the uniqueness of the Veneziano amplitude³⁷.

The other reaction that we have studied in the second chapter is the η -production in pion nucleon scattering. In this process A_2 trajectory is exchanged in the t -channel. There also exists nonzero polarization at pion laboratory energies 11.2 GeV and 5.9 GeV, though the data is scanty. We obtain a good fit to the differential cross-sections for the reaction $\pi^- p \rightarrow \eta n$ using only four parameters. The fit is characterized by a chi-square value 8.5 against an expected 10. Our solution yields an average polarization of 4 percent at 5.9 GeV. The experimental data, though some what inconclusive due to very large errors, are of opposite sign. At high energies (11.2 GeV) both the experimental data as well as our solution indicate very small polarization.

In the first part of the Chapter III, we considered $\bar{K}N$ charge-exchange reaction.⁵² The amplitude for this process contains four free parameters. The cross-section at \bar{K} -meson laboratory energies at 9.8 GeV and 12.3 GeV are compared with our solution. The quality of the fit is characterized by a chi-square value of 21.3 against an expected 20. The amplitude further yields an average positive polarization of 15 percent at 9.8 GeV. The experimental indications also show a positive polarization. As is well known the s-u crossing relates this process to KN charge exchange process. The exchange degeneracy of ρ and A_2 trajectories implies that the cross-sections for the two processes should be same at a given energy. It is impressive that our solutions agree reasonably well with the differential cross-section for $K^+n \rightarrow K^0p$ at K meson laboratory energy of 12 GeV. The only feature that is not completely reproduced is a broad shoulder at $t = -.3 \text{ GeV}^2$ to $-.5 \text{ GeV}^2$.

The hypercharge exchange processes we have studied are $K^-p \rightarrow \pi^-\Sigma^+$ and $K^-n \rightarrow \pi^-\Lambda$. The former has six parameter and the fit to the differential cross-section at 8 GeV gave a chi-square value of 12 against an expected 7. An interesting feature is that our solution yields a small **positive** (.2 percent) polarization in this reaction. We have to wait for the polarization data to check whether this is indeed true. For the reaction, $K^-n \rightarrow \pi^-\Lambda$ the total cross-section was fitted

with a formula involving only two parameters. The fit is good giving a chi-square value of 19 against 11. The formula also predicts polarization which agrees qualitatively with the data at 4.5 GeV.

We have calculated polarization at pion laboratory energies 4 GeV and 7 GeV for the process $\pi^+p \rightarrow K^+\Sigma^+$. The amplitude for this process is obtained by $s-u$ crossing of the amplitude for $K^-p \rightarrow \pi^-\Sigma^+$. The fit to the polarization data was obtained without any free parameters in the amplitudes. Our results agree with the experimental data for $-t < .3 \text{ GeV}^2$, whereas in the region $-t > .4 \text{ GeV}^2$ the polarization is of the order of .7 for all energies, much larger than what we obtain in our model. The existence of large polarization indicates the presence of a large background term⁷⁰. In all our calculations the polarization is produced due to the interference of the Regge term with the non leading terms present in the Stirling approximation of B and C functions of the Veneziano amplitudes. Therefore, the $1/s$ behavior of the polarization is incorporated automatically, this leads to vanishing polarization at high energies. Though differential cross-section for charged pion photo production can be fitted well, it is not possible to describe the asymmetry parameter in a Veneziano model.

We have so far discussed the predictions and usefulness of the Veneziano model to describe meson baryon scattering phenomena in the intermediate and medium high energy region.

However, the model has several short-comings. In principle, since crossing symmetry is included, we should expect the model to be more versatile and thus be capable of predicting the amplitude in the low energy region as well. It is also expected that the parameters which describe the forward scattering phenomena should also be able to give a reasonable description of the processes in the backward directions. It is here that we find several discrepancies, which make the model inexact in its details. The model requires a much larger number of resonances, several of them degenerate. The structure of the terms calls for parity doublets, the presence of particles in daughter trajectories of wrong isospin, etc. The set of parameters, that describe the forward scattering cross-section, do not describe the backward scattering data. In fact, in case of πN CEX scattering the backward scattering cross-sections exceed by an order of magnitude when calculated using the parameters used by Igi and the set of parameters that are determined from FESR results.¹⁰⁶ Indeed, by increasing the number of parameters and the satellite terms, we can reduce the number of unwanted poles in the baryon channels. And it is also possible to describe the forward and the backward scattering data if one includes a large number of parameters. Such attempts have been made by Berger and Fox and Desai and Kumar. Berger and Fox⁶⁰ find it necessary to introduce secondary Veneziano terms and also to include non-Veneziano factors to account for certain changes of sign. In

order to describe the elastic scattering neither one has to introduce the Pomeron trajectory in a nonlocal fashion or one has to keep exotic trajectories in the baryon channel. Another important point to notice here is the fact that the uniqueness of the Veneziano representation cannot be concluded from experimental results. It calls for additional constraints on the amplitude in order to determine the residue functions uniquely.

In the second and the third chapter, we have adopted the point of view that the Veneziano parametrization is the most economical to describe phenomenologically the high energy charge-exchange and hypercharge-exchange reactions. This is supported by the fact that there is substantial agreement between high energy cross-sections and polarization data and the Veneziano like solutions, exist **notwithstanding** the shortcomings of the model.

In the fourth chapter we have considered a nonlinear bootstrap scheme. This imposes certain restrictions on the Veneziano residues. We feel, if this approach succeeds, that it might be possible to determine the Veneziano residue uniquely through this bootstrap scheme.

In this scheme we obtain a sum rule relating an appropriate discontinuity of the four point Veneziano amplitude to an integral over a discontinuity function of a six point

function. The former discontinuity function is proportional to g^2 whereas the latter is of the order of g^4 . This sum rule enables us to impose the bootstrap conditions on the coupling constants.

The principal difficulty in this scheme is caused by our inability to write the discontinuity function in a closed form, in all kinematical regions. Perhaps significant errors are introduced by the extrapolation that we have adopted. There is room for improvement of both the technique and the choice of the starting Dual Resonance Model.

The central theme, on which this bootstrap scheme is based, emphasises that Dual Resonance Model contains a good deal of properties that are characteristic of a unitary theory. This draws support from the fact that the Regge trajectories are very nearly linear and the widths of the higher resonances are indeed small. Hence the corrections to DRM should occur as small parameters. It is not clear that in the multi-loop approach, which attempts to take care of unitarity perturbatively in a very elegant crossing symmetric manner, such corrections indeed be small. In fact, there are divergences due to a variety of reasons, on the contrary, in the approach we have considered here; there are no problems connected with infinities. Instead, unitarity acts as further constraints on the model. Indeed, if such a line of thought merits consideration, further

refinement of the theory would be in starting with a better approximation of DRM. For example one may introduce the trajectory function with proper analytic structure. It is possible to construct a crossing symmetric amplitude¹⁰⁷⁻¹¹¹ that has the correct analytic structure, without introducing the traditional difficulties, such as ancestors or essential singularities. Perhaps a nonlinear equation set up through such amplitudes would result in a better approximation. Our result certainly encourages pursuit of such ideas.

In describing scattering cross-section and the polarization phenomena for charge and hypercharge exchange processes we have introduced a phase to the apparently real Veneziano amplitude. This is achieved by introducing a small imaginary part to the trajectory function. Similarly, in deriving the nonlinear bootstrap conditions we have implicitly assumed that the imaginary part of the trajectory function is small. This is supported by the fact that experimentally observed resonances are rather narrow. Therefore, we feel that the Veneziano amplitude, to a good approximation, describes the real hadronic world. Any correction to the Veneziano function would be small so that the narrowness of the resonance is not affected to a large extent. All our calculations indicate validity of this belief.

REFERENCES

1. Historically, Heisenberg was first to stress the importance of the S-matrix theory in elementary Particle Physics. Z. Physik 120, 513, 673 (1943).

For more details see:

G.F. Chew, S-matrix theory of strong interactions,
W.A. Benjamin, N.Y. 1962.

G.F. Chew, Analytic S-matrix W.A. Benjamin, N.Y. 1966.

S. Frautschi, Regge poles and S-matrix theory,
W.A. Benjamin, N.Y. 1963.

R.J. Eden High energy collision of elementary particles,
Cambridge University Press 1967.

P.D.B. Collin and E.J. Squares in Springer tracts in
Modern Physics, Vol 45, Springer Verlag. (1968).

2. V. Barger and D. Cline, Phys. Rev. Letters, 16, 913 (1966).
3. V. Barger and M. Olsson, Phys. Rev. 151, 1123 (1966).
4. B.R. Desai, D.T. Gregoritch and R. Ramachandran, Phys. Rev. Letters, 18, 565 (1967).
5. L. van Hove, Phys. Letters 24B, 183 (1967).
6. L. Durand, Phys. Rev. 161, 1610 (1967).
7. R. Blankenbecler in Proceedings of Rochester Conference, 1967, Ed. C.R. Hagen, G. Guralnik and V.S. Mathur, 559.
8. K. Igi and S. Matsuda, Phys. Rev. Letters, 18, 625 (1967).
9. A. Logunov, L.D. Loloviev and A.N. Tarkhelidze, Phys. Letters 24B, 181 (1967).
10. R. Dolen, D. Horn and C. Schmid, Phys. Rev. Letters 19, 402 (1967) and Phys. Rev. 166, 1768 (1968).
11. C. Schmid, Phys. Rev. Letters, 20, 628 (1968).
12. C. Schmid, Phys. Rev. Letters 20, 689 (1968).

13. M. Ademallo, H.R. Rubinstein, G. Veneziano and M.A. Vivasoro, Phys. Rev. Letters 19, 1402 (1967).
14. M. Ademallo, H.R. Rubinstein, G. Veneziano and M.A. Vivasoro, Phys. Rev. 176, 1904 (1968).
15. M. Bishari, H.R. Rubinatein, A. Schwimmer and G. Veneziano, Phys. Rev. 176, 1926 (1968).
16. S. Matsuda and K. Igi, Phys. Rev. Letters 19, 928 (1967).
17. C. Schmid's Lecture in Subnuclear Phenomena. Acad. Press (1970).
18. R. Oehme, Nucl. Phys. 16B, 161 (1970). We closely follow Oehme's argument here.
19. P.O.G. Freund, Phys. Rev. Letters, 20, 235 (1968).
20. H. Harari, Phys. Rev. Letters, 20, 1395 (1968).
21. G. Veneziano, Nuovo Cimento, 57A, 190 (1968).
22. C. Lovelace, Phys. Letters, 28B, 264 (1968).
23. K. Kawarabayashi, S. Kitakado and H. Yabuki, Phys. Letters, 28B, 432 (1968).
24. K. Bardakçi and H. Ruegg, Phys. Letters 28B, 342 (1968).
25. M.A. Virasoro, Phys. Rev. Letters, 22, 37 (1969).
26. Chan H.M., Phys. Letters 28B, 425 (1968).
27. C.G. Goebel and B. Sakita, Phys. Rev. Letters, 22, 257 (1969).
28. Z. Koba and H.B. Nielsen, Nucl. Phys. B10, 633 (1969).
29. L. Susskind, Phys. Rev. D1, 1182 (1970).
30. S. Fubini and G. Veneziano Nuovo Cimento, 64A, 811 (1969).
31. K. Kikkawa, B. Sakita and M.A. Virasoro, Phys. Rev. 184, 1701 (1969).
32. K. Bardakçi, M.B. Halpern and J.A. Shapiro, Phys. Rev. 185, 1910 (1969).
33. V.A. Alessandrini, D. Amati, M. LeBellac and D. Olive, In Physics Report 10 'The Operator Approach to Dual Multi-Particle Theory' and references therein.

34. R.K. Logan, J. Beaupre and L. Sertorio, Phys. Rev. Letters, 18, 259 (1967).
35. C.B. Chiu and J. Finkelstein, Nuovo Cimento, 48A, 820 (1967).
36. See Reference 4.
37. J. Maharana and R. Ramachandran, Phys. Rev. D2, 2713 (1970).
38. K. Igi, Phys. Letters 28B, 330 (1968).
39. Y. Hara Phys. Rev. 182, 1906 (1969).
40. M.A. Virasoro, Phys. Rev. 18A, 1621 (1969).
41. K.C. Gupta and S.K. Bose, Phys. Rev. 184, 1571 (1969).
42. S.Y. Chu and B.R. Desai, Phys. Rev. 188, 2215 (1969).
43. Y. Miyata, Prog. Theo. Phys. Japan, 43, 1013 (1969).
44. S. Sakai, Prog. Theo. Phys. Japan 43, 986 (1969).
45. S. Fenster and K.C. Wali, Phys. Rev. D1, 1409 (1970).
46. A.N. Hendry, S.T. Jones and H.W. Wyld, Nucl. Phys., B15, 389 (1970).
47. S.W. McDowell, Phys. Rev. 116, 774 (1960).
48. Virendra Singh, Phys. Rev. 129, 1889 (1963).
49. F.J. Gilman, H. Harari and Y. Zarmi, Phys. Rev. Letters, 21, 323 (1968).
50. For Polarization Data, P. Bonamy et.al. Phys. Letters 23, 501 (1966).

For Differential Cross-Section Data, A.V. Stirling, Phys. Rev. Letters, 14, 763 (1965) and P. Sonderegger et.al. Phys. Letters, 20, 75 (1966).
51. P. Bonamy et.al. unpublished.
52. J. Maharana and R. Ramachandran, Nuovo Cimento, 5A, 603 (1971).
53. For $\pi N \rightarrow \eta n$ see,
O. Miyamura, Prog. Theo. Phys. Japan 42, 305 (1969).
M. Blackmon and K.C. Wali, Phys. Rev. D2, 258 (1970).

54. O. Guisan et.al., Phys. Letters, 18, 200 (1966).
55. P. Bonamy et.al., Nucl. Phys. B16, 335 (1970).
56. K. Igi and J. Storrow, Nuovo Cimento, 62A, 972 (1969).
57. K. Pretzel and K. Igi, Nuovo Cimento, 63A, 609 (1969).
58. T. Inami, Nuovo Cimento, 63A, 987 (1969).
59. C. Lovelace, Nucl. Phys. B12, 253 (1969).
60. E.L. Berger and G.C. Fox, Phys. Rev. 188, 2215 (1969).
61. Bipin R. Desai and Aditya Kumar, Phys. Rev. D4, 2030 (1971).
62. We closely follow Sec. 3.2 of Ref. 52 in this Chapter.
63. M.G. Schmidt, Nucl. Phys. B15, 157 (1970).
64. Data has been taken from P. Astbury et.al. Phys. Letters, 23, 346 (1966).
65. D. Cline, J. Matos and D.D. Reeder, Phys. Rev. Letters, 23, 346 (1969).
66. A. Firestone et.al. Phys. Rev. Letters, 25, 958 (1970).
67. K.V.L. Sarma, Private Communication.
68. D. Bernboum et.al. Phys. Letters, 31B, 484 (1970).
69. W.L. Yen et.al., Phys. Rev. 188, 2011 (1969).
70. S.M. Pruss et.al. Phys. Rev. Letters, 23, 189 (1969).
71. K. Lai and J. Louie, Nucl. Phys. B19, 205 (1970).
72. R.D. Field, Phys. Rev. D5, 86 (1972).
73. J.S. Ball, W.R. Frazer and M. Jacob, Phys. Rev. Letters, 20, 518 (1968).
74. D.P. Roy and S.Y. Chu, Phys. Rev. 171, 1762 (1968).
75. G.F. Chew, M.L. Goldberger, F.G. Low and Y. Nambu, Phys. Rev. 106, 1345 (1957).
76. J.S. Ball, Phys. Rev. 124, 2014 (1961).

77. D.P. Roy, Phys. Rev. Letters, 23, 1417 (1969).
78. R.L. Brower and M.B. Halpern, Phys. Rev. 182, 1779 (1969).
79. I. Bender and H.J. Rothe, Nuovo Cimento Letters 2, 477 (1969).
80. F. Drago, *ibid*, 2, 712 (1969).
81. M. Ahmad, Fayyazuddin and Riazuddin, Phys. Rev. Letters, 23, 504 (1969).
82. D.P. Roy, Phys. Rev. 187, 1890 (1969).
83. M. Ahmad and Fayyazuddin, Phys. Rev. D2, 2718 (1970).
84. A. Boyarski et.al., Phys. Rev. Letters, 20, 300 (1968).
85. C.C. Moorehouse et.al., Phys. Rev. Letters, 25, 835 (1970).
86. In this chapter we follow closely our work J. Maharana and R. Ramachandran on 'Nonlinear ~~Bootstrap~~ in Dual Models (Submitted for Publication).
87. R.P. Feynman, Phys. Rev. Letters, 23, 1415 (1969).
88. J. Benecke, T.T. Chow, C.N. Yang and E. Yen, Phys. Rev. 188 2159 (1969).
89. A.H. Mueller, Phys. Rev. D2, 2963 (1970).
90. N.F. Bali, A. Pignotti and D. Steele, Phys. ~~Rev.~~ D3, 1167 (1971).
91. C.E. De Tar, C.E. Jones, F.E. Low, J.H. Weis, J.E. Young and Chung-I-Tan, Phys. Rev. Letters, 26, 675 (1971).
92. D. Gordon and G. Veneziano, Phys. Rev. D3, 2116 (1971).
93. M.A. Virasoro, Phys. Rev. D3, 2834 (1971).
94. C.E. De Tar, K. Kang, Chung-I-Tan, J.H. Weis and C.S. Hsue, Phys. Rev. D4, 2336 (1971).
95. A. Di Giacomo, S. Fubini, L. Sertorio and G. Veneziano, Phys. Letters, 33B, 171 (1970).
96. G. Veneziano, Phys. Letters, 34B, 59 (1971).

97. G. Veneziano, Talk Presented at the International Conference on Duality and Symmetry in Hadron Physics, Tel-Aviv, Israel, April 1971.
98. S.H.H. Tye and G. Veneziano, Phys. Letters, 36E, 30 (1972).
99. N. Panchapakesan, Letter Nuovo Cimento 4, 235 (1970).
100. K. Bardakci and H. Ruegg, Phys. Letters 28E, 342 (1968).
101. K. Huang and G. Segre, Phys. Rev. Letters, 27, 1095 (1971).
102. Strictly speaking the left handside of the eqn.(4.3.13) is to be multiplied by the multiplicity factor which has a logarithmic energy dependence. This energy dependence is weak compared to the energy dependence of the four and six point discontinuity function. We have ignored this factor. In fact, if all permutations of six point amplitude are summed, this factor can be accounted for.
103. M.Ademallo, H.R. Rubinstein, G. Veneziano and M.A.Virasoro, Nuovo Cimento, 51A, 227 (1967).
104. K. Bardakci and H. Ruegg, Phys. Letters, 28E, 671 (1968).
105. The coupling constant $g_{A_2 \rho \pi}$ is defined through the interaction Lagrangian,

$$\mathcal{L} = \frac{1}{4} g_{A_2 \rho \pi} \epsilon_{\lambda \mu \nu \sigma} [p_{\lambda}^{(A_2)} \epsilon_i^{\rho \alpha} \epsilon^{\sigma} p_{\nu j} p_{\sigma k}^{\pi} | \epsilon_{ijk}$$

where $\epsilon^{\rho \alpha}$ is the A_2 polarization tensor and ϵ^{σ} is the ρ - polarization vector. p 's are the various four momenta of the particles involved.
106. We have checked this explicitly, J. Maharana and R. Ramachandran (Unpublished).
107. G. Cohen - Tannoudji, F. Henyey, G. Kane, Phys. Rev. Letters, 26, 112 (1971).
108. R. Ramachandran and M.O. Taha, Phys. Rev. (To be published).
109. A. Bugrig, L. Jonkovsky and N. Kobylinsky, Letter, Nuovo Cimento, 1, 923 (1971).
110. M. Schmidt, Letter, Nuovo Cimento 1, 1017 (1971).
111. R. Gaskell and A.P. Contogouris, Letter, Nuovo Cimento, 3, 231 (1972).

APPENDIX A

We list below the discontinuity functions of the six point function $\pi+\pi+\eta \rightarrow \pi+\pi+\eta$ which are related to the inclusive cross-section $\pi+\eta \rightarrow \pi+\text{anything}$.

$$\begin{aligned} \text{Disc}_{M^2} \frac{1}{2\pi i} B_6^a &= \frac{1}{\pi} \left[\Gamma^2(1-\alpha(t)) - 2\alpha(t) \Gamma(-\alpha(t)) \Gamma(1-\alpha(t)) + \alpha^2(t) \right. \\ &\quad \left. \Gamma^2(-\alpha(t)) \right] \sin \pi(\alpha(0) - 2\alpha(t)) \int_0^{\alpha(0)-2\alpha(t)} \\ &\quad (\alpha(s))^{\alpha(0)} \Gamma(1+\alpha(0)+2\alpha't) \quad . \quad (A.1) \end{aligned}$$

$$\begin{aligned} \text{Disc}_{M^2} \frac{1}{2\pi i} B_6^b &= \frac{1}{\pi} \left[\Gamma^2(1-\alpha(t)) - 2\alpha(t) \Gamma(-\alpha(t)) \Gamma(1-\alpha(t)) + \alpha^2(t) \right. \\ &\quad \left. \Gamma^2(-\alpha(t)) \right] \sin \pi(\alpha(0) - 2\alpha(t)) (1-\rho)^{2\alpha(t)} \\ &\quad \int_0^{\alpha(0)-2\alpha(t)} (\alpha(s))^{\alpha(0)} \Gamma(1+\alpha(0)+2\alpha't) \quad . \quad (A.2) \end{aligned}$$

$$\begin{aligned} \text{Disc}_{M^2} \frac{1}{2\pi i} (B_6^c + B_6^d) &= \frac{2 \cos \pi\alpha(0)}{\pi} (\alpha(s))^{\alpha(0)} (1-\rho)^{\alpha(t)} \int_0^{\alpha(0)-2\alpha(t)} \\ &\quad \sin \pi(\alpha(0) - 2\alpha(t)) \left[\Gamma^2(1-\alpha(t)) \Gamma(1+\alpha(0)+2\alpha't) \right. \\ &\quad \left. - \alpha(t) \Gamma(1-\alpha(t)) \Gamma(-\alpha(t)) \Gamma(1+\alpha(0)+2\alpha't) \right. \\ &\quad \left. - \alpha(t) \Gamma^2(1-\alpha(t)) \Gamma(\alpha(0)+2\alpha't) + \alpha^2(t) \Gamma(-\alpha(t)) \right. \\ &\quad \left. \Gamma(1-\alpha(t)) \Gamma(\alpha(0)+2\alpha't) - \alpha(t) \Gamma(1-\alpha(t)) \Gamma(-\alpha(t)) \right. \\ &\quad \left. \Gamma(1+\alpha(0)+2\alpha't) - \alpha^3(t) \Gamma^2(-\alpha(t)) \Gamma(\alpha(0)+2\alpha't) \right. \\ &\quad \left. + \alpha^2(t) \Gamma^2(-\alpha(t)) \Gamma(1+\alpha(0)+2\alpha't) \right. \\ &\quad \left. + \alpha^2(t) \Gamma(-\alpha(t)) \Gamma(1-\alpha(t)) \Gamma(\alpha(0)+2\alpha't) \right] \quad . \quad (A.3) \end{aligned}$$

The discontinuity functions eqns. (A.1)-(A.3) have been derived in the limit $s \rightarrow \infty$, t fixed $M^2 \rightarrow \infty$ and $\varphi \rightarrow 0$.

The bootstrap equation for the process $\pi \eta \rightarrow \pi \eta$ takes the following form,

$$\frac{2\pi g_{\pi\eta A_2}^2 (\alpha(s))^{\alpha(0)-1}}{\Gamma(\alpha(0))} = \frac{\alpha'^2 g_{\pi\eta A_2}^2 g_{A_2\varphi\pi}^2}{4\pi\alpha(s)} \int_0^1 d\varphi \int_{t_{\min}}^{t_{\max}} dt f(s, t, \varphi). \quad (A.4)$$

Then we obtain the coupling constant $g_{A_2\varphi\pi}^2$ as

$$g_{A_2\varphi\pi}^2 = \frac{8\pi^2 (\alpha(s))^{\alpha(0)}}{\alpha' \Gamma(\alpha(0)) \int_0^1 d\varphi \int_{t_{\min}}^{t_{\max}} dt f(s, t, \varphi)}. \quad (A.5)$$